REPORT OF INVESTIGATION 77

Open file report

# TEST RESULTS
# OF A
# SETTLING BASIN HYDRAULIC MODEL

by

Harold W. Humphreys

J. Rodger Adams

Nani G. Bhowmik

Illinois State Water Survey

Urbana, 1974

This Study is a Cooperative

Investigation with the City of Chicago

REPORT OF INVESTIGATION 77

Open file report

(not edited for printing)

# TEST RESULTS
# OF A
# SETTLING BASIN HYDRAULIC MODEL

by

Harold W. Humphreys

J. Rodger Adams

Nani G. Bhowmik

Illinois State Water Survey

Urbana, 1974

This Study is a Cooperative
Investigation with the City of Chicago

CONTENTS

# Test Results of a Settling Basin Hydraulic Model

by Harold W. Humphreys, J. Rodger Adams and Nani G. Bhowmik

## ABSTRACT

The Illinois State Water Survey in cooperation with the City of Chicago studied the flow characteristics in a hydraulic model of one of the sixteen settling basins in the Central Water Filtration Plant (CWFP). The study objective was improvement of flow conditions in the prototype settling basins in order to improve the quality of the settled water applied to filters.

A l-to-24 scale model of one of the prototype settling basins was constructed. The model includes the raw water supply channel, the mixing basin with four end around mixing channels including paddle flocculators in each channel, the upper and lower settling basins and the settled water collector.

The model performance was evaluated by making slug tracer studies, obtaining velocity distributions in the upper settling basin and taking time-lapse color photographs of the advance of dye in the upper settling basin.

The original model and several modifications were tested. Modifications tested included turning vanes at a bend in the mixing channels, reduced open area in the slotted baffle wall, various types and locations of screen grids in the upper settling basin, additional outlet ports from the lower settling basin and varied numbers of paddle flocculators in the fourth mixing channel.

Test results are discussed for all modifications. Specific test results are presented for the original model and selected modifications. Results are also given for a dispersion test and for an investigation of turbulent velocity fluctuations in the upper settling basin.

Model test results showed that slug tracers were not sensitive to most of the modifications investigated. Paddle flocculators prevent short circuiting in the mixing channels as well as promote flocculation. An inclined screen at the downstream end of the upper settling basin was not advantageous and can not be recommended for use.

Recommendations for installation in prototype basins are: 1) turning vanes at abrupt channel bends, 2) open area less than 5 percent in slotted baffle walls, 3) full depth screen baffles if three are used in series and if sludge removal equipment is properly designed and 4) training walls in wide basins.

Modifications recommended for trial in CWPP are turning vanes in the bend between mixing channels 3 and 4, and reduction of open area in the slotted baffle wall to 2.6 percent. Four additional outlet valves from the lower settling basin are suggested for reduction of head loss only.

A deaeration system was installed to supply partially degasified water to the model. Deaerated water was required for operation of the thermistor velocity meter which was developed to measure the very low velocity flow in the settling basin.

## INTRODUCTION

The Illinois State Water Survey (ISWS) in cooperation with Department of Water and Sewers, City of Chicago, has studied the flow characteristics in a hydraulic model of one of the sixteen settling basins in the Central Water Filtration Plant (CWFP).

The study objective was the improvement of flow conditions in the prototype settling basin in order to improve the quality of the settled water applied to the filters. Several modifications were tested in the model and their effect on the flow conditions were observed to determine which of the modifications would improve the flow conditions in the prototype.

Partial test results of this study have been presented by Humphreys[1].

Each prototype settling basin, designed for 60 mgd, includes a mixing basin with four end around mixing channels equipped with paddle flocculators in each channel, an upper settling basin, and a lower settling basin. In plan each basin is 172 ft wide by 263 ft 6 in. long and has an average total depth of 31 ft including the upper and lower settling basin. The basin length includes the 82 ft 11 in. wide mixing basin. The prototype is supplied from a raw-water supply channel equipped with a flow metering section.

Discharge from the prototype enters a settled water collector which receives settled water from the four settling basins in a quadrant of the plant. The four settling basins in the quadrant with the one which was modeled are identified as numbers 1, 2, 3 and 4. Settling basin number 3 was selected for modeling. The discharge from settling basin number 4 is the first to enter the settled water collector. The second discharge to enter the settled water collector Is from settling basin number 3, and it is followed by the discharges from basins 2 and 1.

This report describes the model scaling factors, settling basin model, methods for evaluating model performance, model modifications and the test results. A water deaeration system and a thermistor meter for measuring low velocity flow are described in appendices.

Test results include the effects of the model modifications on slug tracers at the outlet ports of the lower settling basin and at the model outlet, velocity distributions in the upper settling basin and the advance of a dye tracer in the upper settling basin. In addition test results on dispersion coefficients, response to a sudden change in discharge, and turbulent velocity fluctuations in the upper settling basin are presented. Notations for symbols used throughout this report are given in the back.

Acknowledgment

This cooperative research was conducted under the administrative supervision of Dr. William C. Ackermann, Chief, Illinois State Water Survey and Mr. James W. Jardine, Commissioner, Department of Water and Sewers, Chicago, Illinois. Thanks are extended to Mr. John B. W. Corey, Chief Water Engineer, Department of Water and Sewers, Mr. N. J. Davoust, Engineer of Water Purification and the Central Water Filtration Plant staff for their cooperation, suggestions and advice. Special credit is due to Dr. F. W. Sollo for his essential contribution in developing the velocity meter.

## MODEL

### Model Scaling Factors

The prototype mixing basins' and settling basins operate with a free water surface. Therefore, for the flow patterns to be similar in the prototype and model, the model was operated in accordance with the Froude law.

The Froude law requires operating the model at the same Froude number that occurs in the prototype.

The Froude number, defined in hydraulic and fluid mechanics text books, is $F = V/(gL)^{0.5}$ where V is a characteristic velocity, L is a characteristic length and g is the acceleration of gravity. The Froude number is nondimensional.

Camp[2] reported that the results obtained in a geometrically similar model did agree with the results obtained in the prototype when the model was operated according to Froude's law. He also found that similar flow patterns were observed when the

peripheral velocity of flocculator paddles was scaled in accordance to the Froude law.

The hydraulic model was constructed so that dimensions in the model divided by corresponding dimensions in the prototype equal a constant length ratio, $L_r$. The constancy of $L_r$ insures geometric similarity of form between the model and prototype.

For the value of $L_r$ equal to 1/24 for this study the scale factors given in Table 1 for area, volume, time, velocity, and discharge were used to scale these quantities between the prototype and model.

## Model Description

A 1:24 scale model of settling basin number 3 was designed and constructed by the Illinois State Water Survey. The model was constructed of clear acrylic so that when dye was used the flow in all parts of the model could be observed and photographed. The model and necessary auxiliary equipment are shown in figures 1 and 2. A plan view of the mixing basin and upper settling basin is shown in figure 3. A longitudinal section of the model is shown in figure 4.

The electrical and float controls in figure 1 are for the two pumps required to operate the model. Since the model was continuously operated the float controls were necessary to prevent operation of the pumps if for any reason the water supply was insufficient.

In the center of figure 1 are two open circular tanks. The smaller constant-head tank in the foreground receives water from the hydraulic laboratory system and supplies water to the larger tank. The larger tank is part of a continuously operated deaeration system described in Appendix A, "Water Deaeration." The partially deaerated water is pumped from the bottom of the larger tank to an elevated constant-level tank just out of view at the upper left corner of figure 1.

The horizontal pipe across the upper part of figure 1 supplies water through a calibrated elbow meter and inflow control valve to the model head box. This water flows from the model head box through the raw-water supply channel (figure 3) and through two inlet ports into mixing channel 1.

Mixing channel 1 contains 7 reel-type flocculators with 4 paddles each. Mixing channels 2, 3 and 4 have 8 reel-type flocculators with 2 paddles each. This type of slow mix equipment is often called paddle flocculators. The term paddle flocculator is used throughout this report.

After flowing through the four end around mixing channels the water passes through the slotted baffle wall (figures 2 and 3) into the upper settling basin. The slotted wall contains six vertical slots in bays one through eight and five slots in bay nine for a total of 53. Figure 5 shows the location and prototype dimensions of the slots.

After passing through the slotted baffle wall (figure 2) the water in the upper settling basin flows from left to right. At the right end of the model the water passes through large floor openings in each bay (figure 3) to the lower settling basin. In the lower settling basin (figures 2 and 4) the flow is from right to left. The water leaves the lower settling basin at the left end wall through the five (1, 2, 3, 4 and 5) outlet ports shown in figure 6 and enters the settled water collector. The settled water collector terminated at the model outlet (figure 1) where an adjustable overflow gate was used to establish the desired water level in the upper settling basin. The water level elevation was determined within 0.001 ft using a standard hook gage installed in a stilling well.

Although settling basin number 4 was not modeled its discharge was simulated. The simulated discharge was measured with a calibrated elbow meter and it entered the upstream end of the settled water collector shown in figure 3.

## EVALUATION OF MODEL PERFORMANCE

The performance of the model was evaluated by making slug tracer studies, obtaining velocity distributions in the upper settling basin with a specially developed velocity meter and taking time-lapse photographs from above the model of the advance of dye in the upper settling basin.

A test began by establishing the flow rate to the settling basin, the simulated flow rate from settling basin number 4 and the water surface elevation in the upper settling basin. After these items were established the model was permitted to run for a sufficient amount of time to insure flow establishment and a constant water temperature in the model. All the paddle flocculators in each mixing channel, (figure 1), were operating and rotating in a counter-clockwise direction with respect to the equipment gallery (figure 3), unless otherwise indicated.

### Slug Tracer Studies

Lithium was selected for the tracer because it does not react with the other chemicals in the laboratory water, and is conveniently determined in tracer samples by atomic absorption. A typical dose of 1.96 grams of lithium was obtained by

dissolving the proper amount of lithium nitrate in deionized water to make 400 ml of solution. This quantity of lithium results in maximum concentrations of approximately 1 mg/1 at the outlet sampling points.

The 400 ml tracer dose was added in about eight seconds to the flow immediately upstream of the metering section in the raw-water supply channel supplying the settling basin. Mixing of the tracer dose with the water supply took place very quickly.

Discrete samples were taken systematically at each of the outlet ports (figure 3) from the lower settling basin, at the water supply inlet to the model, and at the overflow weir at the model outlet. The sampling tube at each outlet port was purged for five to ten seconds immediately before filling a 25 ml test tube. The fastest sampling cycle was 2.5 minutes for five outlet ports and 4.5 minutes for nine outlet ports.

Curves of relative concentration. $c/C_0$, versus relative time $t/T$ , were developed for each or the outlet ports from the lower°settling basin, and for the overflow from the settled water collector. The reference concentration, $C_0$, in mg/1 is the weight of tracer added divided by the water volume of the settling basin. The reference time, $T_0$, in minutes is the water volume of the settling basin divided by the flow rate through the settling basin. The tracer concentration, c, in mg/1 is the concentration of the sample taken at time t. The time, t, in minutes is the time that had elapsed since adding the slug tracer.

Each concentration-time curve may be described by several points on the curve and by several parameters obtained by mathematical manipulation of the curve. Points on the curve are the initial appearance of tracer ($c = 0$, $t = t_i$) and the peak ($c = c_p$, $t = t_p$ ). The curve end point (theoretically $c = 0$, $t$ ) is hard to locate experimentally. However the concentration is nearly zero when the test is terminated after approximately 2.8 detention times.

The time to the peak concentration is one measure of the center of the curve. Two other times also locate the "center" of the distribution. The time at which one half of the recovered tracer has passed the sampling point is called t50. This is determined from the cumulative integral of the distribution. The time to the center of gravity of the distribution curve, $t_{cg}$, is found by taking moments about the axis $t = 0$. In statistics, $t_p$ is the mode, $t_{50}$ is the median, and t is the mean. Figure 7a shows these times in proper relation for a typical tracer curve.

The width or spread of the tracer curve is quantified in the standard deviation, s, or the Morril Index, M.I. The standard deviation is defined by

$$s = [\int_o^\infty c(t)\ (t-t_{cg})^2\ dt/\int_o^\infty c(t)dt]^{1/2} \qquad (1)$$

The Morril Index is the ratio of the time for 90 percent of the tracer to pass to the time for 10 percent of the tracer to pass, or $t_{90}/t_{10}$. The Morril Index correlates quite well with the standard deviation. Since it is commonly used in tracer studies of water treatment processes, the Morril Index is the measure of spread that will be reported.

The skewness or asymmetry of the curve should be included in the numerical description of the tracer distribution. However, Naor and Shinnar3 report that skewness has been found to not be characteristic of the physical properties of the system. Consequently no skewness parameters will be reported.

A computer program written in FORTRAN IV was used to reduce the raw data from the recorder charts of absorption values from the atomic absorption spectrophotometer. The program also computed various parameters describing the tracer distribution, and in its final version plotted the $c/C_o$ versus $t/T_o$ curves.

Several theoretical processes are applied to determine the function of a flow system by tracer tests. Plug flow occurs if all the fluid and tracer move through the system at the local mean velocity. In this case a slug of tracer introduced at the inlet at t = o would appear at the outlet at $t = T_o$. The shape of the slug distribution curve would be a narrow spike with the same width as if the sample were taken just downstream of the introduction point. Two modifications can be made to the plug flow case. If there is "dead space", the effective flow velocity is higher than the design value and the slug will reach the outlet at $t<T$ . The second addition to the plug flow case is to consider diffusion by fluid turbulence. This will result in a wider and lower peaked tracer distribution at the outlet. The tracer distribution would be symmetric with mean time $t_{cg} = T_o$ and would have a Gaussian or normal shape. Dead space may be estimated by methods which are described in the discussion of the outlet tracer curves. Diffusion is very difficult to determine, especially in systems with several components like the settling basin of this study. Similar in effect but generally several times more important is dispersion resulting from non-uniform velocity distribution. This is not predictable and often masks the turbulent diffusion.

Perfect or complete mixing is another theoretical concept applied to settling basin analysis. In perfect mixing, the tracer is completely mixed with the fluid volume in the basin at the instant the tracer is introduced. From this initial

concentration, equal to C , the tracer concentration remaining in the basin at any time, t, is given by $c/C_0 = \exp(-t/T_0)$. The perfect mixing equation can be modified for dead space, short circuiting, or plug flow. A further discussion of the modified perfect mixing equations is included in the section on outlet tracer curves.

*Tracer Curves at Outlet Ports.* Curves of relative concentration, $c/C_0$, versus relative time $t/T_0$, for each outlet port were plotted on a single graph for each slug tracer test. For tests with nine ports, the curves for the five original ports are on one graph and the curves for the four added ports are on a second graph. These graphs permit direct comparison of the tracer distribution at the outlet ports from the lower settling basin. The time of initial detection of tracer and the concentration value and time of the peak are important points on these curves. Computed parameters useful for the port tracer distributions are time to center of gravity, time for 50 percent, and Morril Index, $t_{90}/t_{10}$. The area under each curve is significant, but can not be used except in a comparative way for a given test because flow rates through each outlet port were not obtainable. This also prevents direct comparison between tracer distributions at the settling basin outlets and the distribution at the outlet from the settled water collector channel.

*Tracer Curve at Model Outlet.* Tracer samples collected at the overflow weir define a relative concentration versus relative time curve that is affected by flow in the entire model. This is the tracer distribution reported in most investigations of settling basins by tracer tests. Thus, comparison with other work may be made.

In addition to the parameters described previously, several quantities may be obtained for the outlet tracer distributions. Since the flow rate over the weir is known, the tracer recovery ratio may be calculated. The amount of tracer passing the outlet divided by the amount of tracer in the initial slug is the recovery ratio. A value of 1.0 would indicate complete recovery of the tracer.

Rebhun and Argaman[4] used a modified equation of perfect mixing to analyze settling basin performance. In a discussion of this paper, El-Baroudi[5] suggested fitting the recession part of the distribution itself instead of fitting $1 - \int_0^t c/C_0 \, d(t/T_0)$ The assumed distribution is:

$$c/C_0 \ (t/T_0) = 0, \text{ for } 0 < t/T_0 < \Theta \qquad (2)$$

and

$$c/C_o\ (t/T_o) = a \exp\ [-a(t/T_o - \theta)],\ \text{for}\ \theta < t/T_o < \infty \qquad (3)$$

where $a = 1/[(1-p)\ (1-m)]$
$\theta = p(1-m)$, true plug flow fraction
$p$ = plug flow fraction
$m$ = dead space fraction.

This is physically equivalent to plug flow for the time between zero and $\theta = p(1-m)$ followed by perfectly mixed flow for time after the initial arrival of tracer at the outlet at time $\theta$ with concentration $a = 1/[(1-p)(1-m)]$. The parameters, a, $\theta$, p, m were determined from a straight line fit by eye to plots of log $(c/C_o)$ versus $t/T_o$. A typical plot is given in figure 7b. Note that the data are represented by the straight line only for times larger than 0 and that the rising portion of the curve is not approximated.

Velocity Distribution

A velocity meter described in Appendix B was used to measure the point velocities at various locations in the upper settling basin. The velocity meter output signal was recorded on a Sargent Recorder, Model SRG. Point velocities were determined from the calibration curve given in figure B7.

Preliminary velocity distribution data were collected from the upper settling basin in order to select the sections for collecting the velocity data. Also at this time the approximate locations in the verticals where the point velocity data should be collected were selected. It was observed that velocity data could not be collected with the velocity meter between column rows H and G, figure 3, due to excessive turbulent velocity fluctuations. From dye tests it was observed that the streamlines after column row B are in general curved and follow a downward trend. Thus it was decided to collect the velocity data between the column rows G and F, E and D, and C and B respectively designated as Section 1, Section 2 and Section 3, figure 3.

The preliminary velocity distribution data indicated that sufficient information would be available if data were collected at four points in each vertical. These verticals were located at the middle of each bay. For a few of the tests, especially with the slotted screens of Modification 11, velocity distribution data were collected for five points in each vertical.

Flow velocity was equal to zero at all the wetted perimeters and visual observation of floating particles indicated that the flow velocity was also zero at the water surface.

***Data Collection.*** Some precautions were carried out in order to be sure that the data collected with the velocity meter

were representative and correct. Every day before inserting the velocity meter inside the model it was set in a rectangular box full of freshly deaerated water and the temperature and the output signal for zero velocity were recorded. The temperature of the deaerated water was kept within a range of 24°c to 25°C. Once in a while it was required to make an adjustment so that for a velocity equal to zero, the recorder output would equal 10 mv as shown on the calibration curve, figure B7. This was a check on the repeatability of the meter. The same procedures were repeated at the end of the working day to be certain that the velocity meter had worked properly for the duration of the day.

The depth of water at the section where velocity data were collected was measured with a point gage. The velocity meter was supported from an instrument carriage which could be moved both laterally and longitudinally. The meter was inserted in the water and was placed at the desired location in the vertical. The first step was to record the temperature of the water. Next the meter was switched to record the flow velocity and the output signal from the velocity meter was recorded for approximately 25 minutes before the meter was moved to the next position. It must be emphasized that the velocity data thus collected gives the horizontal component of the velocity vector directed downstream. Initially no attempt was made to locate the velocity direction or the magnitude of the maximum output signal at each location. However, a mechanism to rotate the meter and at the same time to read the angle of deviation from a reference line was incorporated in the design of the meter support and this was utilized for subsequent investigation.

The flow in the model settling basin equivalent to a prototype discharge of 60 mgd is turbulent in nature and consequently the velocity distribution at any point in the basin is not constant but a combination of an average velocity and a turbulent component. Thus the output signal indicated a fluctuating velocity about a mean value at each point where velocity data were collected.

*Data Analysis*. In the analysis of the velocity data, the meter output signal recorded on the chart for the first five minutes was discarded. It was reasoned that approximately this time should be allowed for the flow to reestablish around the meter after the meter was moved to each location. Then the chart readings corresponding to 30 second intervals for the next 15 minutes on the chart were tabulated. These 30 chart readings are given in millivolts and the calibration curve must be utilized to convert these readings into the velocity in feet per second. Initially a few sets of these data were analyzed in two different ways. In the first case velocities corresponding to each chart reading at 30 second intervals were read from the calibration curve and a simple average of

these velocities were computed. In the second case a simple average of the 30 data points in millivolts was computed and the average velocity corresponding to this average value was read from the calibration curve. The two average velocities obtained from the same data in the two different ways were compared with each other. The difference between these two velocities was not significant and it was concluded that the average velocity obtained from the simple average of the 30 chart readings would yield a representative velocity at any particular point. This method of obtaining the average velocity at any particular location was followed for all the data collected in the upper settling basin.

Once the average velocity at each point on all the verticals was determined, the average velocity in each vertical was computed. This average velocity computed for each vertical was assumed to be the average velocity in that particular bay. Knowing the average velocity for each bay, the average velocity, V, for that section was computed.

The ratio, v/V, of each point velocity in each section was computed to give a non-dimensional relative velocity for each point. The values of v/V were used to develop contours of equal velocity or isovels for the section.

## Dye Advance in Upper Settling Basin

Time-lapse photography from above the model was used to follow the advance of a dye tracer in the upper settling basin. The color photographs were taken on l6 mm movie film at the rate of one frame per second. The dye tracer used was 250 ml of a saturated solution of potassium permanganate in deionized water.

The dye was added in approximately eight seconds to the flow immediately upstream of the metering section in the raw-water supply channel. A reference clock was started at the beginning of the dye addition. The clock was located in the area photographed to show the elapsed time throughout each dye test.

The location of the dye front at specific relative times was observed on the time-lapse movies. This provides a more generally available record of the dye advance. The dye front location was determined at relative times $t/T_0$ equal to 0.10, 0.12, 0.16, 0.20, 0.21, 0.28, 0.30 and 0.32. The exact time was not determined and the projected image was not scaled so only qualitative comparisons may be made.

Experience showed that the movement of a dye front can be correlated qualitatively with the velocity distribution in the upper settling basin. Therefore, the dye test is a good

qualitative method for evaluating the effect of a modification and determining the modifications for which additional data should be taken.

The permanent recording of the dye movement by time-lapse photography has proven to be an excellent aid in evaluating the effect of modifications. Therefore, the dye front advance plots will be used to indicate the effect of model modifications on flow conditions in the upper settling basin.

## DESCRIPTION OF MODEL MODIFICATIONS

The original model (figure 3) and several modifications were tested. The modification designations and descriptions are given below. The paddle flocculators in each of the four mixing channels were operating normally except as noted. A summary of the model modifications is given in Table 2.

### Modification 0

This is the original model. There were seven paddle flocculators in mixing channel 1 and channels 2, 3 and 4 had eight paddle flocculators in each channel.

### Modification 1

Four turning vanes shown in figure 8 were installed at the end of mixing channel 3 and the beginning of mixing channel 4. Each vane extended vertically from the mixing channel floor to above the water surface. In the prototype each vane would be 4 ft wide and 2 in. thick. The vane spacing would be 3 ft in mixing channel 3 and 4 ft in mixing channel 4. A half-round nose was attached to the vertical end of the wall between mixing channels 3 and 4. Two paddle flocculators one in channel 3 and one in channel 4, were removed for installation of the turning vanes.

### Modification 1-A

This is modification 1 with the addition of a fifth, vane, shown as a dashed line in figure 8, in front of the two slots in the baffle wall.

### Modification 2

Each slotted opening area in the slotted wall at bay 1 was reduced by 20 percent. Modification 1-A was also installed in the model.

Modification 3

Nine turning vanes shown in figure 9 were installed at the end of mixing channel 3 and the beginning of mixing channel 4. Each vane extended vertically from the mixing channel floor to above the water surface. In the prototype each vane would be 4 ft wide and 2 in. thick. The vane spacing would be 1.5 ft in mixing channel 3 and 2 ft in mixing channel 4 except for the vanes close to the paddle shaft, see figure 9. A half-round nose was attached to the vertical end of the wall between mixing channels 3 and 4. The paddle flocculators in channel 4 were not operating.

Note: The turning vanes and half-round nose in Modification 3 were installed for Modifications 4 through 26.

Modification 4

The paddle flocculators were operating in the normal direction in each of the four mixing channels.

Modification 5

Two paddle flocculators immediately downstream from the turning vanes in mixing channel 4 were removed. Therefore, five paddle flocculators were operating in mixing channel 4.

Modification 6

This is Modification 4 with the seven paddle flocculators in mixing channel 4 rotating in the direction reversed from normal operation. The paddle flocculators in channels 1, 2, and 3 were operating in the normal direction.

Note: Modification 7 through 14 had either one, two, or three baffle screens installed in the upper settling basin at the locations shown on figure 10. Each baffle screen was fabricated from woven brass wire cloth with 10 by 10 meshes per lineal inch and an open area of 56.3 percent. Each screen had in each bay across the upper settling basin the slot openings required for clearance of the prototype sludge scrappers. The slot openings extending the full width of the bay were 0.75 feet deep. All three screens had bottom slots above the basin floor but only screens 2 and 3 had upper slots at an elevation of 14.0 ft, prototype. The top elevation

of baffle screen 1 was at 16.0 ft, prototype. Screens 2 and 3 extended above the water surface of the upper settling basin. The bottom elevation of each screen was at the settling basin floor. Each screen extended across the full width of the settling basin.

Modification 7

Baffle screen 1 (figure 10) was installed. The five paddle flocculators of Modification 5 were operating in mixing channel 4.

Modification 8

This is Modification 7 with the installation of baffle screen 2 and seven paddle flocculators were operating in mixing channel 4.

Modification 9

This is Modification 8 with baffle screen 3 installed between screens 1 and 2. Five paddle flocculators were operating in mixing channel 4.

Modification 10

Baffle screens 1, 2, and 3 (figure 10) were installed. The first paddle flocculator immediately downstream from the turning vanes in mixing channel 4 was removed. Therefore, six paddle flocculators were operating in channel 4.

Modification 11

Baffle screens 1, 2, and 3 installed.

Modification 12

Baffle screen 1 was installed.

Modification 13

This is Modification 12 after removing the first paddle flocculator immediately downstream from the turning vanes in Channel 4.

Modification 14

Baffle screens 2 and 3 were installed (figure 10).

Modification 15

Baffle screens 1, 2, and 3 were installed and the slot openings at the settling basin floor in screens 1 and 2 were closed.

Modification 16

A sloping screen was installed at the downstream end of the upper settling basin. The screen was fabricated from woven brass wire cloth with 10 by 10 meshes per lineal inch and an open area of 56.3 percent. The bottom edge of the screen was on the upper settling basin floor at column row A (see figure 3). The top edge of the screen was located at elevation 22 ft, prototype, on the settling basin end wall.

> Note: For Modifications 17 through 21 four additional outlet ports were drilled in the downstream end wall of the lower settling basin. The butterfly valve disk was not modeled for these four outlets. Therefore, the additional outlets were drilled so that the net area of each outlet would be the same as the net open area as an original outlet which has the butterfly valve disk installed. The location and identification of the four additional outlets are shown in figure 6.

Modification 17

The sloping screen of Modification 16 was installed.

Modification 18

The sloping screen of Modification 17 was removed.

Modification 19

Three baffle screens were installed in the upper settling basin at the location shown on figure 10. Each baffle screen was fabricated from woven brass wire cloth with 10 by 10 meshes per lineal inch and an open area of 56.3 percent. Each screen extended from the settling basin floor to above the water surface and across the full width of the upper settling basin.

Modification 20

This is Modification 19 after removal of training walls in the upper settling basin (figure 3).

Modification 21

This is Modification 20 after the removal of three baffle screens in the upper settling basin.

Modification 22

This is Modification 21 with the 4 additional outlet ports closed.

Modification 23

This is Modification 22 after three baffle screens were installed in the upper settling basin at the locations shown in figure 10. The screens were those used for Modification 19.

Modification 24

This is Modification 23 after installing the training walls in the upper settling basin at the locations shown on figure 3.

Modification 25

This is Modification 4 after reducing the slot open area in the slotted baffle wall (figure 5). The area of the original 53 slots in the baffle wall were reduced to one-half of the area of the original slots. The area reduction was made at the center part of each slot. Therefore, there were 106 small openings in the baffle wall. This change in slot open area is in agreement with Kawamura , who recommends less than 5 percent open area. He found good performance with 3 percent open area. The percent open area is 5.2 percent for the original slots and 2.6 percent for the reduced slots. The three baffle screens were removed.

Modification 26

This is Modification 25 after installation of the three baffle screens of Modification 24.

## TEST RESULTS

For all tests, except as noted, the flow had reached steady state with essentially equal discharge through the model and for the simulated basin 4 flow. The water surface elevation was 20.5 ft. Most tests were run for a flow rate of 60 mgd, and most graphs are for tests at this discharge. Quantities are given in either prototype units or dimensionless relative units.

Results of evaluation of the hydraulic performance of the model settling basin are given in three sections. First the effects of the 26 model modifications are described in terms of slug tracer tests, velocity distributions and dye advance patterns. Velocity data or slug tracer results were not obtained for all modifications because time-lapse photography indicated that more detailed data were not necessary. Where results of one type of test were similar within a group of modifications, graphical results are given only for a typical case.

Tracer results at the model outlet are presented next. The last section describes the three special studies conducted in the model settling basin.

For a description of each modification, see the section on model modifications. Tracer test parameters are defined in the section describing evaluation of model performance by slug tracer tests. Dimensions on the velocity distribution figures are in prototype units. See figure 3 for bay designations and the locations where velocity data were collected.

## Modification 0

*Slug Tracer Tests.* Four lithium tracer tests were made at 60 mgd in the original model. Results from test No. 1 are shown in figure 11. This is typical for the original model. Port 5 has a very high peak concentration. Ports 1 and 4 have intermediate peak concentrations and ports 2 and 3 have low peak concentrations. The irregular pattern is common to many of the tracer concentration-time curves. In the four tests the ratio of highest to lowest peak value ranged from 2.9 to 4.8. Though actual tracer amounts are unknown because the flow rates through the individual ports were not measured, the extreme range of peak concentrations and areas under the curves indicate that the tracer is not uniformly divided among the 5 ports. Morril Index values showed port 3 to have the widest distribution (average M.I. = 2.75), and port 1 to have the narrowest distribution (average M.I. = 2.28). The Morril Index ordered from highest to lowest put the other ports in the sequence 2, 4, 5.

Slug tracer tests were run at discharges of 80 and 100 mgd. Peak concentrations were higher than for 60 mgd, but the order of high or low values was the same. The times to peak were closer to the detention time for the higher discharges than for 60 mgd. The spread of ratios of high to low peak concentrations ranged from 2.3 to 3.3. These values are somewhat lower than the ratios at 60 mgd. The Morril Index showed a trend to narrower distributions with higher discharges. Averages of M.I. for 5 ports were 2.50 for 4 tests at 60 mgd, 2.08 for 2 tests at 80 mgd, and 1.82 for 2 tests at 100 mgd. The variation of

M.I. among the ports was different but no definite pattern was discerned. The higher peak concentration and narrower distribution might be expected at increased discharges and reduced detention times. As there were no substantial changes in tracer results at discharges above 60 mgd, all additional tracer tests were run at 60 mgd.

*Velocity Distribution.* The velocity distributions obtained for Modification 0 at sections 1, 2 and 3 in the upper settling basin (figure 3) are shown in figure 12.

The isovels developed for section 1 are shown in figure 12a. Two distinct cores of flow separated by an area of near zero velocity in bay 2 are present in this section. One high velocity area is in bay 1 and the other large area of high velocity is in bays 4 through 8.

Velocity distribution at section 2 shown in figure 12b also indicates the presence of two cores of high velocity. The low velocity area is in bay 3. In bays 1 and 2 the velocity is high with the largest value in bay 1. Another high velocity area is in bays 4 through 8. A low velocity zone is present across the entire section near the floor.

Figure 12c shows the velocity distribution at section 3. A high velocity area in bays 1 and 2 is evident near the water surface. Another high velocity area is in bays 6 through 9. Between these two high velocity areas a lower velocity area is present in bays 3 and 4. A zone of approximately zero velocity is evident near the floor for the entire width of the section.

The two important flow characteristics present in the unmodified upper settling basin are clearly demonstrated by these three figures. One of the characteristics is the presence of two cells of high velocity flow for the entire length of the upper settling basin. These cells maintained their individual shape with some lateral spreading and with a general shift toward the water surface as they moved in the downstream direction. The other flow characteristic is the absence of any significant flow in bay 2 at section 1. • This indicates that very little flow is coming out into bay 2 through the slotted wall.

These velocity distributions in the upper settling basin are undesirable since they are neither uniform nor balanced. Corrective measures had to be installed to eliminate these cores of flow and thus alter the existing flow pattern in the upper settling basin. The most logical place to initiate these measures was the turn-around corner between the mixing channels 3 and 4.

*Dye Advance.* Figure 13 shows the locations of the dye front for discharges corresponding to 60 mgd and 80 mgd in the prototype. The overall pattern of the dye advance in figure 13b is similar to that in figure 13a. The high velocity area in bay 1 is evident for both discharges. Although the details of the dye fronts are not identical for the two discharges at the same value of $t/T_0$, the general shape and position of the fronts are the same. The dye advance also correlates qualitatively with the overall velocity distribution and emphasizes the effect of velocity distribution on movement of dissolved material in the upper settling basin.

Time-lapse photography could not be used after the dye front reached the downstream end of the upper settling basin and began to enter the lower settling basin. The dye front in the lower settling basin had to be observed through the sides of the model. The relatively diffused dye and shadows from dye remaining in the upper settling basin complicated visual observation. Nevertheless several flow features were evident in all dye tests. Since no modifications, except the modifications with 4 additional outlet ports, affected the dye movement in the lower settling basin the description that follows applies to all modifications. The additional outlet ports only modified the dye pattern after it had passed the lower cross collector.

The dye did not smoothly turn the corner through the floor openings between the upper and lower portions of the settling basin. Instead it dropped through the floor openings and rebounded from the lower floor to fill the entire height of the lower settling basin near column row B, figure 3. The lateral shape of the dye front remained similar to what it had been in the upper settling basin and advanced until it reached the cross collectors, where the beam supporting the upper cross collector causes an abrupt contraction in flow area of the lower settling basin as shown in figure 4. The dye streamed off of this beam and left a clear space under the mixing basin floor. A similar flow pattern was observed at each of the beams beneath the openings at the end of each mixing channel wall.

There is a lower cross collector equipment room which can be located with reference to figures 3 and 4. This lower equipment room has the same width as the equipment gallery and extends from the slotted baffle wall to the wall between mixing channels 3 and 4. An eddy was visible upstream of this equipment room. Behind this equipment room the dye expanded gradually leaving a large dead zone against the settling basin wall. The dye tended to stream from alongside the lower equipment room directly toward outlet port number 5.

## Modification 1

*Slug Tracer Test.* No tracer test was run for Modification 1.

*Veloeity Distribution.* Figure 8 shows the types of model modifications made in the settling basin.

Velocity distribution data were collected at section 1 and the related isovels were developed. The velocity distribution obtained for section 1 showed that a very high velocity cell was concentrated in bay 1. To the left were two more cells but their high velocity points were smaller and the cells extended over a larger area than the cell in bay 1. This was an undesirable velocity distribution at section 1.

Velocity distributions were not obtained at sections 2 and 3 since the velocity data (figures 12a, 12b and 12c) for the model without modification showed that the high velocity cell in bay 1 could be expected to persist for the full length of the upper basin.

The high velocity cell present in bay 1 indicated that this vane arrangement did not prevent an excessive amount of the flow from passing through the baffle wall slots in bay 1.

*Dye Advance.* Since velocity distributions had shown the poor flow conditions for this modification before the time-lapse photography technique was used, dye test results are not presented.

## Modification 1A

*Slug Tracer Test.* Modification 1A reduced the peak concentration at port 1 to a level comparable to the value at ports 2 and 3. Ports 4 and 5 had peak concentrations similar to those for Modification 0. The Morril Index showed that port 1 had the widest distribution, and port 3 had a median width for this condition.

*Velocity Distribution.* The position of the vane at the beginning of mixing channel 4 nearest the baffle wall (figure 8) was not effective in preventing direct flow of the water to the two baffle wall slots of bay 1 adjacent to the outside wall of the model. Therefore, an additional vane, shown as a dotted line in figure 8, was installed in front of the two slots.

The velocity distribution data were collected at sections 1, 2, and 3 for this modification and the isovels for each section were developed. These results are discussed but not presented.

Bay 1 in Section 1 had an area of average velocity and a larger area of less than average velocity. The highest velocity area was in bays 3 and 4.

At section 2 the high velocity area was small and was located in bays 3 and 4. In bays 1 and 2 the velocity was less than average.

Velocity distribution for section 3 showed only one high velocity area that was located in bays 4 and 5 just above mid-depth. Although the overall velocity distribution was better than the distribution obtained for modification 0, the distributions obtained at sections 1 and 2 were not satisfactory.

*Dye Advance.* No dye advance is shown since the velocity distribution indicated poor flow condition.

Modification 2

*Slug Tracer Test.* Tracer distributions at the outlet ports from the lower settling basin were similar to those for Modification 1A.

*Velocity Distribution.* The velocity distribution data were collected at sections 1, 2, and 3 and the corresponding isovels were developed. These results are discussed but not presented.

Bay 1 at section 1 had one small area of average velocity and the remaining area had a velocity well below average. The high velocity area was in bays 3 and 4.

The high velocity area for section 2 was large. It extended over the upper part of bays 3 through 8.

At section 3, there was a high velocity area in bays 4 and 5. Also, there was a small core of higher velocity in bay 2.

Modifications 1-A and 2 did improve the velocity distributions in the upper settling basin when compared to the results obtained for the original model and Modification 1. However, these improvements were still unsatisfactory.

*Dye Advance.* No dye advance is shown since the velocity distribution indicated poor flow conditions.

Modification 3

*Slug Tracer Test.* The peak concentrations for Modification 3 have a pattern similar to that for Modifications 1A and 2. This indicates that turning off the paddle flocculators in the fourth mixing channel cancels the positive effect of the Modification 4 turning vanes.

*Velocity Distribution.* Figures l4a, l4b and 14c show the velocity distributions obtained at sections 1, 2 and 3 respectively.

Figure l4a shows that for section 1 bay 9 has a high velocity area. A second high velocity area is located in bay 4.

Figure l4b shows that the velocity distribution for section 2 has a high velocity area in bay 9 and a smaller high velocity area in bay 4.

At section 3, figure l4c shows the highest velocity area continues to be located in bay 9. A smaller high velocity area is located in bays 4 and 5.

The three velocity distributions show that the highest velocity area persisted in bay 9 for the entire length of the upper settling basin, and this flow condition is unsatisfactory.

These velocity distributions also indicate that when the paddle flocculators in mixing channel 4 were not operating, the high velocity flow from mixing channel 3 to mixing channel 4 traveled very fast along the left hand wall of mixing channel .4 and delivered an excess amount of flow to bay 9. This effectively starved other bays from their share of discharge. Therefore, the paddle flocculators serve dual purposes, they break-up the flow concentration in the mixing channel in addition to their normal purpose of assisting in the formation of floc.

*Dye Advance.* Note the rapid movement in bay 9 that is apparent in figure 15. Without the fourth row of paddle flocculators, dye is moved rapidly along the left wall of mixing channel 4 and out into bay 9.

Modification 4

*Slug Tracer Tests.* Peak concentration values were changed significantly. The peak value at port 5 was reduced approximately 50 percent from that obtained for Modification 0. The peak value at port 1 was also lowered while the peak value at port 3 was

raised. The spread of high to low peaks was reduced to 1.7 in test 14 and 2.1 in test 15. The concentration versus time results for test No. 14 are shown in figure 16. The Morril Index was reduced to an average of 2.27 for 5 ports in both tests of Modification 4. The reduction in M.I. was more at the middle ports (2, 3, 4) than at ports 1 or 5. Nine turning vanes in the bend between mixing channels 3 and 4 result in a significant improvement over the original model.

*Velocity Distribution.* The velocity distributions obtained for Modification 4 at sections 1, 2 and 3 in the upper settling basin are shown in figures 17a, 17b and 17c

Figure 17a shows that at section 1 there is a small area or cell of high velocity in bay 3. A second cell with a smaller velocity is located in bays 6 to 8.

At section 2, figure 17b, there is only one small high velocity area and it is located in bays 3 and 4.

Figure 17c, shows the velocity distribution for section 3 has only one small high velocity area located in bays 3 and 4. This high velocity region has enlarged in area and reduced in magnitude when compared with section 2.

The velocity distributions in figure 17 for Modification 4 show that of the two high velocity cells at section 1 only the cell in bay 3 persisted for the length of the settling basin. Also, the magnitude in this cell became smaller as it increased in size and spread to include parts of bays 3 and 4. These velocity distributions show a marked improvement when compared with those in figure 12 for the original model.

*Dye Advance.* Figure 18 shows the locations of the dye front for discharges corresponding to 60 mgd and 80 mgd in the prototype. The overall pattern of the dye advance in figure 18b is similar to that in figure l8a. The high velocity area is evident in bay 3 for both discharges.

Figures 13 and 18 indicate that performing dye tests at two discharges for determining modification effects is not necessary. Satisfactory comparisons can be made at discharges equivalent to 60 mgd in the prototype.

## Modification 5

*Slug Tracer Test.* No slug tracer test was taken since dye advance observations showed no improvement over Modification 4.

*Velocity Distribution.* Velocity distributions were measured and the isovels were developed for model Modification

5 at sections 1, 2 and 3 in the upper settling basin. These results are discussed but not shown.

At section 1, small areas of high velocity were present in each of bays 5 and 3. At section 2, the area of highest velocity was in bays 5 and 6. The next highest velocity extended over a very small area in bay 8. The next highest area of velocity was in bays 2 and 3.

At section 3, the high velocity areas were located in bays 5 and 6, 8 and in 2 and 3. The highest velocity area was in bays 5 and 6, and the next highest velocity area was in bay 8. The next highest velocity area was in bays 2 and 3. These results were similar to those obtained at section 2.

These velocity distributions indicated that the removal of two paddle flocculators immediately downstream from the vanes in mixing channel *k* were not effective in developing an uniform and balanced velocity distribution in the upper settling basin.

*Dye Advance.* No dye advance plots are shown.

## Modification 6

The dye advance for Modification 6 showed that reversing the direction of rotation of the paddle flocculators in mixing channel *k* would distort the velocity distribution. Random surface currents, indicated by floating particles, were evident for approximately one-third of the surface area in the upper settling basin downstream from the baffle wall. Thus velocity distribution and slug tracer tests were not collected for this modification.

## Modifications 7, 8, 9, and 10

Time-lapse photographs of the dye advance in the upper settling basin were taken for all of these modifications. The dye advances indicated no improvements in the velocity distribution as a direct result of the installation of these various modifications. Hence, no velocity data were collected for any of these modifications. No slug tracer test was made either.

## Modification 11

*Slug Tracer Tests.* Three slug tracer tests were made on this modification. The results of Test 22 are shown in figure 19. The very irregular tracer distribution is' typical of all three tests. Ports 1 and 5 had high peaks, ports 3 and *k* had intermediate peaks, and port 2 had the lowest peak in tests 21 and 22. Test 20 was different with peak concentrations

ranging from highest at port 5, to lowest at port 3. Port 2 had a peak slightly higher than port 3 while ports 1 and 4 had nearly equal peaks midway in value between port 2 and port 5. The ratio of highest to lowest peak averaged 2.5. The Morril Index averaged 2.26 for tests 21 and 22 but averaged 2.63 for Test 20. The width of individual port tracer distributions was wider in test 20 than in tests 21 and 22, except that port 3 had similar Morril Index values in all three tests.

*Velocity Distribution.* As described in the section on Model Modification, Modification 11 consisted of Modification 4 and the addition of three baffle screens downstream of the training walls (figure 10).

Figures 20a, 20b and 20c, show the velocity distributions obtained at sections 1, 2 and 3 respectively.

Figure 20a shows for section 1 a relatively high velocity area near the basin floor extending across the basin. The peak velocity of this area is located in bays 4 through 6. This concentration of high velocity is associated with the slot openings in the baffle screens. These slots are required for clearance of the sludge scrappers. There are two slots in the baffle screens for each bay and the vertical positions for the slots are indicated on figure 20a. Also, section 1 is only one-half of a bay downstream from baffle screen 2, figure 10. The second highest velocity area located in bay 3 is small.

Figure 20b shows that for section 2 the highest velocity area is in bays 5 and 6. An area of zero velocity near the water surface extends across the settling basin width.

At section 3, figure 20c shows the highest velocity area is across bays 5, 6, 7, 8 and into bay 9. The area of zero velocity near the water surface is located in bays 5 through 9. This area of zero velocity is about one-half of that shown for section 2, figure 20b.

Presence of the high velocity zone close to the basin floor at section 1 would prevent the normal settling of the setteable particles in the upper settling basin.

*Dye Advance.* The dye advance for this modification is shown in figure 21. The wavey front at $t/T_0$ equal to 0.20 is the result of dye shooting out along the floor from the slots in the screens. In comparison to modification 4, figure 18, the dye front is not peaked in bay 3, and is generally smoother in appearance. The slightly earlier arrival at the end of the settling basin is a result of the dye moving along the floor.

## Modification 12

*Dye Advance.* Visual observation and time lapse dye advance

photographs indicated the presence of high velocity flow near the bottom slot and also above the baffle screen. This made it unnecessary to collect any velocity distribution in the upper settling basin. Also, no tracer test was made.

## Modification 13

Plow distribution was similar to that observed for Modification 12, therefore velocity data were not collected and no tracer test was made.

## Modification 14

*Slug Tracer Test.* Modification 14 gave tracer results not much different from those for Modification 11.

*Velocity Distribution.* Velocity distributions at sections 1, 2 and 3 were obtained and the respective isovels were developed. These results are discussed but not presented.

For section 1 a relatively high velocity area near the basin floor extended across the basin. The peak velocity area located in bays 4 through 6 was very narrow. This high velocity area was very similar to that obtained at section 1, figure 20a, for Modification 11.

At section 2 the highest velocity area was in bays 4 and 5.

For section 3, the highest velocity area shifted to bays 5 and 6. The next highest velocity areas occurred in bay 1 and in bays 8 and 9. An area of zero velocity near the water surface was located in bays 8 and 9.

Presence of the high velocity zone close to the floor at section 1 would prevent the normal settling of the settleable particles in the upper settling basin.

*Dye Advance.* Two screens as in Modification 14 were less effective than the three screens were for Modification 11.

## Modification 15

*Slug Tracer Test.* The results of a tracer test on Modification 15 were similar to those for Modification 11 and 14.

*Velocity Distribution.* Isovels were developed from the velocity data obtained at sections 1, 2, and 3. The results are discussed but not presented.

For section 1 a relatively high velocity area extended across the basin at the level of the slot openings in the baffle screens. The peak velocity of this area was located in bay 5. Two other smaller peak velocities were located in bays 3 and 9. An area of zero velocity near the basin floor extended across bays 1 through 7. This zero velocity area was associated with the closing of the slot openings at the bottom of the baffle screens.

For section 2 the highest velocity area was in bay 4. Also, a smaller peak velocity was located in bays 8 and 9. These peak velocities were smaller than the peak velocity obtained at section 1.

At section 3, the highest velocity area was in bays 8 and 9. The next highest peak velocity was located in bay 4.

These velocity distributions showed the high velocity areas at each section were at approximately the elevation of the slot openings in the baffle screens for the length of the upper settling basin. The flow adjusted itself from three high velocity areas at section 1 to two high velocity areas at section 2 and section 3. The existence of two high velocity areas was undesirable, therefore these velocity distributions were not an improvement when compared with the distributions obtained for Modification 4, figure 17.

*Dye Advance.* The blocked bottom slots in the screens did not produce improved flow conditions in comparison with Modification 4.

Modification 16

*Slug Tracer Tests.* Concentration distributions for one of two slug tracer tests of this modification are shown in figure 22. The other test had a ratio of highest to lowest peak value of 3.6, which is much higher than the ratio 1.7 for test 26. The Morril Index for both tests was similar to that for Modification 4.

*Velocity Distribution.* Figures 23a and 23b show the velocity distributions obtained at section 1 and 3 respectively. The velocity distribution was not obtained at section 2.

Figure 23a shows that at Section 1 the highest velocity area is in bays 3 and 4. The next highest velocity area is in bay 8.

Figure 23b shows the velocity distribution for section 3 has only one small high velocity area located in bay 4.

These two velocity distributions are similar in many

respects to the distributions obtained for Modification 4, figure 17, therefore the velocity distribution for section 2 was not obtained.

The sloping screen did not improve the flow distribution in the upper settling basin when compared with that obtained for Modification 4.

*Dye Advance.* Figure 24 shows the locations of the dye front for a discharge corresponding to 60 mgd in the prototype. The overall pattern of the dye advance although differing in detail, is similar to that obtained for Modification 4, figure 18a.

## Modification 17

*Slug Tracer Test.* The original 5 ports had tracer distribution graphs similar to those for Modification 16. The 4 new outlet ports had higher peak concentrations, but similar Morril Index values.

*Dye Advance.* The overall pattern of the dye advance is similar to that obtained for Modification 16, figure 24. Thus velocity data were not collected.

## Modification 18

*Slug Tracer Test.* This is Modification 4 with the 4 additional outlet ports from the lower settling basin. Tracer distributions for Test 30 are shown in figure 25a for ports 1, 2, 3, 4, 5 and in figure 25b for ports 1-2, 2-3, 3-4, 4-5. Peak concentrations at the new ports were higher than at adjacent original ports. The time to peak was generally later for the original ports than for the additional ones. Ratios of high to low peaks were 1.9 for 5 ports and 3.0 for 9 ports. Morril Index values were not unusual with a 5 port average of 2.35 and a 9 port average of 2.40. Thus the additional ports have higher, later peaks and slightly wider distributions than the original ports.

*Dye Advance.* Figure 26 shows the locations of the dye front for a discharge corresponding to 60 mgd in the prototype. The overall pattern of the dye advance is similar to that obtained for Modification 16, figure 24, and Modification 17. Consequently no velocity data were collected.

## Modification 19

*Slug Tracer Test.* Figures 27a and 27b show the results of a tracer test. The 5 original ports have a ratio of highest

to lowest peak concentration of 2.5. Addition of the 4 new ports increased this ratio to 2.6. Except for ports 2 and 3 which have low peak values, the peak concentrations are grouped quite closely. Time to peak values show earlier peaks for the new ports than for the original ports. The distribution width was similar to Modification 18, with an average Morril Index of 2.48.

*Dye Advance.* The three full depth screens flattened the dye front in bays 3 and 4. Compare figure 28, Modification 19, with figure 26, Modification 18. No velocity distribution was taken for this modification.

Modification 20

*Slug Tracer Test.* The ratio of peak concentration was 4.5 and the Morril Index showed relatively wide tracer distributions with an average value of 2.54.

*Dye Advance.* Removal of the training walls had no effect on dye movement, see figures 29 and 28. Velocity distributions were not taken.

Modification 21

*Slug Tracer Test.* Results of a slug tracer test were similar to those for Modification 20.

*Dye Advance.* The effect of the training walls is shown clearly in figure 30. Note the slow moving areas in bays 1 and 9. The screens had corrected for the lack of training walls in Modification 20. See figure 29. Velocity data were not collected.

Modification 22

*Dye Advance.* The return to 5 outlet ports had no detectable effect on flow in the upper settling basin. The difference between figure 31, Modification 22, and figure 30, Modification 21, are probably test to test variations. The dead zone in bay 1 is clearly shown in figure 31. Neither a tracer test nor a velocity distribution was taken.

Modification 23

*Slug Tracer Test.* Tracer distributions at the outlet ports from the lower settling basin were similar to those for Modifications 20 and 21.

*Dye Advance.* A dye front plot is not shown for this case since it is essentially the same as the plot for Modification 20 in figure 29. Thus velocity data were not collected.

## Modification 24

*Slug Tracer Test.* This is Modification 4 with 3 full depth screen grids in the upper settling basin. Tracer test results are given in figure 32. The ratio of highest to lowest peak concentration is 6.0, the largest value for this ratio in any test. The average Morril Index is 2.60, almost the same as for Modification 23, which differs only by not having training walls.

*Velocity Distribution.* Figures 33a, 33b and 33c show the velocity distribution at sections 1, 2, and 3 respectively.

Velocity distribution for section 1, figure 33a indicates the presence of a reasonably well balanced velocity distribution about the center of the upper settling basin. A small zone of high velocity, v/V = 1.5, is located in bays 2 through 9. Except for this localization of high velocity, the overall velocity distribution is much better than the velocity distribution obtained at this section for other modifications.

Figure 33b, shows the velocity distribution obtained at section 2. The highest velocity, v/V = 2.0, is located near the water surface in bays 4, 5 and 6. Overall velocity distribution appears to be good.

Figure 33c shows the velocity distribution obtained at Section 3. This velocity distribution is symmetrically distributed about the center of the upper settling basin. Concentration of high velocity zones are absent and the vertical velocity distributions from bays 2 to 8 appear to be almost identical. Presence of the settling basin sidewalls modified the vertical velocity distribution in bays 1 and 9. But still these velocity distributions are quite similar.

The velocity distributions for Modification 24 are better distributions than those obtained for any of the previous modifications.

*Dye Advance.* Figure 34 shows the dye front locations for this modification. The full depth screens result in a pattern similar to that for Modification 20 in figure 29.

## Modification 25

*Slug Tracer Test.* Tracer distributions for this modification are shown in figure 35. With the open area in the slotted baffle

wall reduced to 50 percent of the original, the ratio of extreme peak concentrations was 2.9. Port 5 had a very high peak as it did for Modification 24, but the lowest peak at port 2 was nearly twice what it was for Modification 24. The average Morril Index was 2.30, about the same as for Modification 4.

*Velocity Distribution.* Figures 36a, 36b and 36c show the velocity distribution at sections 1, 2 and 3 respectively.

The velocity distribution at section 1, figure 36a, indicates the presence of two horizontal cores of flow separated by a zero velocity area. This zero velocity area is located at about one-quarter depth above the settling basin floor. Below the zero velocity area the flow velocity is directed in the upstream direction as shown with negative sign in figure 36a. The reverse flow area above the basin floor at this section is the direct result of the modifications installed in the slotted baffle wall. The slot areas were reduced by 50 percent and as a result the average jet velocity from the slots was increased by 100 percent. The entrainment of the surrounding water by the high velocity jets initiated the reverse flow zone near the basin floor. However, this reverse flow area may be beneficial in the sludge removal operation in the upper settling basin.

Two high velocity areas above the zero velocity zone are located in bays 4 and 5 and in bay 9.

Figure 36b shows the velocity distribution at section 2. The highest velocity area is located in bay 3. The next highest velocity area is located in bay 9. It appears that these two high velocity areas correspond to the two high velocity areas present at section 1, figure 36a. The zero velocity areas are located near the basin floor in bays 1, 2 and 3 and also in bays 6 and 7.

Figure 36c shows the velocity distribution at section 3. The two high velocity areas present at section 1 and 2 are still present at this section. However these high velocity areas have expanded and also diminished in magnitude. The highest velocity area, $v/V = 1.5$, is now located in bays 3 and 4. The next highest velocity area, $v/V = 1.25$, is located in bays 2, 3, 4, 5 and 6 and also in bays 8 and 9.

*Dye Advance.* Without screens, a more uneven dye front pattern is visible in figure 37. This should be compared with Modification 4 in figure 18. Modification 25 shows improvement, especially in bay 9.

## Modification 26

*Slug Tracer Test.* This modification combines the full depth screen grids and the reduced port area in the slotted baffle wall. Figure 38 presents the tracer results for this modification. The ratio of highest to lowest peak concentration is 3.6. Ports 1 and 5 have high peak concentrations while ports 2, 3, 4 have low peaks. This is similar to the results for Modification 25, the other case with the changed baffle wall. The average Morril Index is 2.49. The full depth screens tend to increase the width of the tracer distributions.

*Velocity Distribution.* No velocity data were collected for this modification since time lapse photographs of the dye advance indicated the flow pattern to be similar to that present for Modification 24, figure 34.

*Dye Advance.* The full depth screens smooth the dye front. Delay or retardation of flow can also be observed by comparing figure 39 with figure 37. This effect is more striking between Modifications 20 and 21 than between Modifications 24 and 25. See figures 29 and 30.

## Tracer Results at Model Outlet

Table 3 summarizes various parameter values for outlet tracer distributions. Data are given for 25 of 38 lithium tracer tests. For a prototype discharge of 60 mgd the tests listed are those for which other results are discussed in this report. Four tests of the original model at discharges of 80 and 100 mgd are included to show the effect of flow rates above the design value of 60 mgd.

*Original Model, $Q_p$ = 60, 80, 100 mgd.* Discharge did effect the time to peak, peak concentration and Morril Index. Average time to peak was 0.637 for 60 mgd, 0.780 for 80 mgd and 0.850 for 100 mgd. The average Morril Index was 2.4l at 60 mgd, 1.99 at 80 mgd and 1.76 at 100 mgd. Average peak concentration was 0.753 at 60 mgd, 0.783 at 80 mgd, 0.850 at 100 mgd. The time to center of gravity did not show a trend with discharge. The plug flow fraction also varied with discharge. It averaged 0.64 at 60 mgd, 0.76 at 80 mgd, and 0.82 at 100 mgd. The dead space fraction did not vary with discharge .

The tracer distribution became narrower with a higher peak concentration occurring at a later time as the discharge increased. The constant time to center of gravity suggests an adjustment in velocity distribution and turbulent mixing but no change in dead space.

*Modified Model, $Q_p$ = 60 mgd.* Five typical outlet tracer curves are shown in Fig. 40. Tests 2 and 15 were selected to show results for Modifications 0 and 4, respectively. Test 22, Modification 11, shows a high peak concentration. Test 30, Modification 18, shows a distribution with a high Morril Index. Test 27, Modification 16, has a low peak concentration.

The recovery ratio ranged from 0.69 to 0.88 with a median of 0.8l. Peak concentrations ranged from 0.647 at $t/T_0$ = 0.663 to 0.989 at $t/T_0$ = 0.663 with a median of 0.752 at $t/T_0$ = 0.662. The similarity of times to these three peak values is fortuitous as is shown by the peak concentrations at the extreme and median times to peak. The range of time to peak is from 0.580 with a peak of 0.712 to O.763 with a peak of 0.832. The median time to peak is 0.667 with a peak of 0.839.

The time to center of gravity ranged from a high of 1.023 to a low of 0.845 with a median of 0.910. The Morril Index ranged from 2.06 to 2.59 with a median of 2.35.

Two parameters defined by Rebhun and Argaman[4] are the plug flow fraction and the dead space fraction. The dead space fraction ranged from -0.08 to 0.l4. Negative values have dubious physical interpretation but are a result of the curve fit. The median value for the dead space fraction is 0.04 which is close to an estimate of 0.05 to 0.07 from settling basin geometry. The plug flow fraction ranged from 0.56 to 0.71 with a median value of 0.64. This is close to the median time to peak. Such agreement would be expected from the method of determining the plug flow fraction.

Unfortunately the main result of the analysis of tracer distribution curves at the model outlet is that they are not sensitive to the types of modifications tried in this study. The recovery ratio reflects the finite sampling time and may have been affected by the base line determination. All parameters indicate a reasonably good performance for the original configuration. Modification 4 shows some improvement though other types of tests are more informative. None of the other modifications appear to cause a definite change in outlet tracer distribution.

## Special Studies

Several tests were made to investigate particular types of information not obtained by the usual methods of evaluation. Results are reported for (1) dispersion in a slug tracer test, (2) a step change in flow rate, and (3) velocity fluctuations in the upper settling basin.

*Dispersion Test.* Use of the diffusion equation is theoretically most attractive but its use is limited by practical

difficulties. Empirical dispersion coefficients vary widely and can be obtained from tracer tests only if the tracer distribution is measured at two or more locations. For settling basins the supply conduit, flocculation basin, settling basin proper, and settled water collector all have different dispersion coefficients. This would require obtaining tracer distributions at a number of locations and might not separate the significant effects of inlet and outlet devices.

A slug tracer test was designed to yield data useful in determining dispersion coefficients. A sampling tube was installed in the center of the turn from mixing channel 1 to mixing channel 2. Another sampling tube was installed just upstream from the turning vanes in mixing channel 3. Both tubes were at mid-depth and pointed into the flow. For this test the tracer distribution was measured at these two places in the mixing basin and at the model outlet.

McQuivey and Keefer[7] give the defining equation for the longitudinal dispersion coefficients.

$$D_x = (\bar{V}^3/2)\ (s_2^2 - s_1^2) \ /\ (x_2 - x_1) \qquad (4)$$

where

$D_x$ = longitudinal dispersion coefficient
$\bar{V}$ = mean velocity
$s^2$ = variance of tracer distribution
$x$ = longitudinal coordinate, positive downstream
2,1 = denote downstream and upstream tracer distributions

Application of this formula to the data for mixing channels 1 and 3 resulted in $D_x = 0.00957\ ft^2/sec$ in the mixing channels. This value of $D_x$ was used to determine $s^2$ half way along mixing channel 4 for use as $s_1^2$ in determining $D_x$ in the settling basin The value of $D_x$ in the settling basin was found to be $0.0116\ ft^2$ / sec. Note that this value includes effects of the slotted baffle wall, the passage from upper to lower settling basin, the outlet valves, and the settled water collector.

The tracer distribution at each of the three locations is shown in figure 4l. Local values of $T_0$ and $C_0$ are used to provide easy comparison of the shape of the distributions. The tracer distribution at the end of mixing channel 1 includes the effects of tracer introduction, mixing in the metering section of the raw water supply channel, entering the mixing basin, and cross mixing by one row of flocculators. Time to peak is O.986 and time to center of gravity is 1.087. This indicates arrival very close to theoretical and a slightly skewed distribution. The Morril Index is 1.86.

From mixing channel 1 to the end of mixing channel 3 the tracer flows through two channels, each with flocculators. Time to peak is 0.994 and time to center of gravity is 1.059. Plow time is closer to theoretical than at the end of mixing channel 1. The Morril Index is 1.42. The cross mixing by the flocculators has made the tracer distribution relatively narrower during flow through the mixing channels.

At the model outlet the time to peak is 0.662 and the time to center of gravity is 0.960. The Morril Index is 2.30. These values are similar to those reported for other outlet tracer distributions, see table 3. This distribution is quite different from the two distributions obtained in the mixing channels. The time to center of gravity is earlier and in agreement with dead space estimates. The much earlier time to peak suggests short circuiting in the settling basin. The wider distribution indicated by the Morril Index is expected after longer times and distances from tracer introduction.

*Unsteady Flow Dye Tests.* The low lift pumps providing head for flow through the CWFP are operated to give step changes in inflow rates to the settling basins. The change in flow rate may be 12.5 mgd per basin (one 200 mgd pump) or 20 mgd per basin (one 320 mgd pump). This is a large proportion of typical flows of 40 to 60 mgd per basin. During the time the flow through the settling basin is adjusting to the new inflow rate the settling floc may be disturbed. This could result in passing more turbidity to the filters.

Model testing can determine the nature of hydraulic action during the adjustment to a sudden change in discharge, but cannot ascertain the effect of hydraulic variations on the floc itself. Two types of tests were run with suddenly changed flow rates for Modification 4. The change in water surface elevation with time was recorded. Time-lapse movies were taken with the dye front at two locations in the upper settling basin when the flow was changed. For all tests the tailgate had been set to give a water surface elevation of 20.5 ft in the settling basin for a discharge of 80 mgd in basins 3 and 4. Both discharges were then set at 60 mgd and the water level allowed to stabilize before beginning a test. Note that in the model the inflow rate is set by control valves and the water level is determined by the flow over the outlet weir. The weir discharge relation is probably different from the prototype discharge condition between the settling basins and filters.

With discharges at 60 mgd and the outlet weir set for 80 mgd the water surface elevation was 19.9 ft. The discharge to the model was increased abruptly to approximately 80 mgd. After the water level had stabilized, the simulated discharge from basin 4 was increased to approximately 80 mgd.

Always waiting for equilibrium, the discharges were reduced to approximately 60 mgd, first in basin 4, then in basin 3.

Response to sudden discharge change was instantaneous. In all four steps, equilibrium was reached within 45 minutes, prototype time. The rate of response is indicated by the time in which a percentage of the total water level change took place. The relative water level change reached 40 percent in 5 minutes, 80 percent in 15 minutes, and 90 percent in 25 minutes. Response was the same for increasing or decreasing discharge.

During this test, the velocity meter was in operation at the same longitudinal location in the upper settling basin as the point gages used to measure water levels. No unusual velocity patterns were observed. With the changing flow depth, the mean velocity is nearly the same at 60 and 80 mgd. The velocity change that did occur was not accompanied by high turbulence or surges.

For the time-lapse movies of a dye cloud during a change in discharge the discharge in basin 3 was increased about 1 minute before the discharge in basin 4 was increased. No movies of a decreased discharge were taken. For one test the discharge in basin 3 was increased at $t/T_0 = 0.116$. For the second test the increase was at $t/T_0 = 0.152$. The approximate position of the dye front at these times may be seen in figure 18 which shows the dye advance for Modification 4 at 60 mgd.

No significant change in dye front patterns or dye advance were observed directly or from the films. When the flow was increased at $t/T_0 = 0.116$, the dye was passing through all floor openings at $t/T_0 = 0.28$. When the flow was increased at $t/T_0 = 0.152$, the dye had reached all the floor openings at $t/T_0 = 0.30$. These times are based on $T_0$ for 60 mgd and 19.9 ft water surface elevation. The dye front advances faster after the discharge is increased. Note the position of the dye fronts at $t/T_0 = 0.28$ and 0.30 in figure 18.

*Turbulent Velocity Fluctuations.* Turbulence is a fluid flow phenomenon that causes random fluctuations of the velocity at a point in the flow.

Hinze[8] has defined turbulence in the following way: "Turbulent motion is an irregular condition of flow in which the various quantities show a random variation with time and space coordinates, so that statistically distinct average values can be discerned." The present analysis is primarily concerned with the turbulence that is produced by water flowing through the slots in the slotted baffle wall of the upper settling basin and downstream from the baffle screens.

The momentary value of velocity at a point in a vertical in the settling basin is written as

$$V_1 = v + v' \tag{5}$$

where v is the average flow velocity at the point of measurement and v' is the fluctuating component of the velocity and by definition $\bar{v}' = 0$. Therefore, the absolute value of the fluctuation, i.e., $|\bar{v}'|$ gives a measure of the turbulent motion.

An important parameter of the turbulence is the root-mean-square velocity fluctuation, also known as the standard deviation, is given by

$$\sigma = (\overline{v'^2})^{1/2} \tag{6}$$

where the overbar indicates averaging. This is also called "intensity of turbulence."

The relative intensity of turbulence can then be defined by the ratio,

$$\text{Relative Intensity of turbulence} = \sigma/v \tag{7}$$

Equation 7 was utilized to compute the turbulent velocity fluctuation at section 1 in the upper settling basin.

Modification 4. Velocity data collected in the upper settling basin for all modifications indicated the presence of turbulent flow with varying degrees of turbulent fluctuation. These turbulent fluctuations were more pronounced at section 1, especially for the modifications where no baffle screens were installed.

The relative intensity of turbulence, $\sigma/v$, was computed from velocity data collected at section 1 for Modification 4. Figure 42 shows a plot of relative depth of flow, y/D, versus the relative intensity of turbulence, $\sigma/v$, for Modifications 4 and 24. Data shown are for section 1 only. For Modification 4, the magnitude of the relative intensity of turbulence is always more than 0.2. This indicates the presence of excessive turbulent motion at section 1 for Modification 4. Although the turbulent velocity fluctuations data were not analyzed for Modification 0, the velocity meter output signals indicated the presence of an even more pronounced turbulent motion at section 1.

Modification 24. Velocity data collected from the settling basin for modifications with baffle screens indicated a marked reduction in the turbulent velocity fluctuation. In some instances the velocity meter output signal corresponding to the point velocity remained almost constant with time.

Pigure 42 shows the relationship between relative depth, y/D, and the relative intensity of turbulence, σ/v, for Modification 24, section 1. It appears that the relative intensity of turbulence varies from a minimum value of 0.03 to a maximum value of 0.1 for the relative depth variation of 0.3 to 0.8. However, the values of the relative intensities of turbulence are much higher near the floor and also close to the water surface. The point velocities at these two locations are very small compared to the corresponding average velocity in the vertical. Thus for small fluctuations in turbulent velocity, the magnitude of the relative intensity of turbulence would be expected to increase at these two locations.

A comparison of the values of relative intensities of turbulence for Modifications 4 and 24, figure 42, will indicate that the installation of baffle screens in the settling basin can substantially decrease the turbulent velocity fluctuations.

## CONCLUSIONS AND RECOMMENDATIONS

Several conclusions are drawn from the laboratory studies performed on a scale model of a settling basin in CWFP. Based on these conclusions, recommendations are made for implementation in CWFP. In addition, recommendations for consideration in the design of settling basins in new water treatment plants are presented.

### Conclusions of Model Study

1. Paddle flocculators are installed in the mixing channels to promote flocculation. In addition, they are important to maintain flow distribution and to prevent short circuiting. These two facts can be seen by comparing for Modifications 3 and 4, respectively, figures 14 and 17 for velocity distribution, and figures 15 and 18 for the relative positions of the dye front in the fourth mixing channel. Removal of any paddle flocculators resulted in distorted flow distribution in the upper settling basin. Reversed rotation of the paddle flocculators in mixing channel 4 did not improve the velocity distribution in the upper settling basin.

2. Installing turning vanes in the 180 bend between mixing channels 3 and 4 improved the hydraulic performance of the settling basin. The vanes must be spaced properly. A spacing between the vanes of approximately 0.1 times the mixing channel width was effective for Modification 4, see figure 9.

3. Baffle screens installed in the upper settling basin immediately downstream from the training walls may or may not be advantageous.

The three screens of Modification 11 with open slots required to accommodate sludge removal equipment resulted in a distorted velocity profile. The high velocity zone, shown in figure 20a, near the basin floor would prevent normal settling of settleable particles. Also, the high velocity zone would hinder sludge removal.

The three full depth screens of Modification 24 resulted in a substantially improved velocity distribution, see figure 33, in the upper settling basin when compared with the velocity distributions obtained for other modifications. One or two screens were not as effective as three screens. Installation of three full depth screens in a new treatment plant would require a different arrangement of sludge removal equipment from that commonly used in present day practice.

The three full depth screens substantially decreased the turbulent velocity fluctuations at section 1 in the upper settling basin, see figure 42. This reduction in turbulent velocity fluctuations should increase the removal of settleable particles.

4. An inclined screen installed at the downstream end of the upper settling basin had only local effects. There was no effect on the hydraulic performance of the settling basin.

5. The addition of four outlet ports, shown in figure 6, from the lower settling basin had no discernable effect on the outlet tracer distribution or the velocity distribution in the upper settling basin. However, the velocity and the head loss at the outlets from the lower settling basin are reduced. The reduction in head loss is proportional to $V^2$. Therefore, increasing from 5 to 9 outlet ports will reduce the head loss to approximately one-third of the head loss for 5 outlet ports.

6. Training walls are necessary in a wide settling basin. The dye front locations in figures 30 and 31 for Modifications 21 and 22, respectively, show that the flow distribution was unsatisfactory after removal of the training walls.

7. Reduction of open area in the slotted baffle wall from 5.2 percent to 2.6 percent was beneficial. The flow distribution was improved in the upper settling basin as shown in figures 36 and 37 for Modification 25.

8. Tracer distributions at the outlet ports from the lower settling basin were useful when significant changes in flow pattern resulted from a modification. Since discharge through each port could not be measured, these tracer distributions could not be completely analyzed. Only qualitative interpretations could be made from the outlet port tracer results.

The turning vanes of Modification 4 did reduce the high peak concentration which occurs at port 5 for Modification 0. Compare these two modifications in figures 11 and 16.

The four additional outlet ports had no effect on tracer distributions at the original five ports. Compare figure 25a for Modification 18 with figure 16 for Modification 4.

Screen grids in the upper settling basin had no discernable effect on tracer distributions at the five outlet ports. Figure 27b shows the tracer distribution for the additional four ports for Modification 19. Comparing figure 27b with figure 25b for Modification 18, indicates a reduction of peak concentration at the added ports which is the result of the full depth screens.

9. Slug tracer distributions for the model outlet were not sensitive to the types of modifications investigated. The tracer distributions did provide an indication, see Table 3, of the settling basin performance. However, major changes in the settling basin are required before a definitive indication is obtained from the outlet tracer distribution.

10. Structural geometry that obstructs flow passage has a detrimental effect on hydraulic performance by creating zones of separation or dead space. Dead space was evident upstream and downstream from the lower cross collector equipment room and at the abrupt step of the cross collector beam in the lower settling basin. The constriction of mixing channel 4 by the equipment gallery (figure 3) prevents full utilization of the mixing channel and bay 9 of the upper settling basin.

Recommendations for modifications in the Central Water Filtration Plant

1. Install turning vanes as shown in figure 17 for Modification 4 in the mixing channels of settling basin number 3.

2. Reduce the open area by 50 percent in the slotted baffle wall of settling basin number 3.

3. Four additional outlet butterfly valves from lower settling basin may be installed if head loss reduction is desired.

4. Do not install baffle screens in the upper settling basin since these screens near the training walls interfere with sludge removal.

5. Do not install inclined screen at downstream end of upper settling basin near the floor openings since this has only limited local influence.

6. Prototype tracer and turbidity tests should be conducted before and after any modification is installed. These tests will determine the effect of the modification on settling basin performance.

General recommendations for new settling basins

1. Turning vanes are useful and should be installed at abrupt 90 and 180 degree channel bends.

2. Slotted baffle walls between flocculating and settling basins should have open areas of less than 5 percent.

3. Training walls are necessary and should be installed in wide settling basins.

4. Baffle screens or grids are helpful if they are installed near the upstream end for the full width and depth of the settling basin. A minimum of three screens in series is required. The location of the screens and design of sludge removal equipment must be coordinated.

5. Inclined screens near outlets are not useful.

6. Equipment rooms and other structures should not obstruct flow areas. If significant blockage is unavoidable, hydraulics should be considered and the design should minimize interference with fluid flow paths.

7. Hydraulic model studies can be beneficial and should be conducted prior to final design of distribution channels, settling basins, outlet and inlet sections, and other major elements for large water treatment plants.

## REFERENCES

1. Humphreys, Harold W. 1973. Hydraulic Model Study of A Settling Basin. Presented at 1973 Annual Conference of American Water Works Association and submitted to Journal AWWA for publication.

2. Camp, Thomas R., Sedimentation and the Design of Settling Tanks. Transactions ASCE, 111:895-958 (1946).

3. Naor, Pinhas and Revel Shinnar, "Representation and Evaluation of Residence Time Distributions," I & EC Fundamentals, V. 2, No. 4, November 1963.

4. Rebhun, M. and U. Argaman, "Evaluation of Hydraulic Efficiency of Sedimentation Basins," Proceedings ASCE, V. 91, No SA5, October 1965.

5. El-Baroudi, H. M., Discussion of "Evaluation of Hydraulic Efficiency of Settling Basins" by M. Rebhun and Y. Argaman, Proceedings of ASCE, V. 92, No. SA3, June 1966.

6. Kawamura, Susumu, "Coagulation Considerations," Journal AWWA, June, 1973.

7. McQuivey, R. S. and T. N. Keefer, "Turbulent Diffusion and Dispersion in Open Channel Flow," Stochastic Hydraulics, U. of Pittsburg, 1973.

8. Hinze, J. 0., Turbulence, McGraw-Hill Book Company, Inc., New York, p. 1, 1959.

## NOTATIONS

$C_o$ = tracer reference concentration in milligrams per liter and equal to the ratio of the weight of tracer added to the volume of water in the settling basin

$c$ = tracer concentration of sample in milligrams per liter

$C_p$ = peak concentration in milligrams per liter

$D$ = total depth of flow in feet

$D_x$ = longitudinal dispersion coefficient in square feet per second

$F$ = Froude number expressed as $V/(gD)^{0.5}$, non-dimensional

$g$ = acceleration of gravity in feet per second per second

$L$ = length in feet

$L$ = length ratio, non-dimensional

M.I. = Morril Index expressed as $t_{90}/t_{10}$, non-dimensional

$m$ = dead space fraction in the settling basin, non-dimensional

$p$ = plug flow fraction, non-dimensional

$Q$ = discharge in model as equivalent prototype discharge in million gallons per day, mgd

$s$ = standard deviation in minutes

$T_\circ$ = reference time in minutes equal to the ratio of the water volume of the settling basin to the flow rate through the settling basin

$t$ = time after start of a test in minutes

$t_{cg}$ = time of center of gravity of the concentration plot in minutes

$t_.$ = time of initial appearance of the tracer in the outlet ports in minutes

$t_P$ = time of peak concentration in minutes

$t_{10}$ = time in minutes when 10 percent of the tracer has passed through the settling basin

$t_{50}$ = time in minutes when 50 percent of the tracer has passed through the settling basin

$t_{90}$ = time in minutes when 90 percent of the tracer has passed through the settling basin

$V$ = characteristic velocity in feet per second

$V$ = average velocity at a section in the upper settling basin in feet per second

$v$ = average velocity at a point in the upper settling basin in feet per second

$v'$ = fluctuating component of the velocity at a point in the upper settling basin in feet per second

$v_x$ = instantaneous velocity at a point in the upper settling basin in feet per second

$x$ = longitudinal coordinate in feet

$y$ = vertical distance of a point above the basin floor in feet

$G$ = true plug flow fraction, non-dimensional

$a$ = intensity of turbulence in feet per second

TABLE 1

Prototype to Model Scale Factors

| Quantity in Prototype | To Obtain Quantity in the Model, Multiply by | |
|---|---|---|
| Length | $L_r$ | = 1/24 |
| Area | $L_r^2$ | = 1/576 |
| Volume | $L_r^3$ | = 1/13,824 |
| Time | $L_r^{0.5}$ | = 1/4.90 |
| Velocity | $L_r^{0.5}$ | = 1/4.90 |
| Discharge | $L_r^{2.5}$ | = 1/2,822 |

Table 2

Model Modifications

| Modification | No. of Turning vanes Mixing 3 | Channel 4 | Baffle Screen No. With Slots | Without Slots | Nine Outlet Ports | Channel 4 Paddle Flocculators Operating | Training Walls Removed |
|---|---|---|---|---|---|---|---|
| 0 | 0 | 0 | | | | 8 | |
| 1 | 4 | 4 | | | | 7 | |
| 1-A | 4 | 5 | | | | 7 | |
| 2[1] | 4 | 5 | | | | 7 | |
| 3 | 9 | 9 | | | | 0 | |
| 4 | 9 | 9 | | | | 7 | |
| 5 | 9 | 9 | | | | 5 | |
| 6[2] | 9 | 9 | | | | 7 | |
| 7 | 9 | 9 | 1 | | | 5 | |
| 8 | 9 | 9 | 1,2 | | | 7 | |
| 9 | 9 | 9 | 1,2,3 | | | 5 | |
| 10 | 9 | 9 | 1,2,3 | | | 6 | |
| 11 | 9 | 9 | 1,2,3 | | | 7 | |
| 12 | 9 | 9 | 1 | | | 7 | |
| 13 | 9 | 9 | 1 | | | 6 | |
| 14 | 9 | 9 | 2,3 | | | 7 | |
| 15[3] | 9 | 9 | 1,2,3 | | | 7 | |
| 16[4] | 9 | 9 | | | | 7 | |
| 17[4] | 9 | 9 | | | Yes | 7 | |
| 18 | 9 | 9 | | | Yes | 7 | |
| 19 | 9 | 9 | | 1,2,3 | Yes | 7 | |
| 20 | 9 | 9 | | 1,2,3 | Yes | 7 | Yes |
| 21 | 9 | 9 | | | Yes | 7 | Yes |
| 22 | 9 | 9 | | | | 7 | Yes |
| 23 | 9 | 9 | | 1,2,3 | | 7 | Yes |
| 24 | 9 | 9 | | 1,2,3 | | 7 | |
| 25[5] | 9 | 9 | | | | 7 | |
| 26[5] | 9 | 9 | | 1,2,3 | | 7 | |

Note: 1. Rav 1, slotted opening area reduced 20 percent
2. Reversed rotation of channel A paddle flocculators
3. Screens 2 and 3, slot opening closed at settling basin floor
4. Inclined screen at downstream end of upper settling basin
5. Slotted open area in baffle wall reduced 50 percent

TABLE 3

Tracer Test Results at Model Outlet*

| Modification | Test Number | Prototype** Discharge mgd | Water Temperature °C | Recovery Ratio | Peak Values $c/C_o$ | $t/T_o$ | $t_{cg}/T_o$ | Morril Index $t_{90}/t_{10}$ | Plug Flow Fraction p | Dead Space Fraction m |
|---|---|---|---|---|---|---|---|---|---|---|
| 0 | 1 | 60 | 24.3 | 0.82 | 0.809 | 0.609 | 0.865 | 2.33 | 0.65 | 0.11 |
| 0 | 2 | 60 | 24.1 | 0.81 | 0.768 | 0.612 | 0.845 | 2.26 | 0.68 | 0.14 |
| 0 | 4 | 60 | 24.1 | 0.79 | 0.647 | 0.663 | 0.978 | 2.49 | 0.62 | 0.02 |
| 0 | 5 | 60 | 24.3 | 0.81 | 0.690 | 0.663 | 0.973 | 2.56 | 0.61 | 0.01 |
| 0 | 3 | 80 | 24.6 | 0.82 | 0.844 | 0.812 | 0.971 | 1.83 | 0.81 | 0.00 |
| 0 | 6 | 80 | 25.1 | 0.80 | 0.723 | 0.747 | 0.969 | 2.14 | 0.71 | 0.01 |
| 0 | 7 | 100 | 26.1 | 0.83 | 0.903 | 0.850 | 0.948 | 1.75 | 0.81 | 0.02 |
| 0 | 8 | 100 | 26.7 | 0.75 | 0.798 | 0.851 | 0.908 | 1.77 | 0.82 | 0.01 |
| 3 | 16 | 60 | 23.1 | 0.86 | 0.760 | 0.761 | 1.023 | 2.42 | 0.64 | 0.01 |
| 3 | 17 | 60 | 22.8 | 0.79 | 0.832 | 0.763 | 0.995 | 2.21 | 0.67 | 0.05 |
| 4 | 14 | 60 | 23.4 | 0.81 | 0.771 | 0.709 | 0.960 | 2.38 | 0.61 | 0.00 |
| 4 | 15 | 60 | 23.8 | 0.80 | 0.752 | 0.662 | 0.932 | 2.34 | 0.63 | 0.05 |
| 4 | 36 | 60 | 26.2 | 0.76 | 0.677 | 0.662 | 0.960 | 2.30 | 0.64 | 0.01 |
| 11 | 20 | 60 | 22.1 | 0.73 | 0.728 | 0.714 | 0.952 | 2.25 | 0.62 | 0.01 |
| 11 | 21 | 60 | 22.1 | 0.86 | 0.989 | 0.663 | 0.897 | 2.12 | 0.66 | 0.04 |
| 11 | 22 | 60 | 22.2 | 0.80 | 0.960 | 0.660 | 0.858 | 2.06 | 0.66 | 0.10 |
| 16 | 26 | 60 | 23.8 | 0.76 | 0.749 | 0.652 | 0.941 | 2.56 | 0.59 | 0.05 |
| 16 | 27 | 60 | 26.1 | 0.69 | 0.650 | 0.712 | 0.910 | 2.14 | 0.66 | -0.01 |
| 18 | 30 | 60 | 23.9 | 0.84 | 0.750 | 0.673 | 0.967 | 2.40 | 0.62 | 0.05 |
| 19 | 31 | 60 | 22.6 | 0.88 | 0.783 | 0.673 | 1.016 | 2.57 | 0.56 | -0.08 |

TABLE 3 (continued)

| Modification | Test Number | Prototype** Discharge mgd | Water Temperature °C | Recovery Ratio | Peak Values $c/C_o$ | $t/T_o$ | $t_{cg}/T_o$ | Morril Index $t_{90}/t_{10}$ | Plug Flow Fraction p | Dead Space Fraction m |
|---|---|---|---|---|---|---|---|---|---|---|
| 20 | 32 | 60 | 24.3 | 0.87 | 0.837 | 0.674 | 0.978 | 2.51 | 0.66 | 0.04 |
| 21 | 33 | 60 | 24.5 | 0.77 | 0.712 | 0.580 | 0.962 | 2.59 | 0.56 | 0.04 |
| 24 | 35 | 60 | 26.9 | 0.83 | 0.839 | 0.667 | 0.935 | 2.35 | 0.64 | 0.09 |
| 25 | 38 | 60 | 26.9 | 0.87 | 0.706 | 0.734 | 1.009 | 2.17 | 0.71 | -0.02 |
| 26 | 37 | 60 | 26.0 | 0.78 | 0.727 | 0.694 | 1.009 | 2.54 | 0.59 | -0.03 |

* Upper settling basin water surface elevation equivalent to 20.5 ft in the prototype.

** Model discharge corresponded to prototype discharge listed.

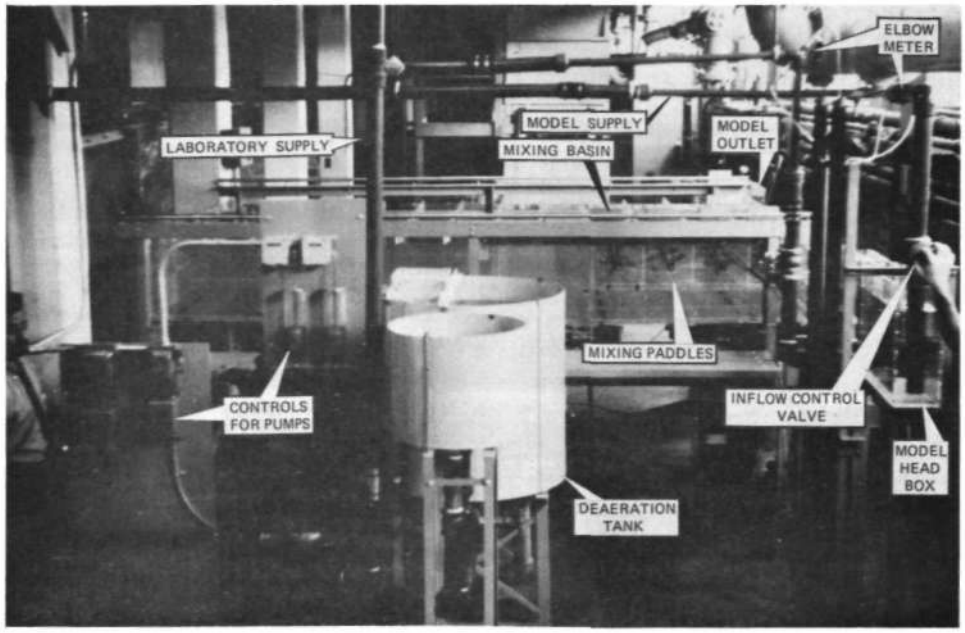


**Figure 1. Equipment for model operation and model inlet**

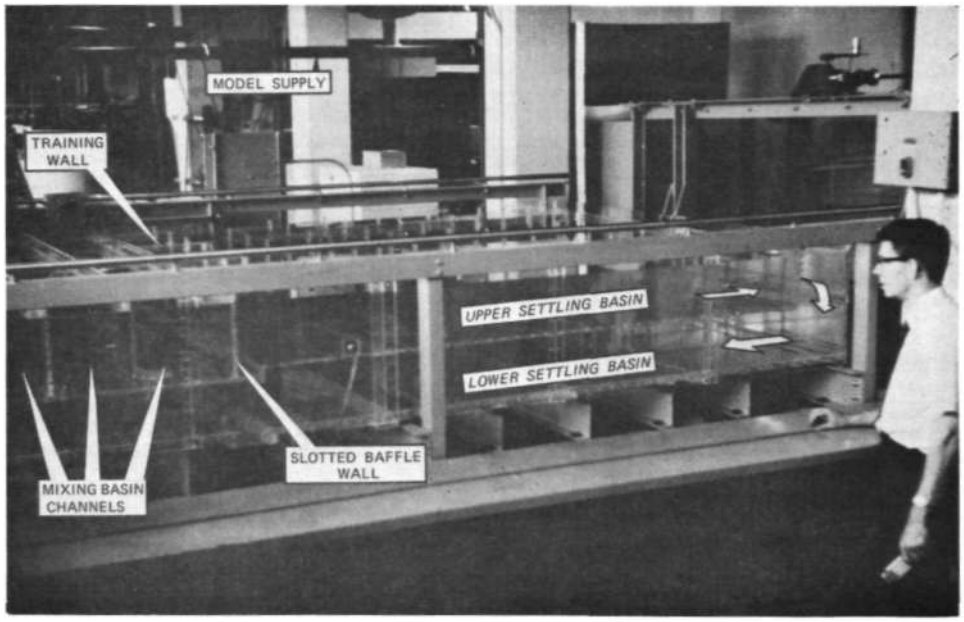


**Figure 2. Side view of upper and lower settling basin**

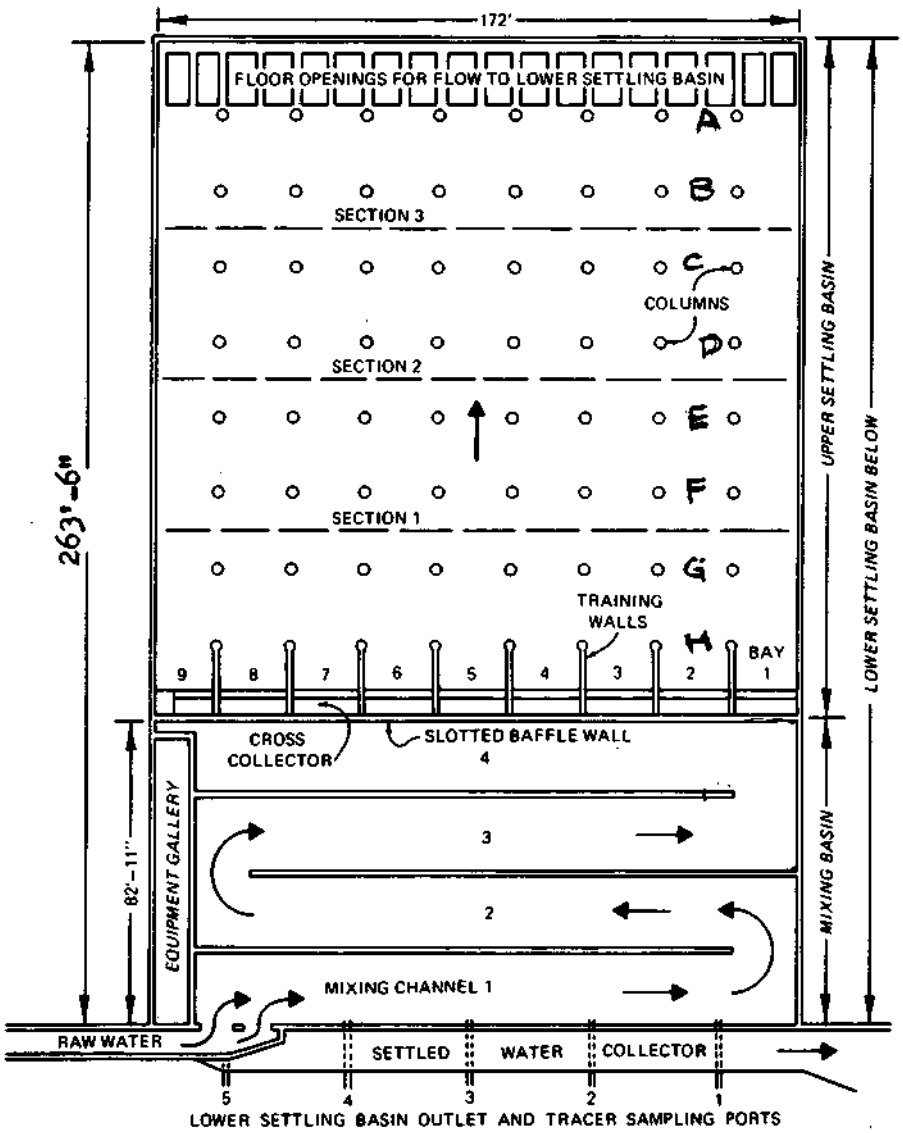


Figure 3. Plan view of mixing basin and upper settling basin

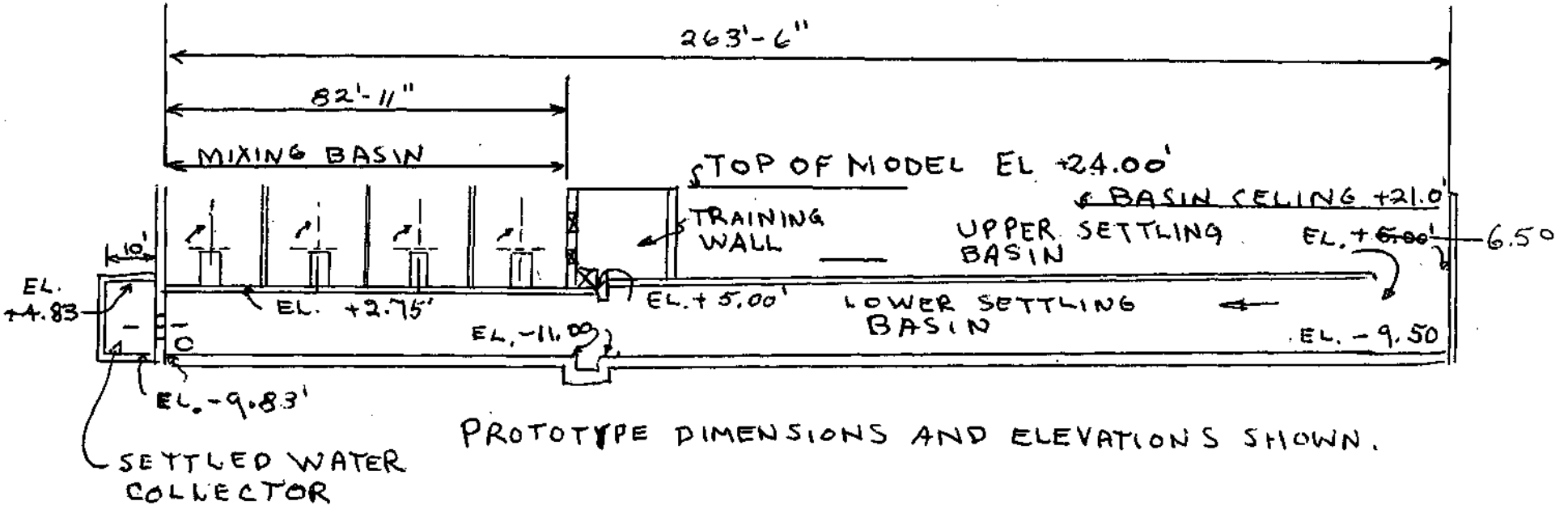


**Figure 4. Longitudinal section of model in Bay 3 as viewed from right side of model**

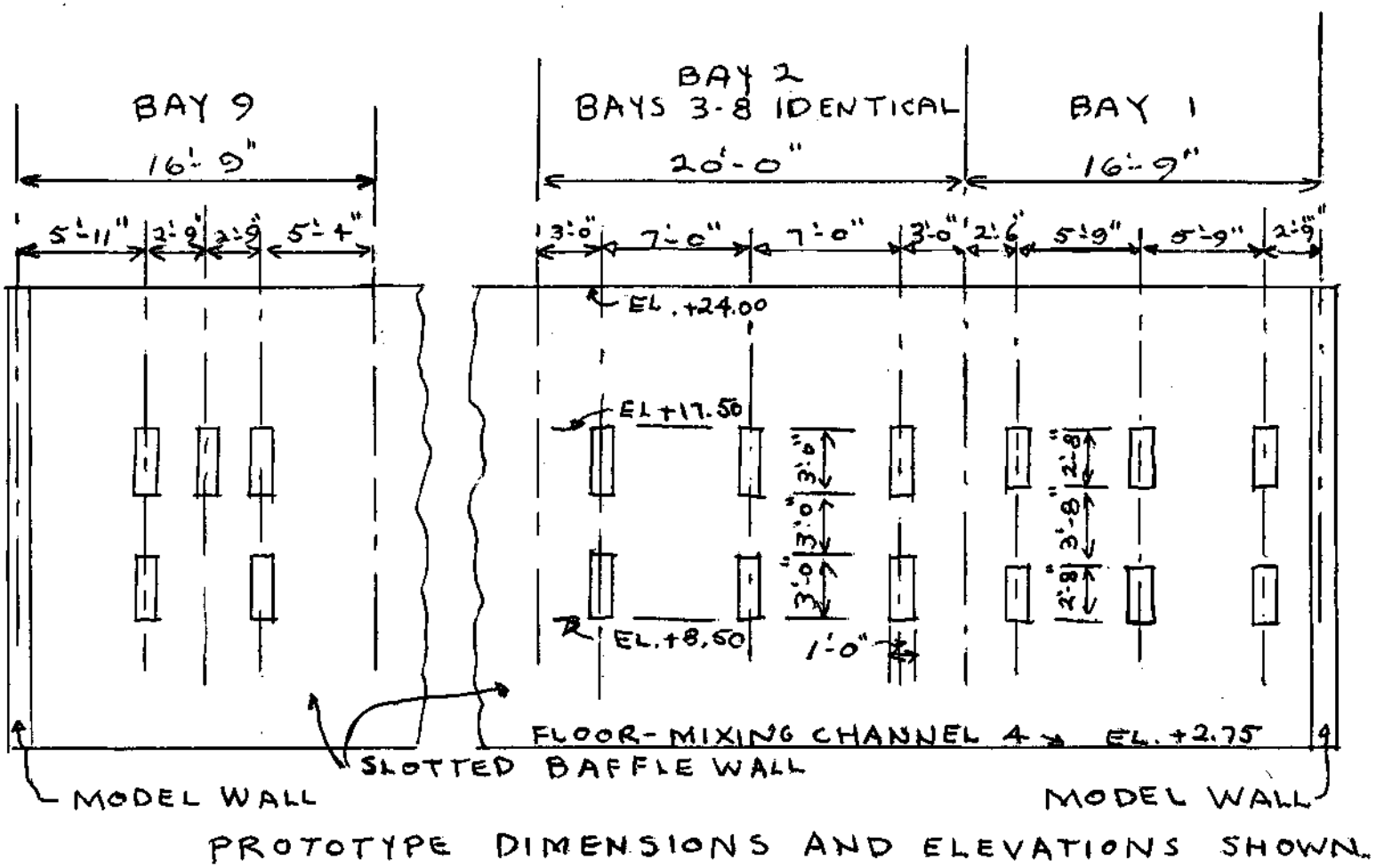


**Flgurs 5. Locations of slots in baffle wall**

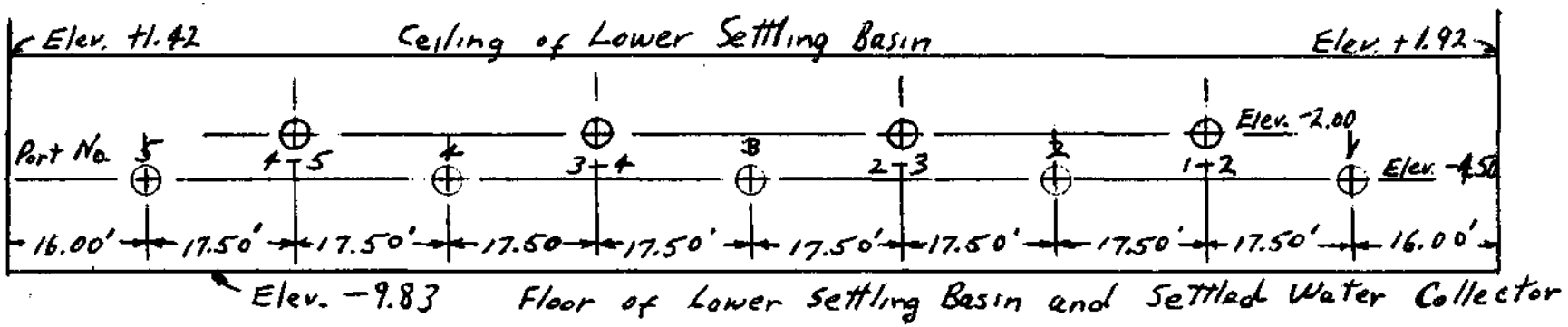


Not to scale. All dimensions and elevations are in prototype feet.
View is from settled water collector channel.

FIGURE 6. LOCATION OF OUTLET VALVES

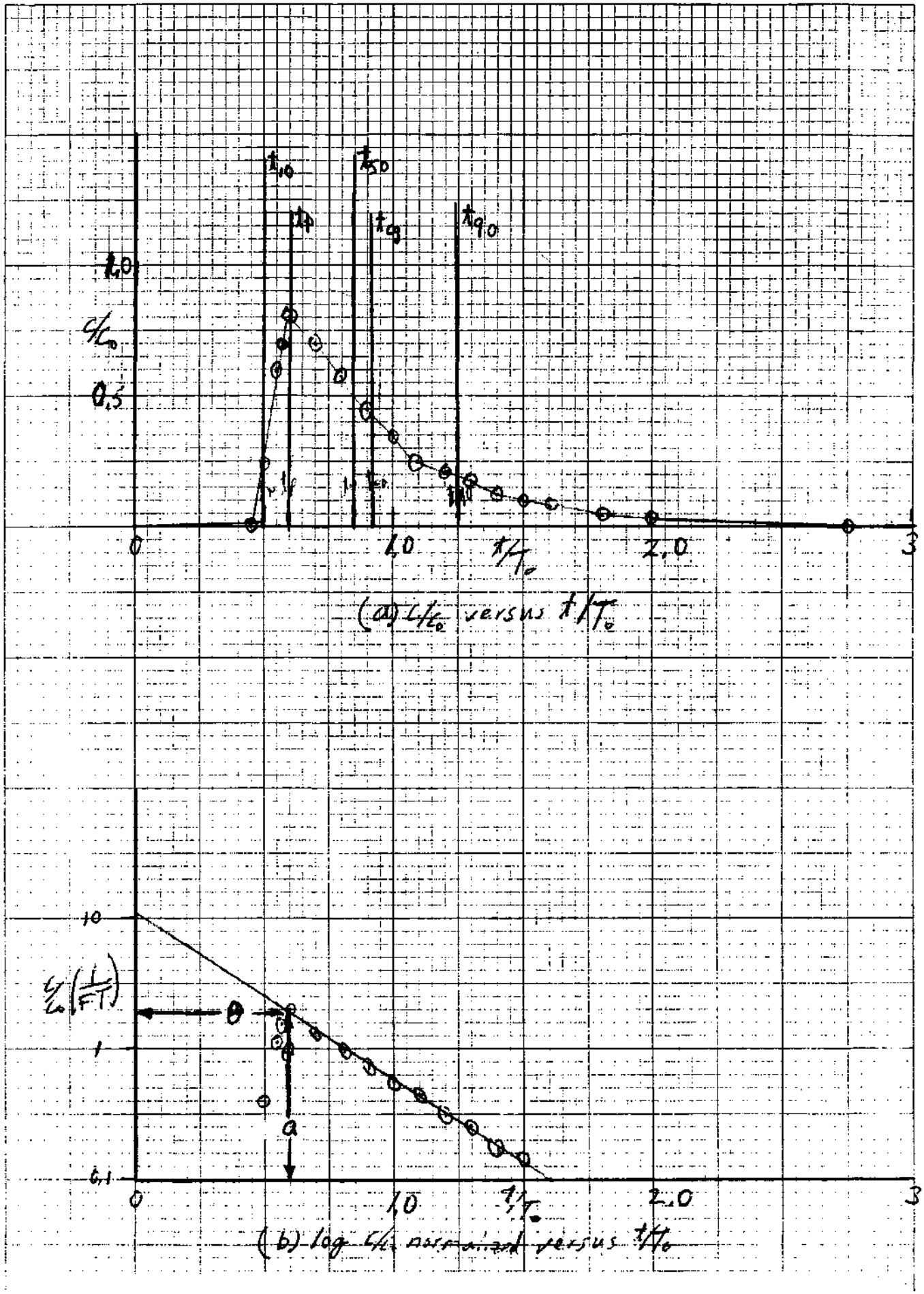


Figure 7. Typical Tracer Distribution Graphs

10/12/72
NGB

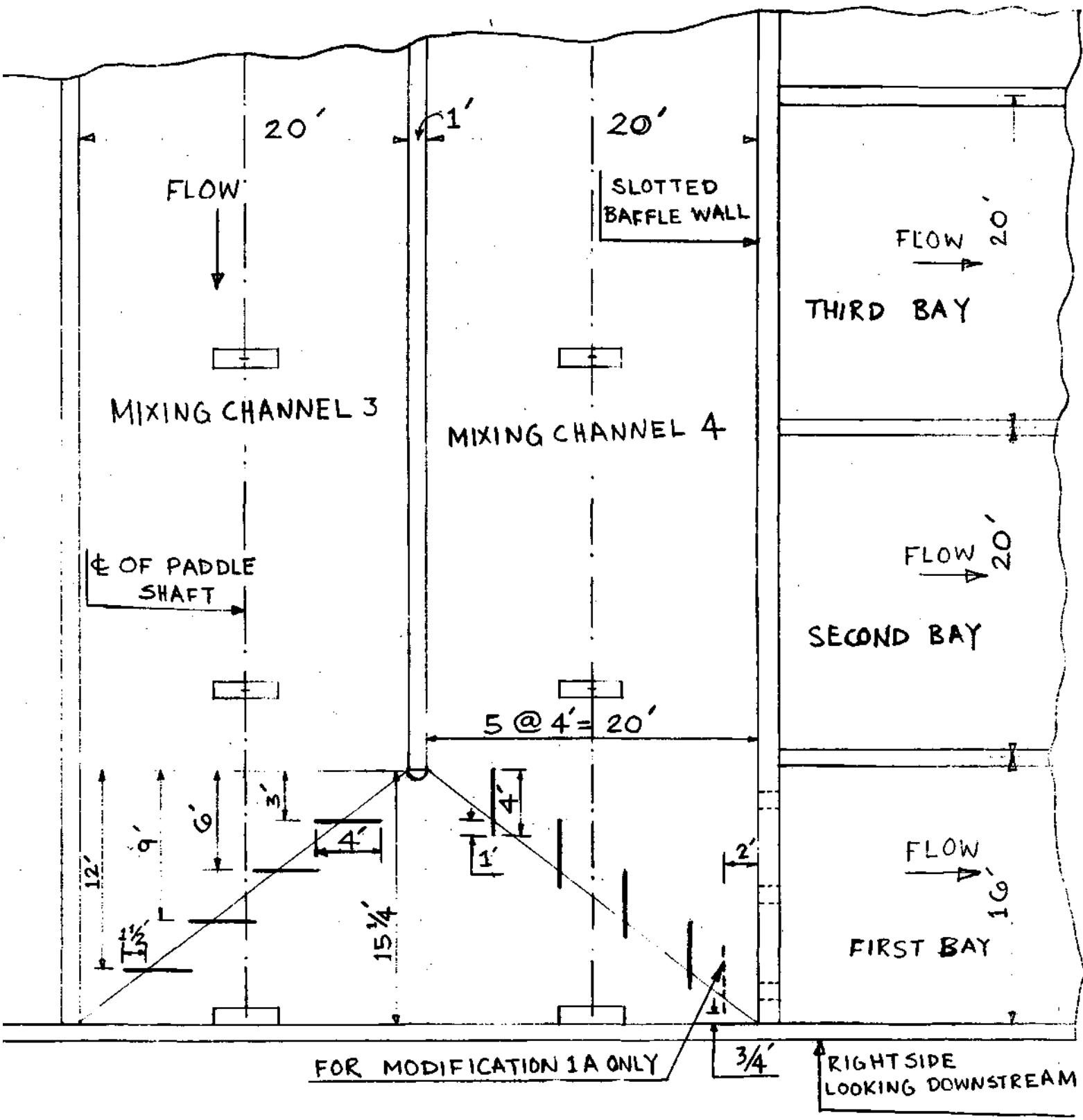


**FIGURE. 8, MODIFICATIONS 1 AUD 1A. STRAIGHTENING VANES IN MIXING CHANNELS 3 AND 4.**

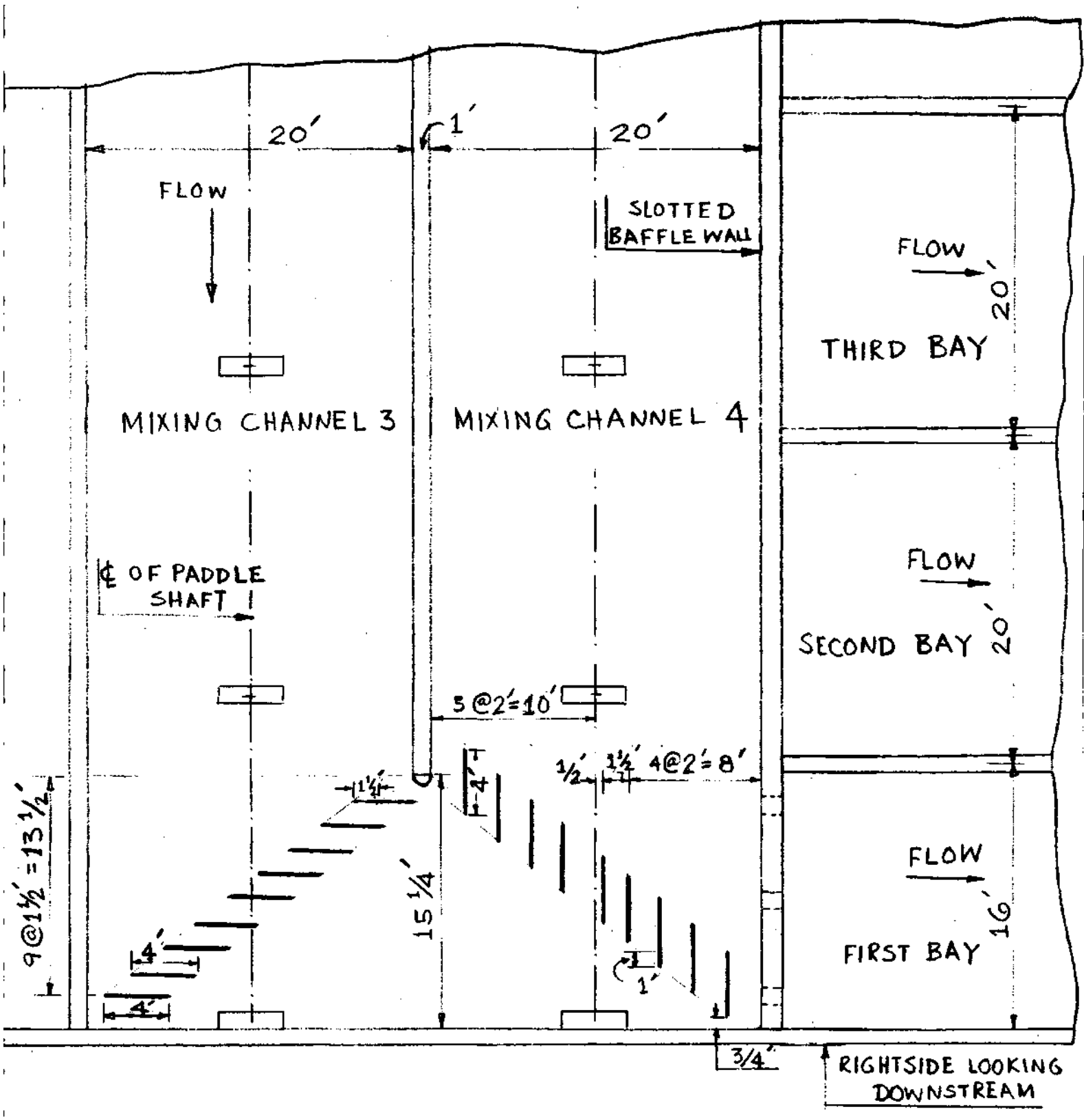


FIGURE. 9. MODIFICATION 4. NINE STRAIGHTENING VANES IN EACH OF THIRD AND FOURTH MIXIN6 CHANNELS.

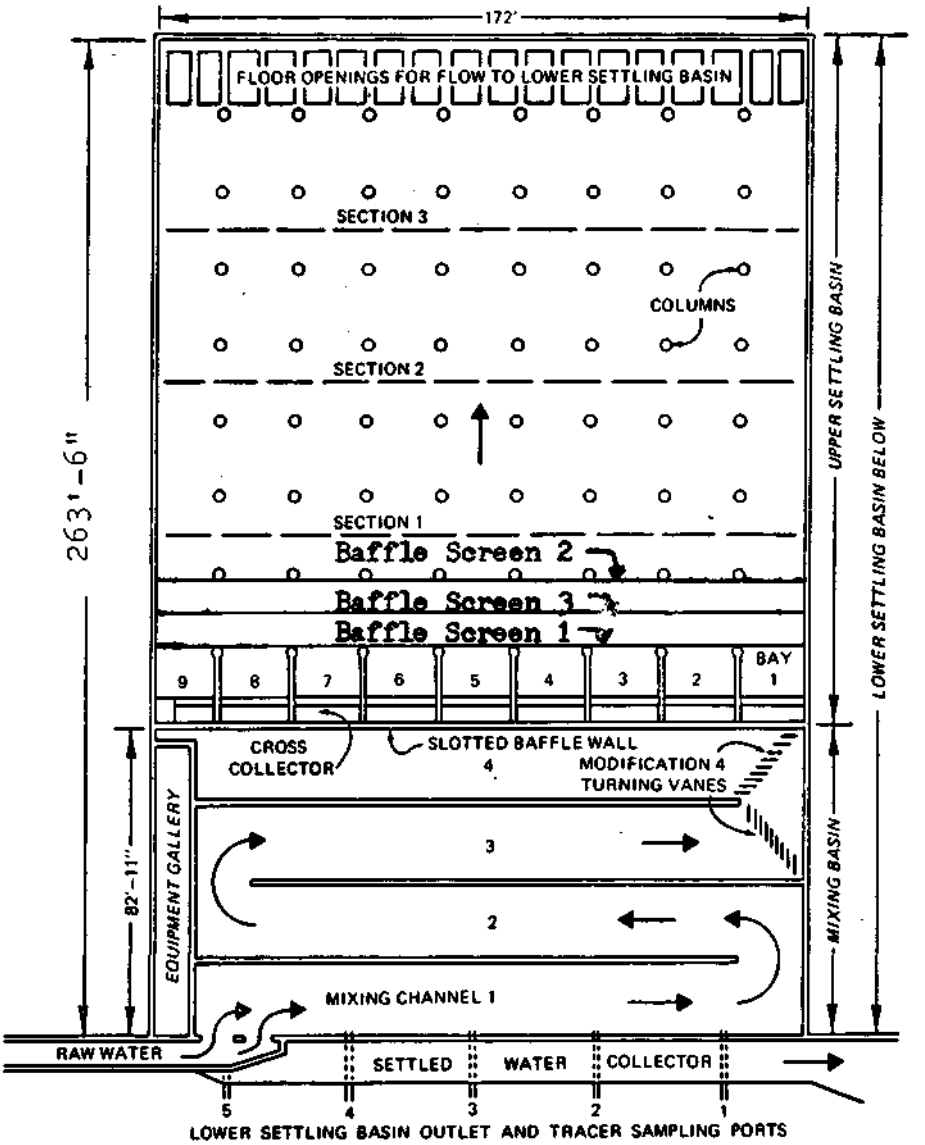


Figure 10. Location of baffle screens in upper settling basin

Figure 11. Tracer Results, Modification 0

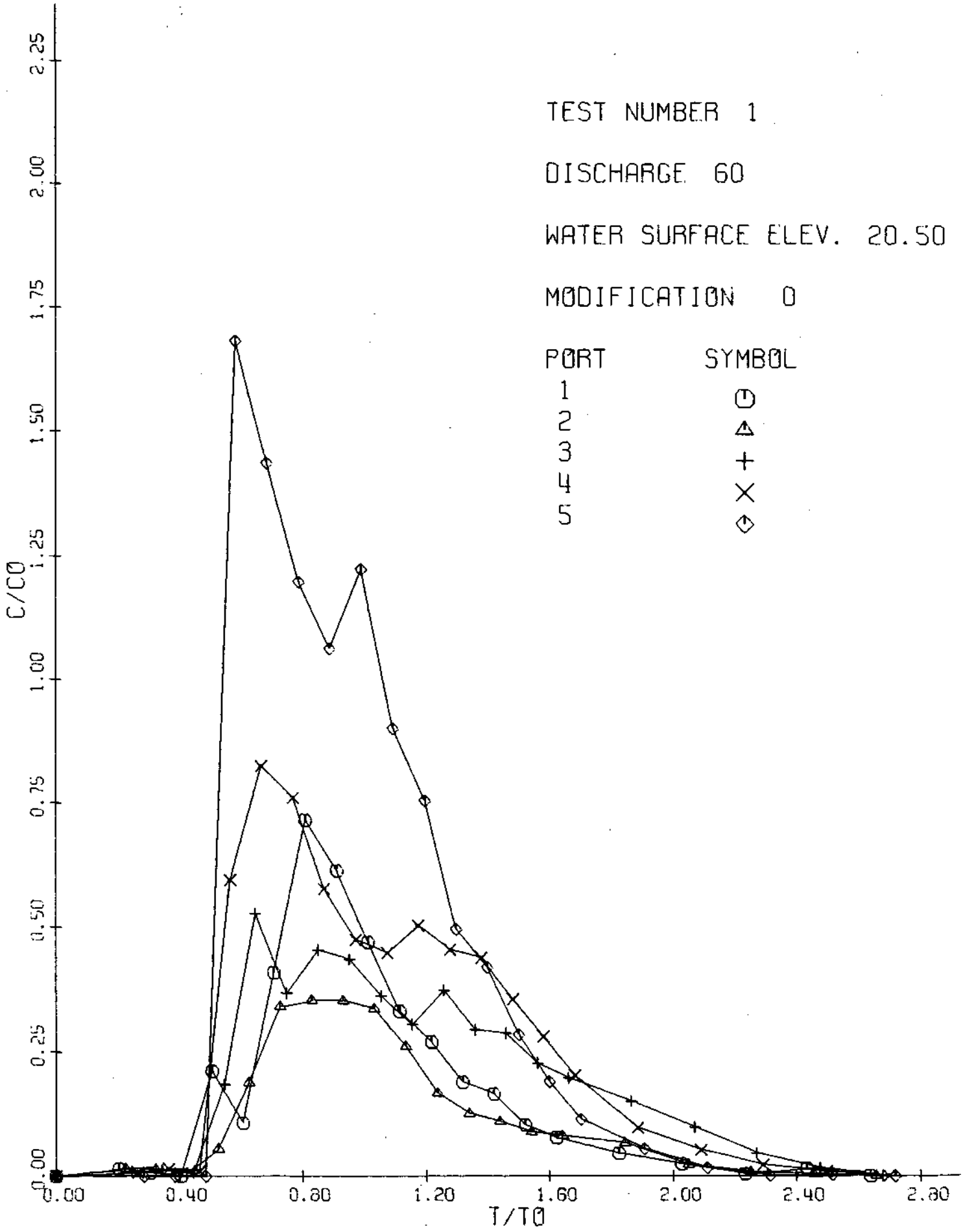

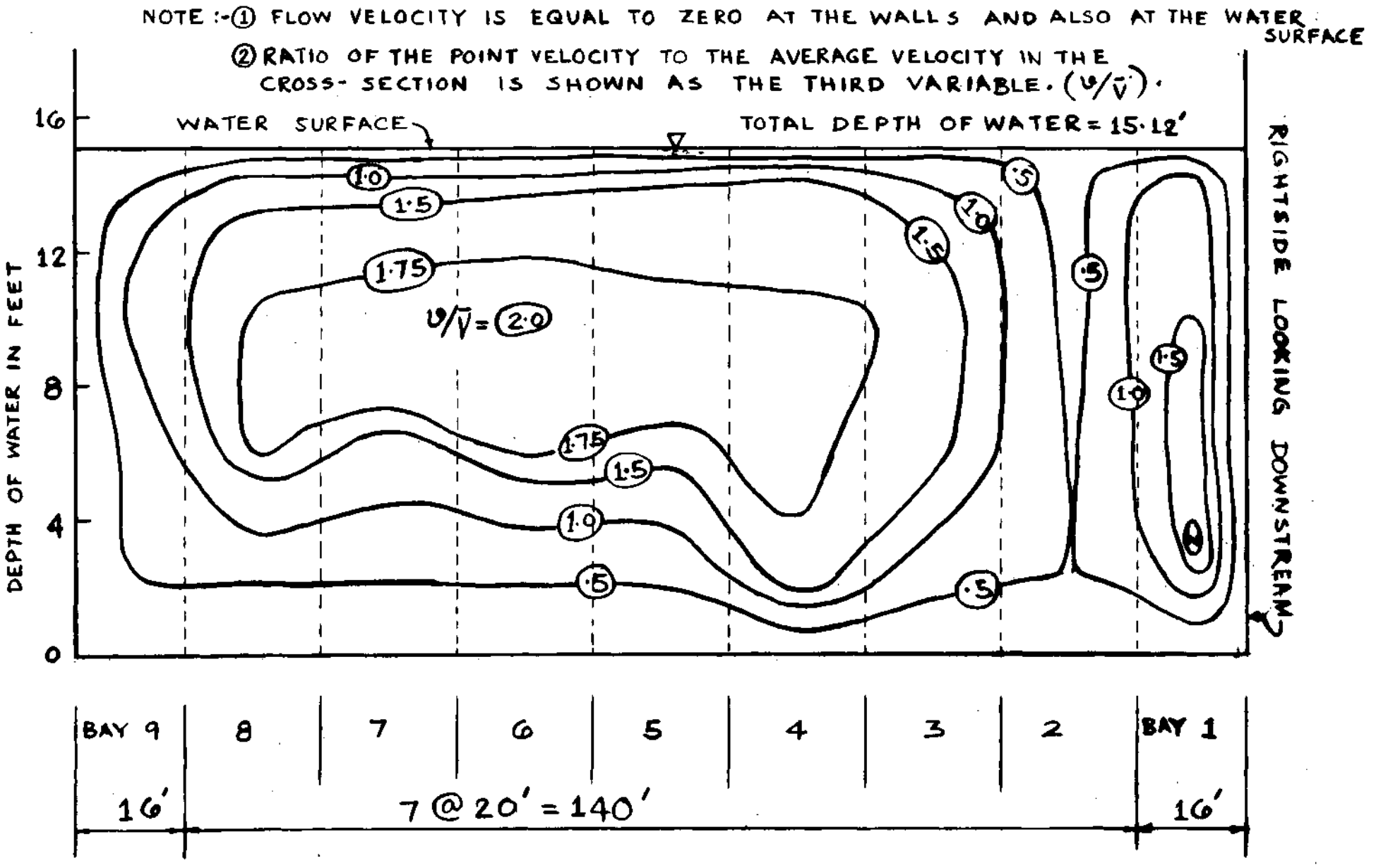


FIGURE. 12a. VELOCITY DISTRIBUTION IN THE. UPPER SETTLING BASIN ATSECTION 1 FOR MODIFICATION 0.QP = 60 MGD, PROTOTYPE WATER, SURFACE ELEVATION = 20.5

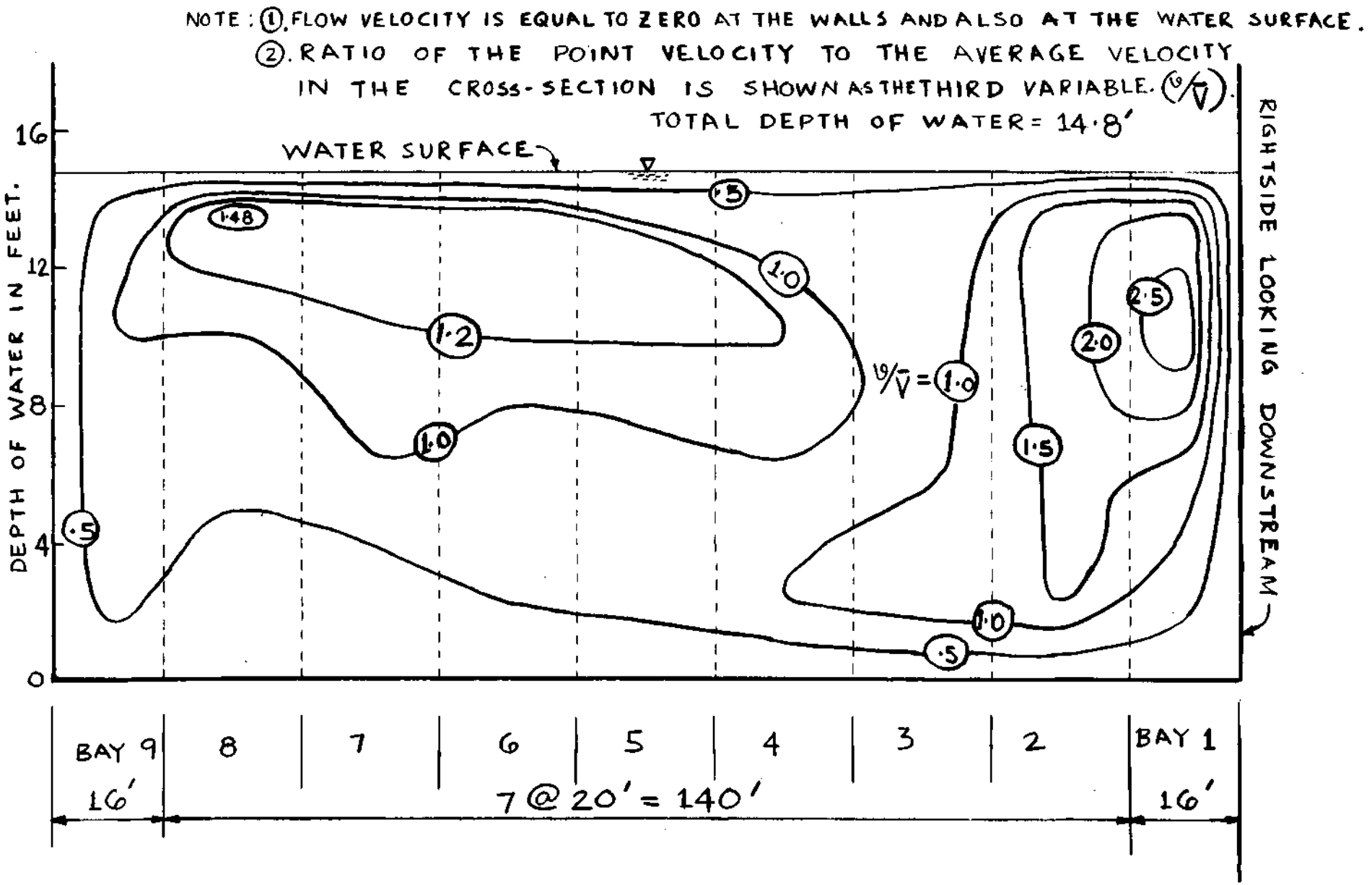


FIGURE. 12b. VELOCITY DISTRIBUTION IN THE UPPER SETTLING BASIN AT SECTION 2 FOR MODIFICATION 0. Qp = 60 MGD, PROTOTYPE WATER SURFACE ELEVATION = 20.5'

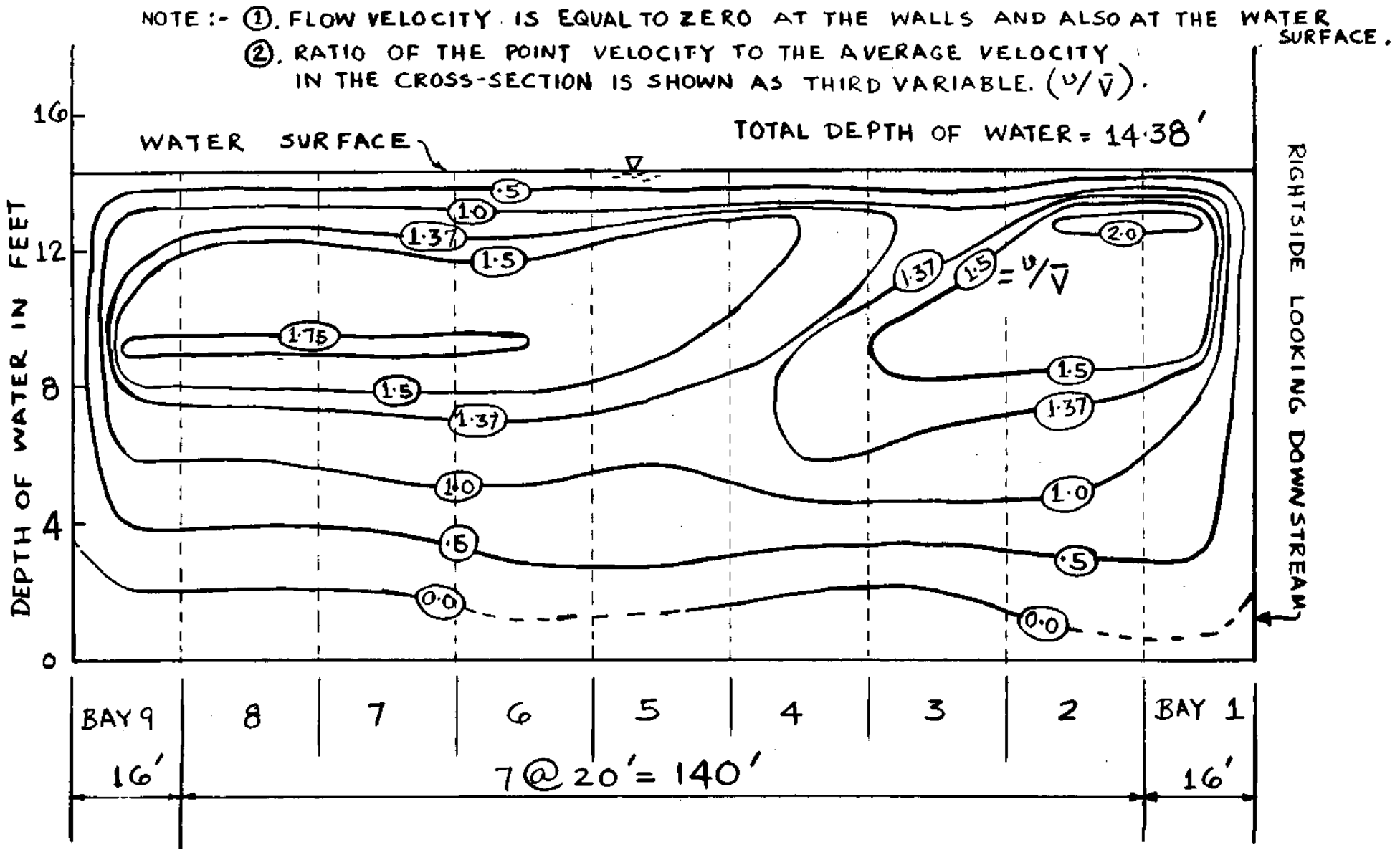


FIGURE 12c. VELOCITY DISTRIBUTION IN THE UPPER SETTLING BASIN AT SECTION 3 FOR MODIFICATION 0. QP = 60 MGD, PROTOTYPE WATER SURFACE ELEVATION = 20.5'

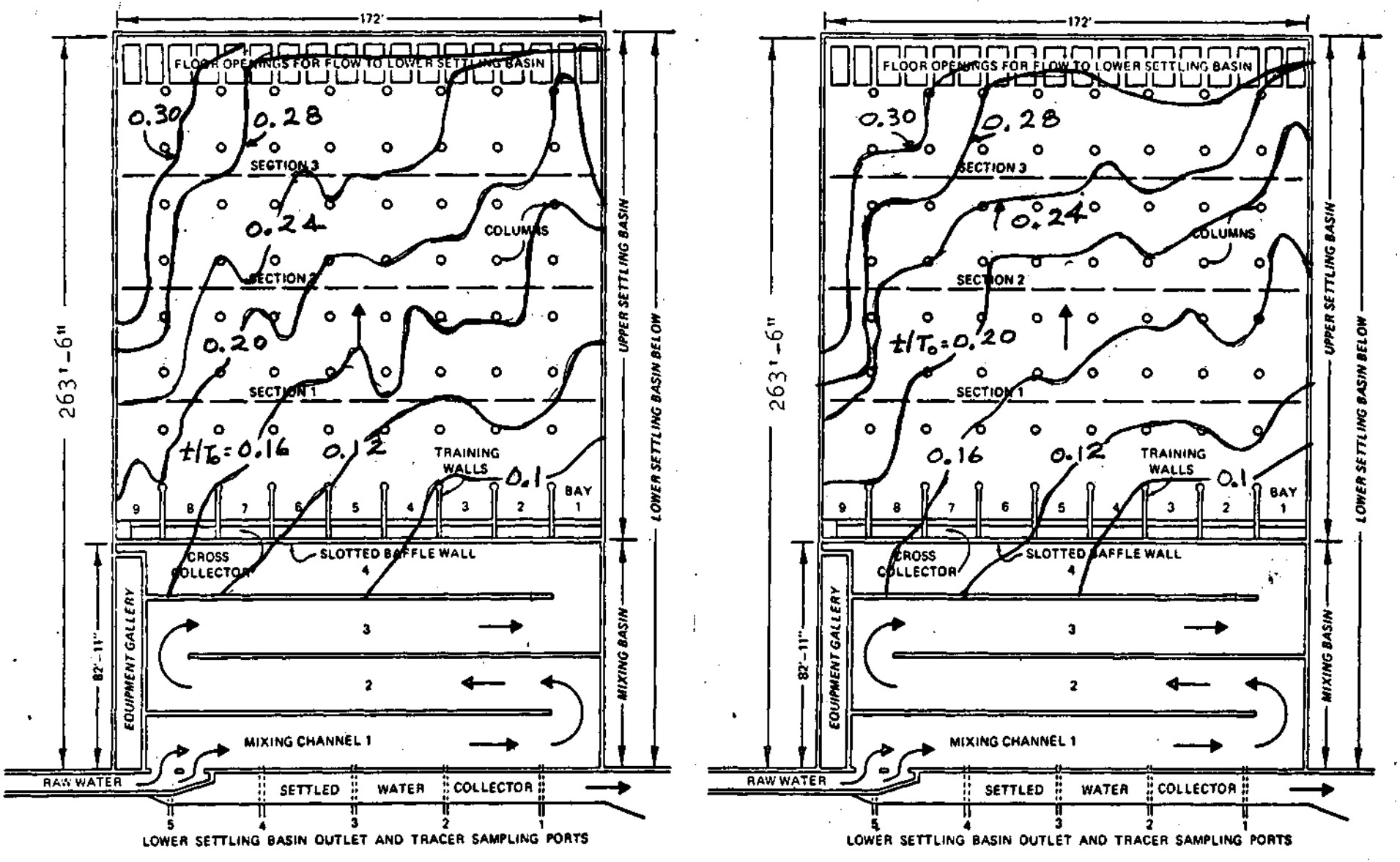


(a). MODIFICATION O
$Q_p$ = 60 MGD., W.S. ELEV. = 20.5 FT.

(b). MODIFICATION O
$Q_p$ = 80 MGD., W.S. ELEV. = 20.5 FT.

FIGURE, 13 . DYE FRONT LOCATION IN UPPER SETTLING BASIN AS OBSERVED FROM MOVIES FOR INDICATED RELATIVE TIME $t/T_0$ .

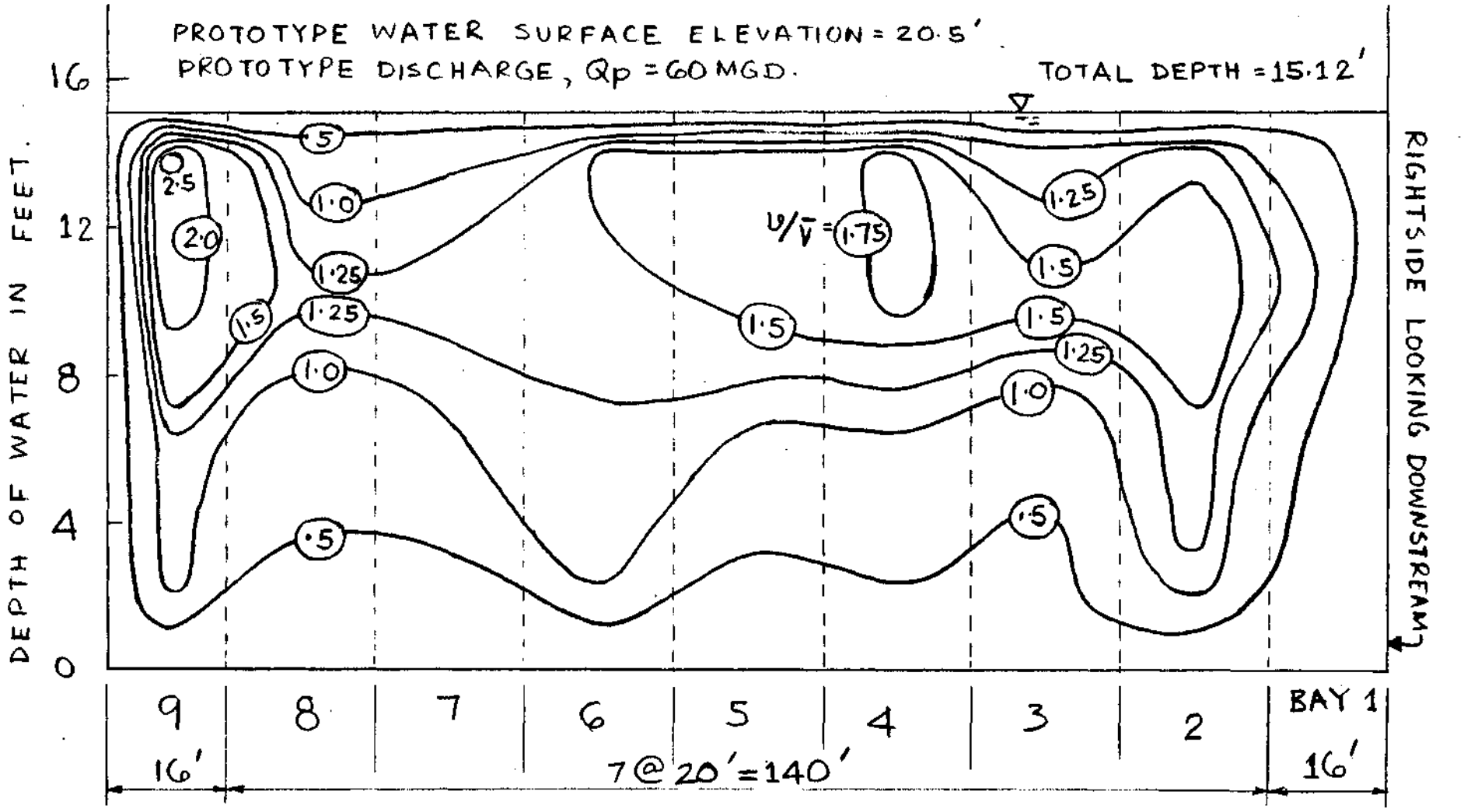


NOTE :- ① FLOW VELOCITY IS EQUAL TO ZERO AT THE WALLS AND ALSO AT THE WATER SURFACE.

② RATIO OF THE POINT VELOCITY TO THE AVERAGE VELOCITY IN THE CROSS-SECTION IS SHOWN AS THE THIRD VARIABLE, $(v/\bar{v})$.

FIGURE, 14a. VELOCITY DIST RIBUTION IN THE UPPER SETTLING BASIN AT SECTION 1 FOR MODIFICATION 3.

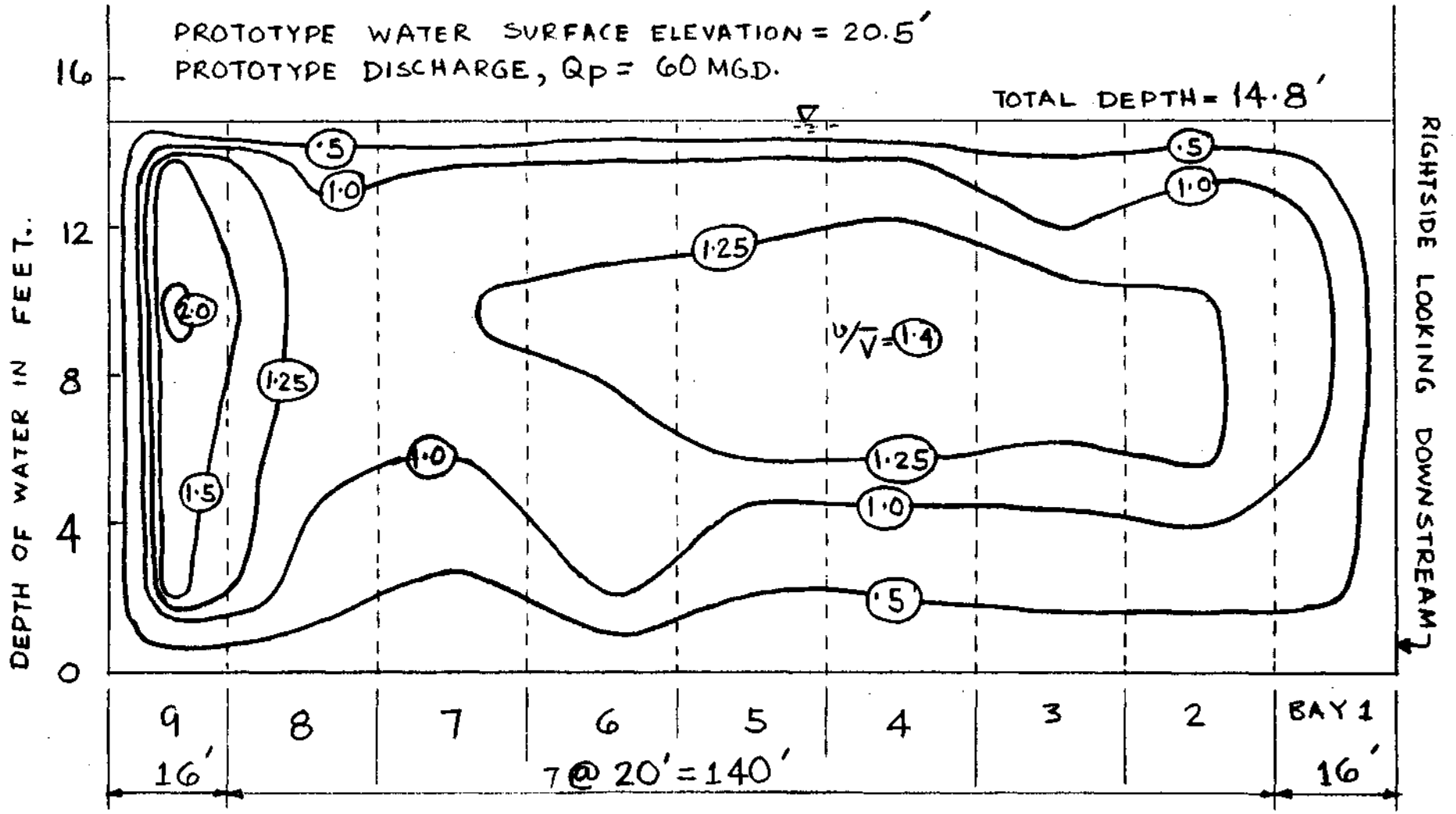


NOTE:- ① FLOW VELOCITY IS EQUAL TO ZERO AT THE WALLS AND ALSO AT THE WATER SURFACE.

② RATIO OF THE POINT VELOCITY TO THE AVERAGE VELOCITY IN THE CROSS-SECTION IS SHOWN AS THE THIRD VARIABLE ($v/\bar{v}$).

FIGURE 14b. VELOCITY DISTRIBUTION IN THE UPPER SETTLING BASIN AT SECTION 2. FOR MODIFICATION 3.

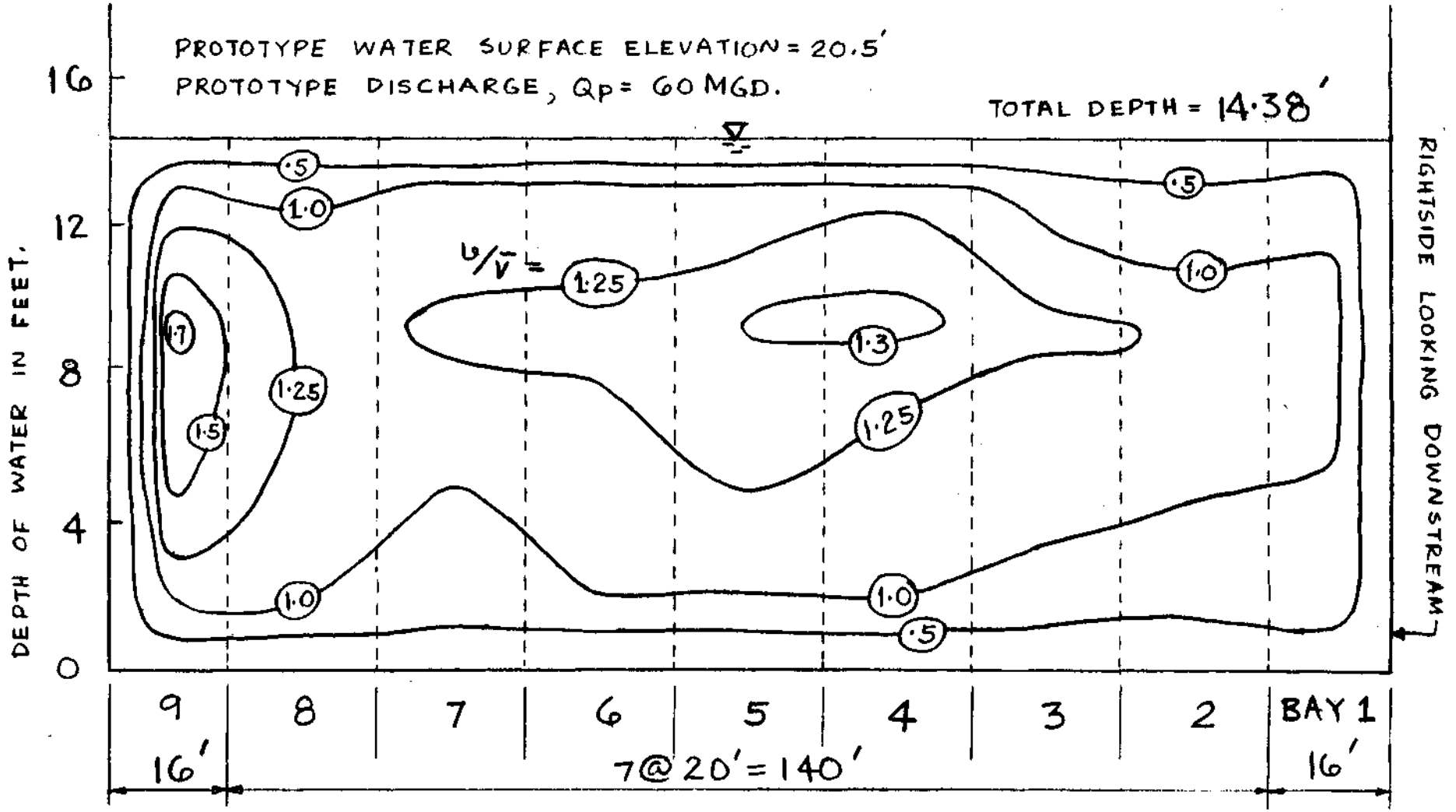


NOTE:- ① FLOW VELOCITY IS EQUAL TO ZERO AT THE WALLS AND ALSO AT THE WATER SURFACE.

② RATIO OF THE POINT VELOCITY TO THE AVERAGE VELOCITY IN THE CROSS-SECTION IS SHOWN AS THE THIRD VARIABLE, $(v/\bar{v})$.

**FIGURE 14c. VELOCITY DISTRIBUTION IN THE UPPER, SETTLING BASIN AT SECTION 3 FOR MODIFICATION 3.**

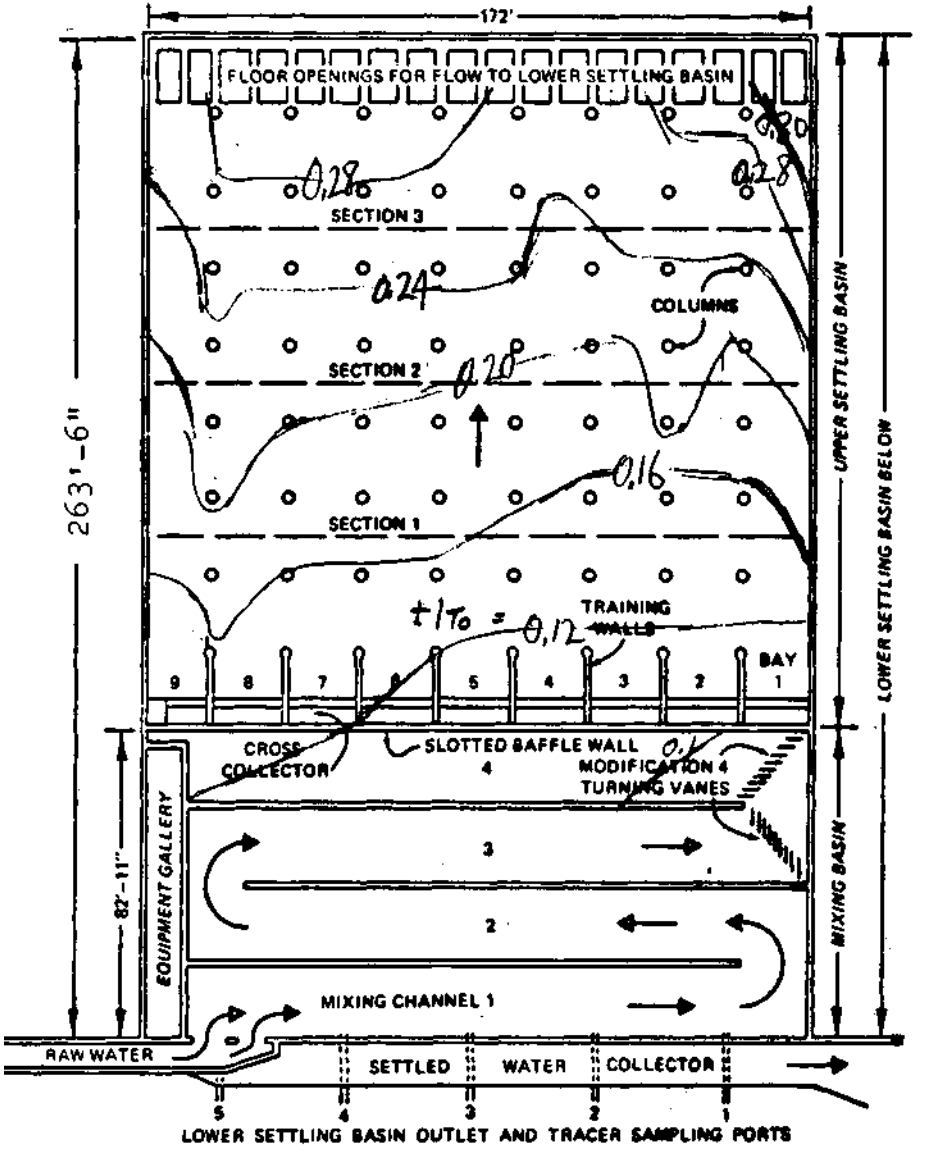


Figure 15. Dye front location in Upper Settling basin, Modification 3

Figure 16. Tracer Results, Modification 4

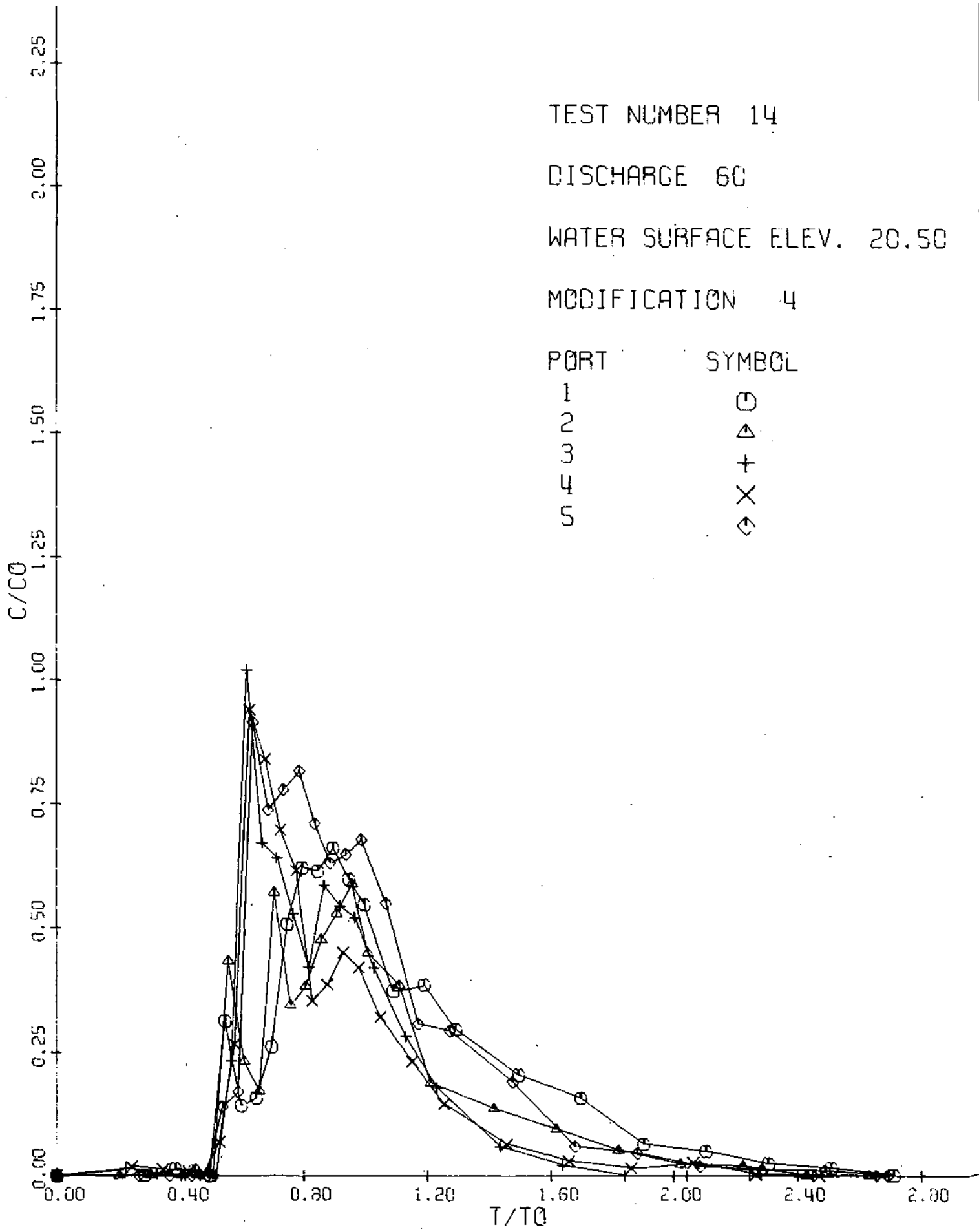

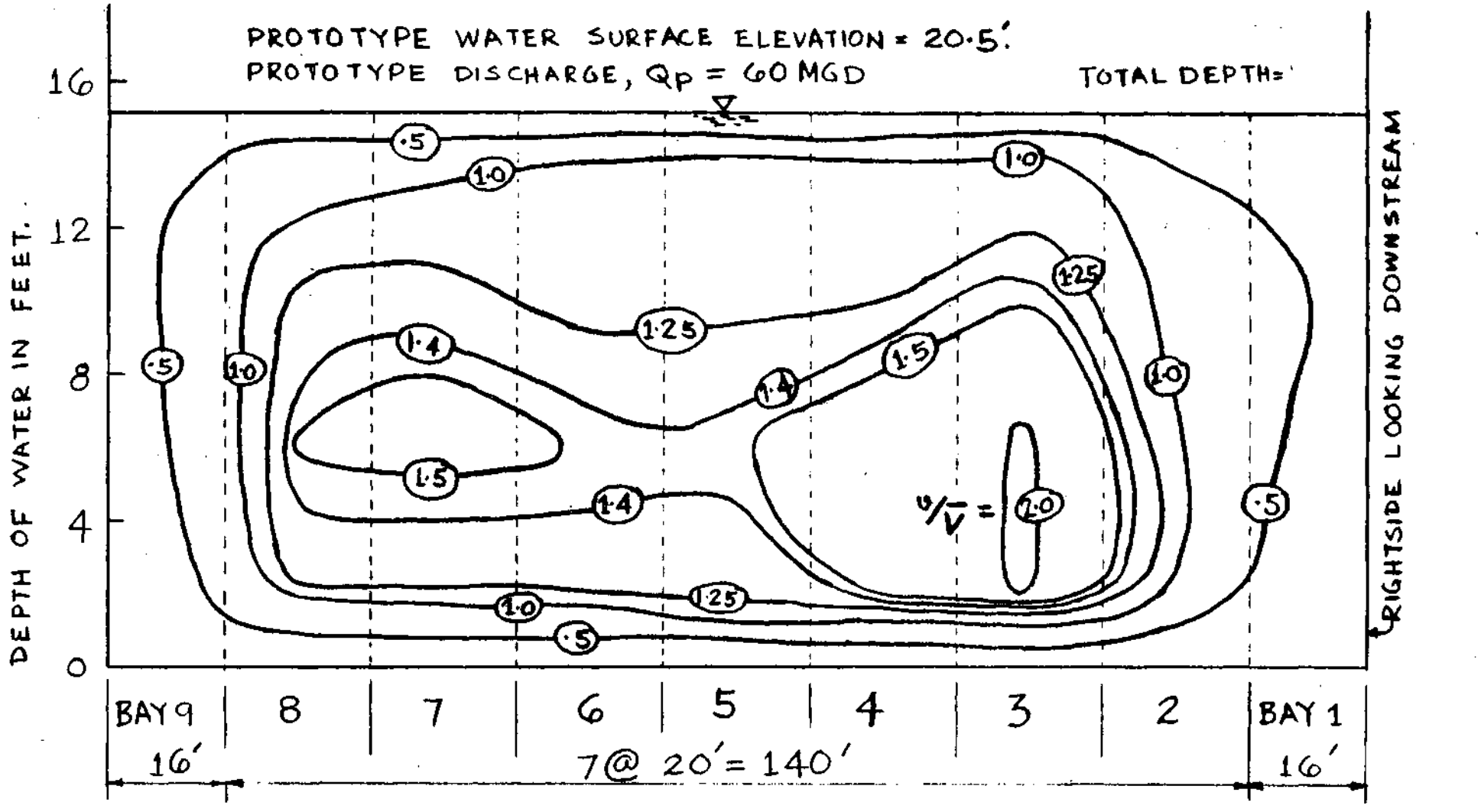


NOTE :- ① FLOW VELOCITY IS EQUAL TO ZERO AT THE WALLS AND ALSO AT THE WATER SURFACE.
② RATIO OF THE POINT VELOCITY TO THE AVERAGE VELOCITY IN THE CROSS-SECTION IS SHOWN AS THE THIRD VARIABLE, $v/\bar{v}$.

FIGURE 17a. VELOCITY DISTRIBUTION IN THE UPPER SETTLING BASIN AT SECTION 1FOR MODIFICATION 4.

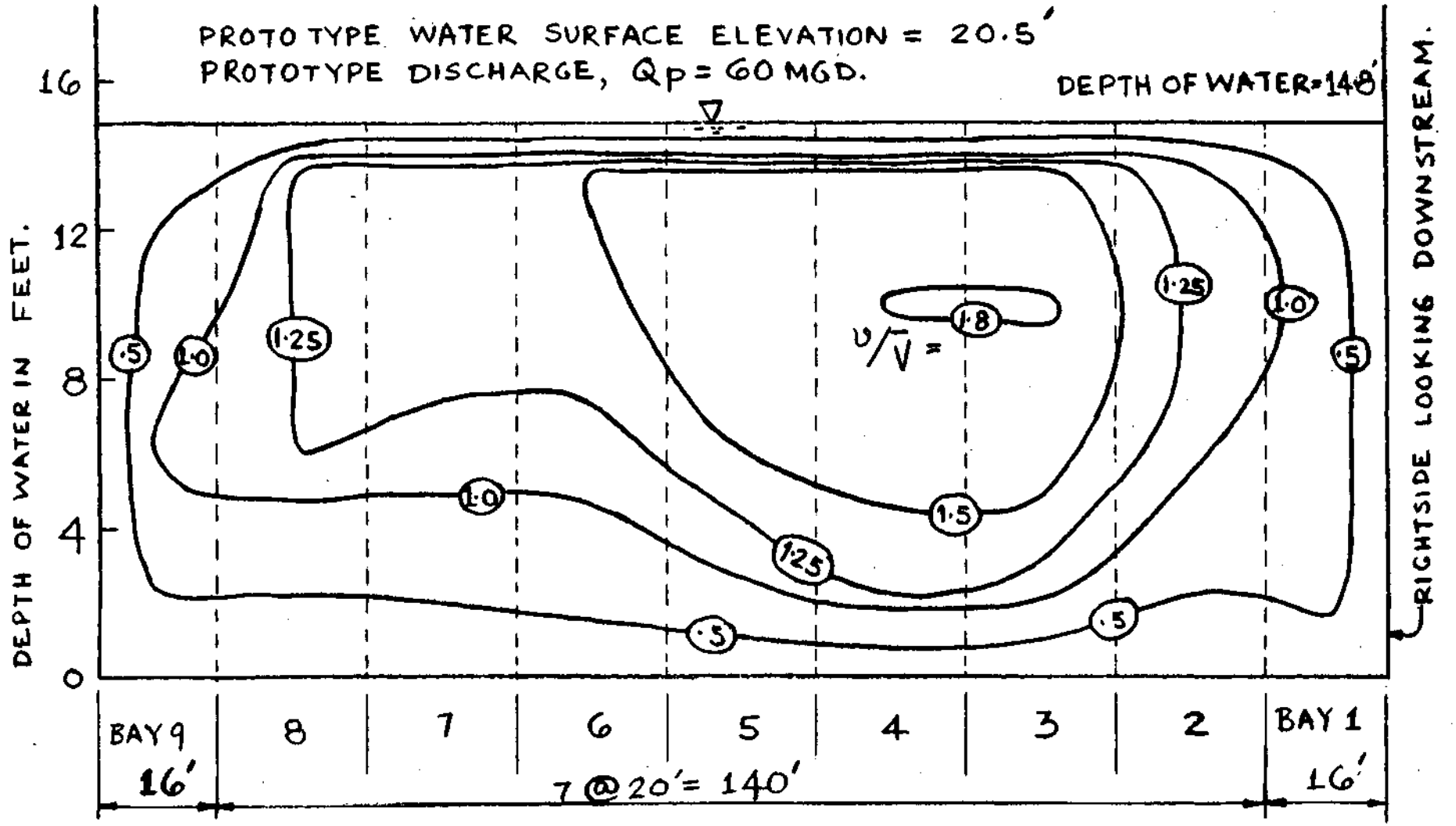


NOTE:- ① FLOW VELOCITY IS EQUAL TO ZERO AT THE WALLS AND ALSO AT THE WATER SURFACE.

② RATIO OF THE POINT VELOCITY TO THE AVERAGE VELOCITY IN THE CROSS-SECTION IS SHOWN AS THE THIRD VARIABLE, $v/\bar{V}$.

FIGURE 17b. VELOCITY DISTRIBUTION IN THE UPPER SETTLING BASIN AT SECTION 2 FOR MODIFICATION 4-.

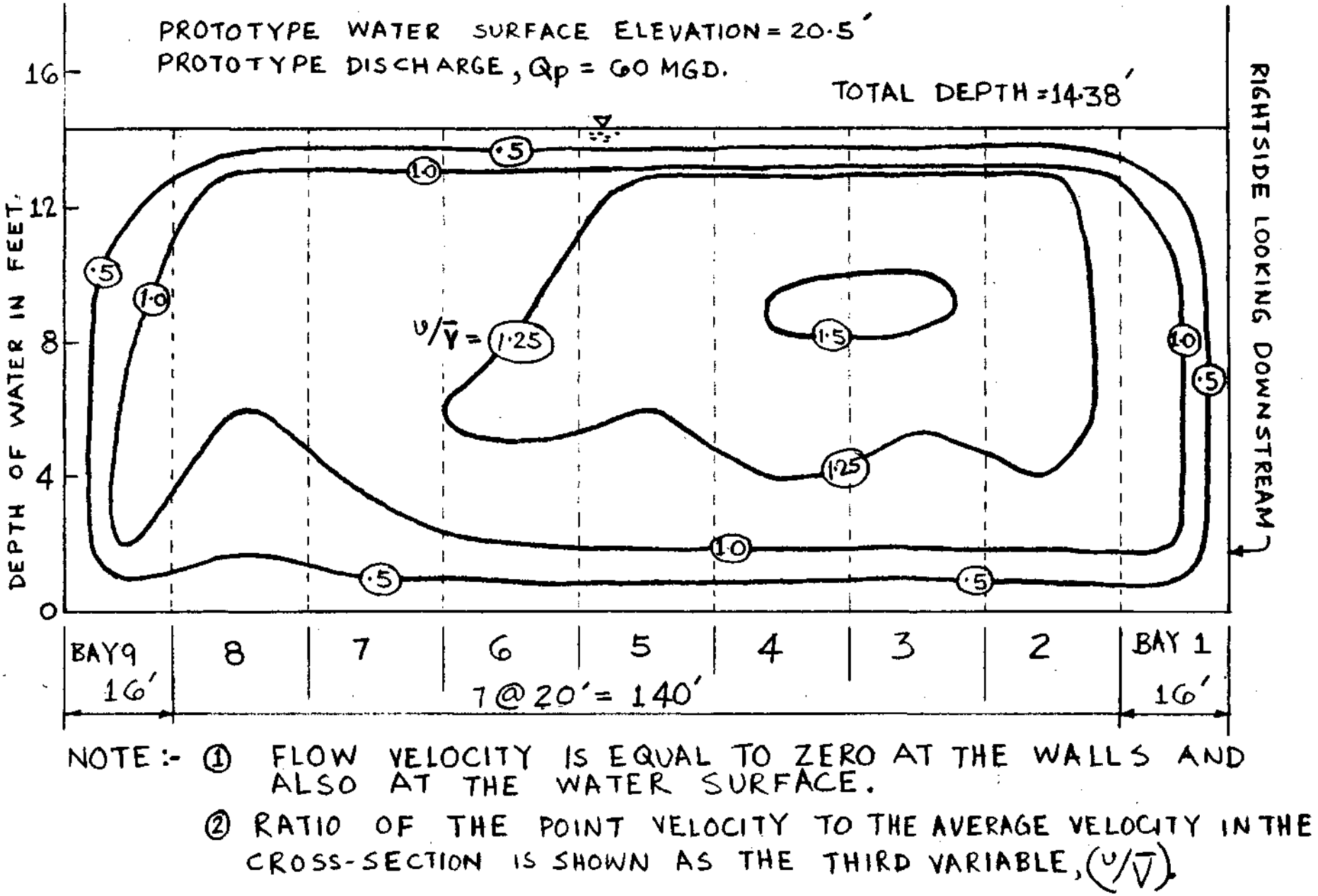


NOTE :- ① FLOW VELOCITY IS EQUAL TO ZERO AT THE WALLS AND ALSO AT THE WATER SURFACE.

② RATIO OF THE POINT VELOCITY TO THE AVERAGE VELOCITY IN THE CROSS-SECTION IS SHOWN AS THE THIRD VARIABLE, $(v/\bar{V})$.

FIGURE 17c. VELOCITY DISTRIBUTION) IN THE UPPER SETTLING BASIN AT SECTION 3 FOR MODIFICATION 4.

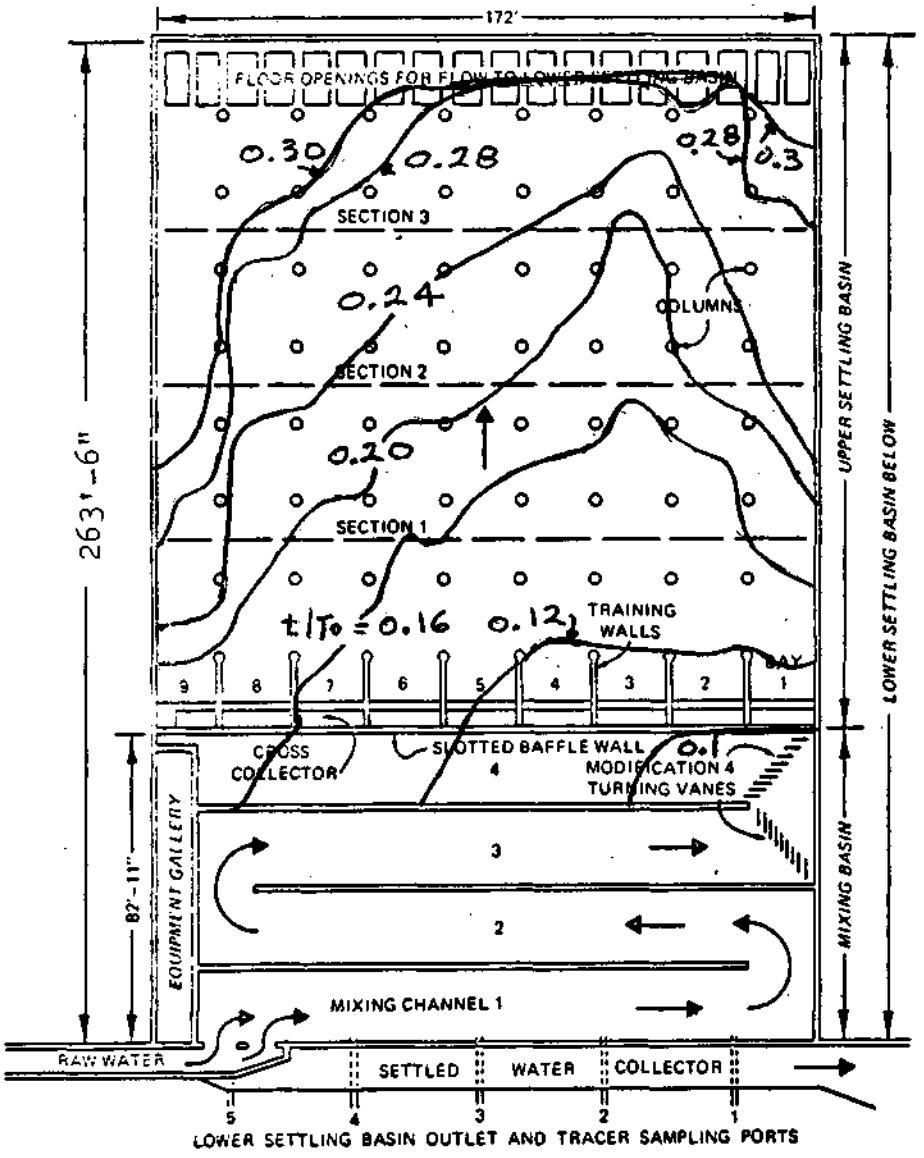


(a). MODIFICATION 4
$Q_p$ = 60 MGD., W.S. ELEV. = 20.5 FT.

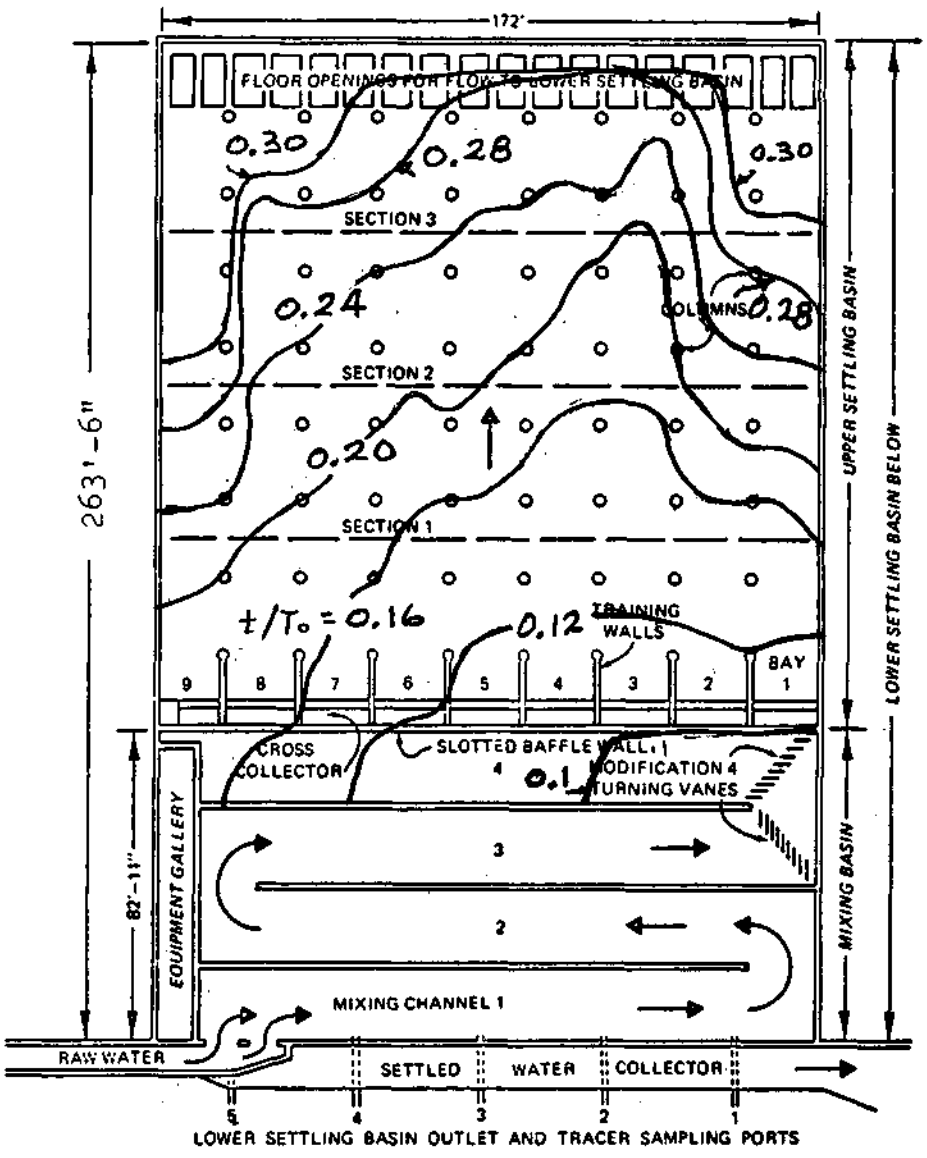


(b). MODIFICATION 4
$Q_p$ = 80 MGD., W.S. ELEV. = 20.5 FT.

FIGURE *18.* DYE PROMT LOCATION IN UPPER SETTLING BASIN AS OBSERVED FROM MOVIES FOR INDICATED RELATIVE TIME $t/T_o$.

Figure 19. Tracer Results, Modification 11

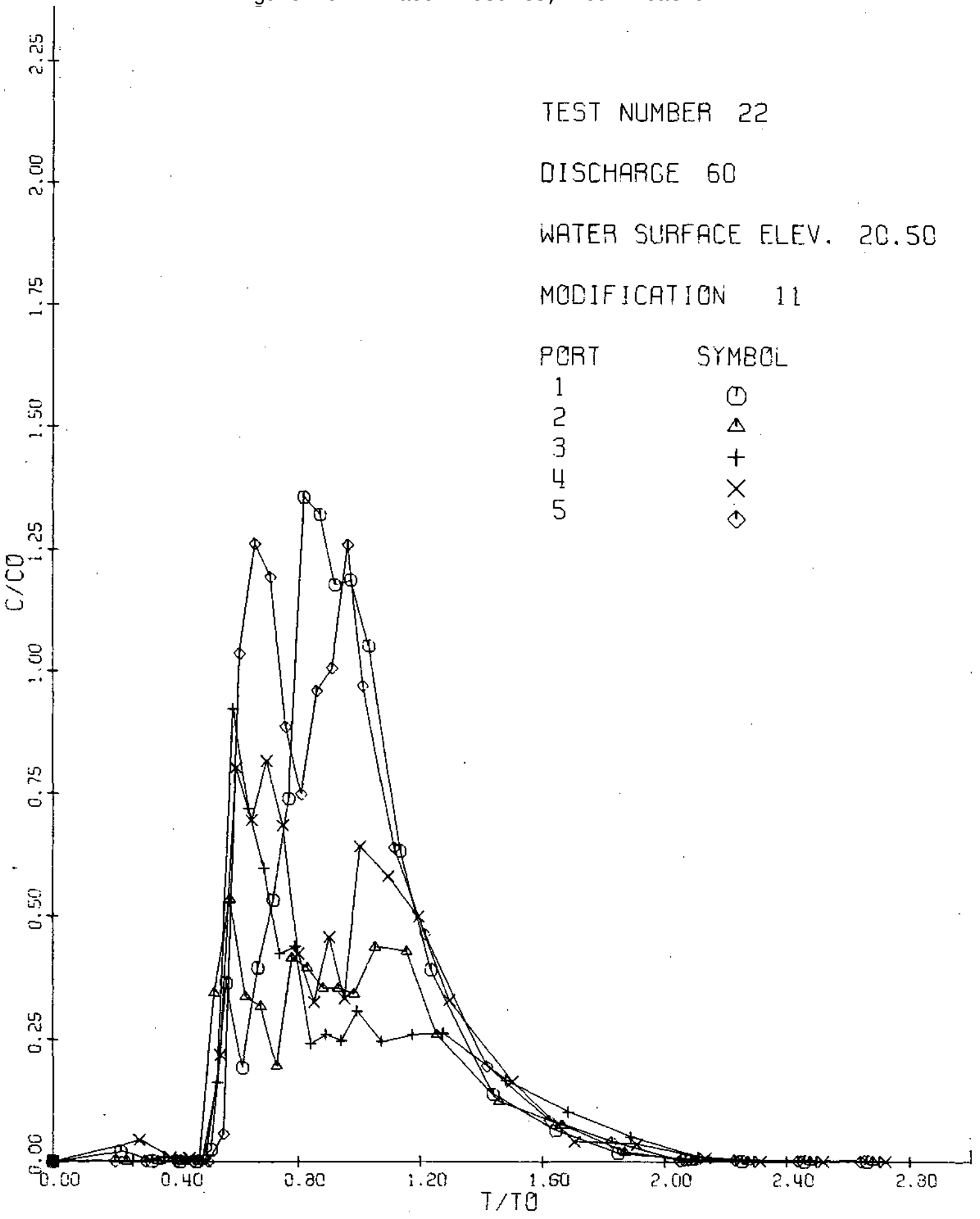

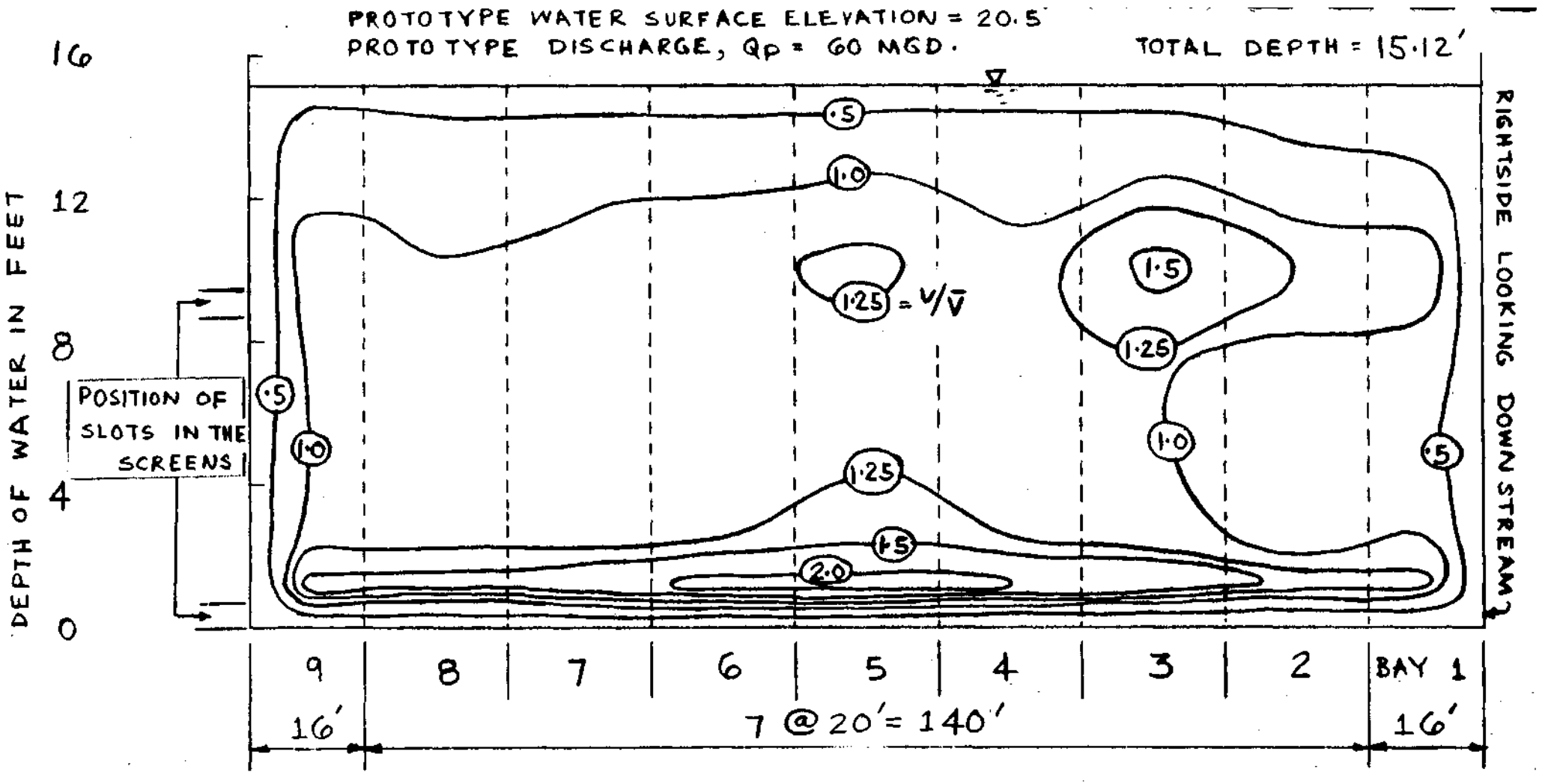


NOTE:- ① FLOW VELOCITY IS EQUAL TO ZERO AT THE WALLS AND ALSO AT THE WATER SURFACE.

② RATIO OF THE POINT VELOCITY TO THE AVERAGE VELOCITY IN THE CROSS-SECTION IS SHOWN AS THE THIRD VARIABLE, $(V/\bar{V})$.

FIGURE 20a. VELOCITY DISTRIBUTION IN THE UPPER. SETTLING BASIN AT SECTION) 1 FOR MODIFICATION 11.

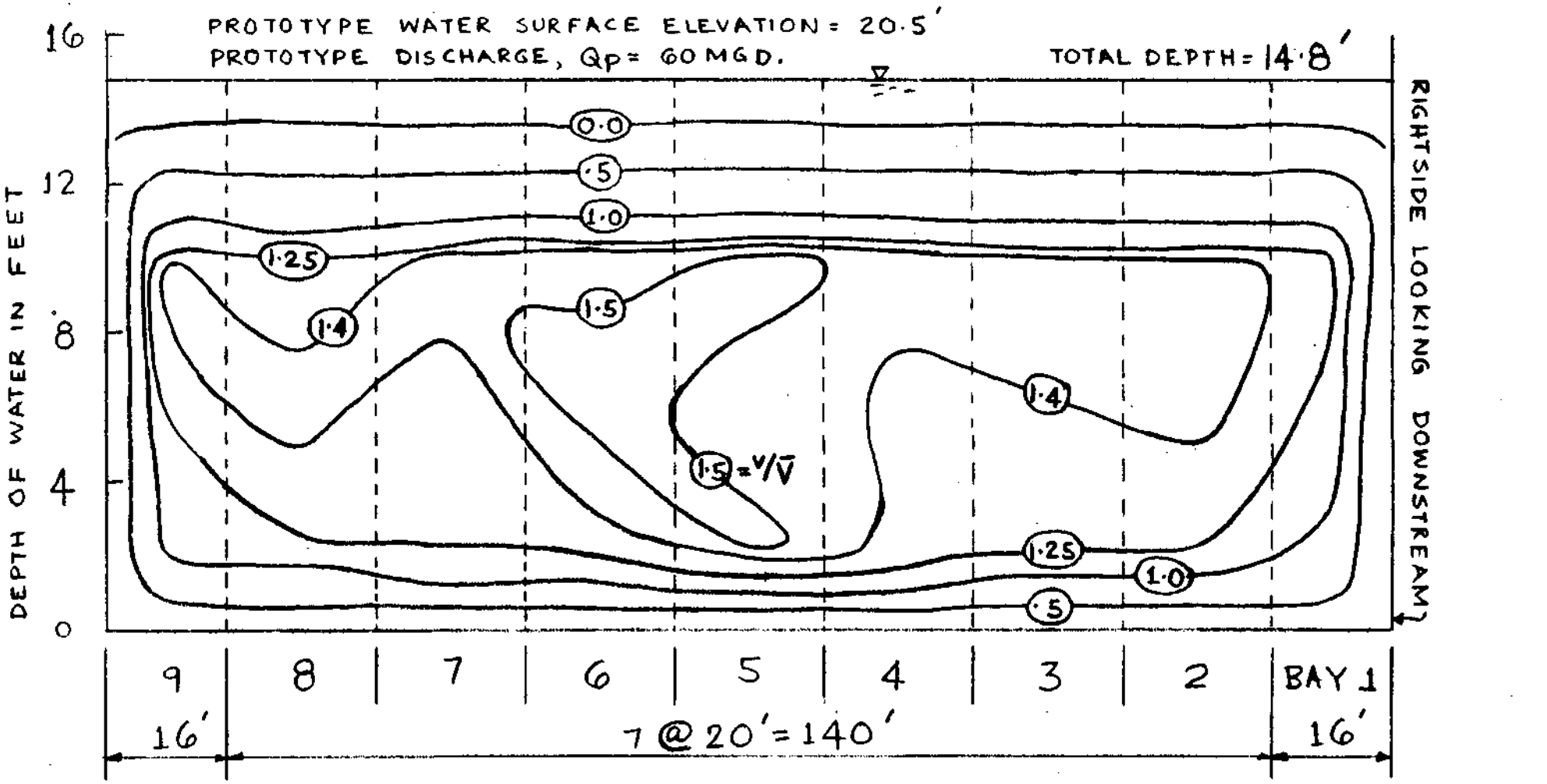


NOTE :- ① FLOW VELOCITY IS EQUAL TO ZERO AT THE WALLS AND ALSO AT THE WATER SURFACE.

② RATIO OF THE POINT VELOCITY TO THE AVERAGE VELOCITY IN THE CROSS-SECTION IS SHOWN AS THE THIRD VARIABLE, $(V/\bar{V})$.

**FIGURE 20b. VELOCITY DISTRIBUTION IN THE UPPER SETTLING BASIN AT SECTION 2 FOR MODIFICATIOK) 11.**

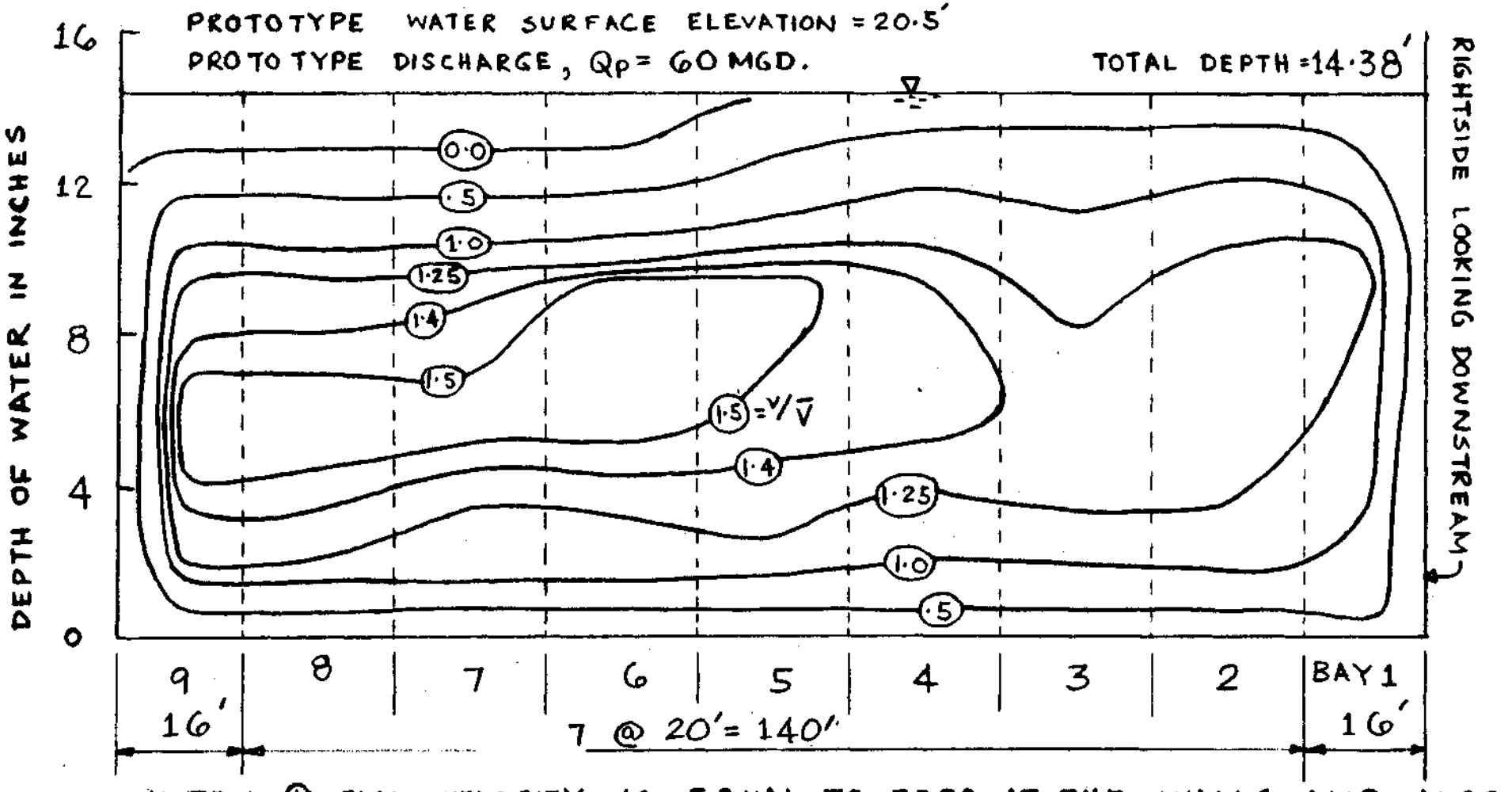


NOTE :- ① FLOW VELOCITY IS EQUAL TO ZERO AT THE WALLS AND ALSO AT THE WATER SURFACE.

② RATIO OF THE POINT VELOCITY TO THE AVERAGE VELOCITY IN THE CROSS-SECTION IS SHOWN AS THE THIRD VARIABLE, $(V/\bar{V})$.

**FIGURE 20c. VELOCITY DISTRIBUTION IN THE UPPER SETTLING BASIN AT SECTION 3 FOR MODI FICATION 11.**

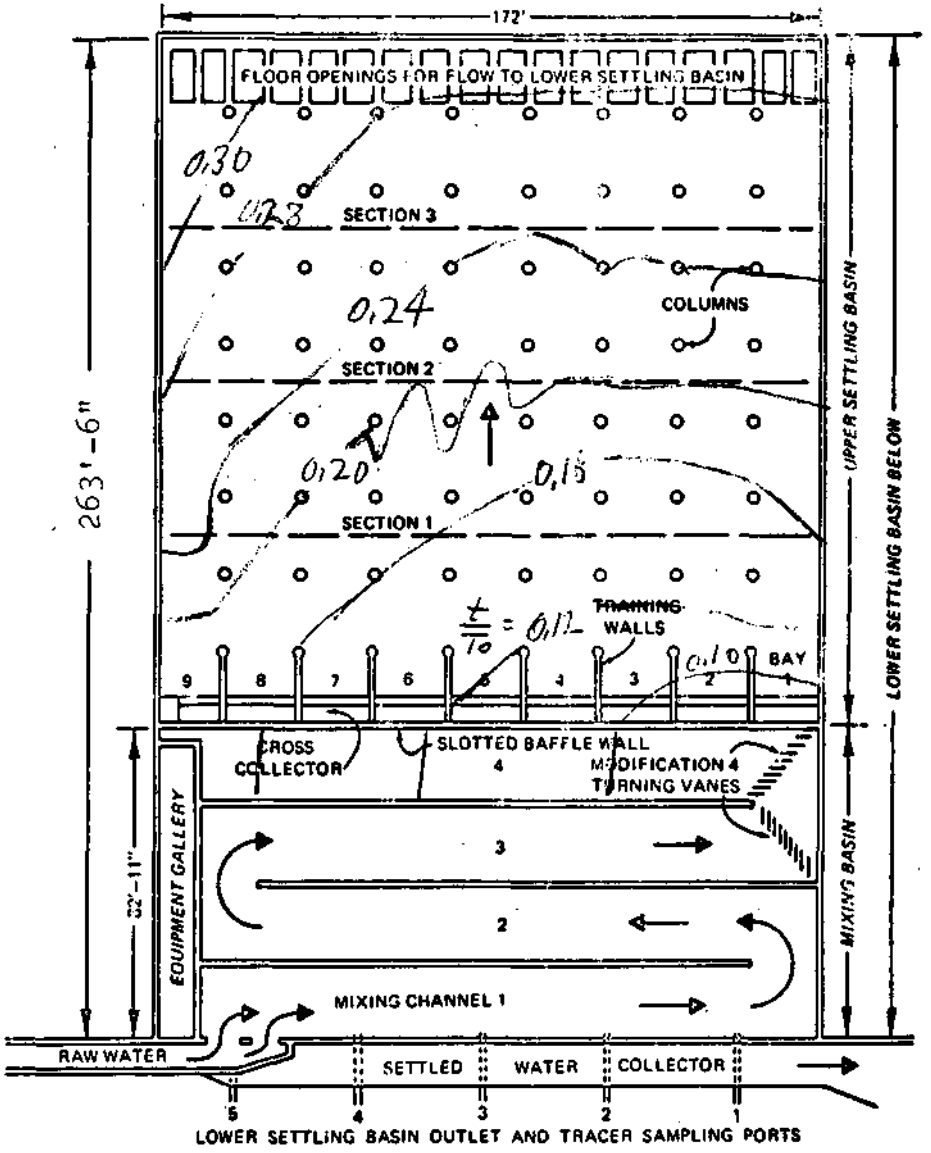


Figure 21. Dye front location in upper settling basin, Modification 11

Figure 22. Tracer Results, Modification 16

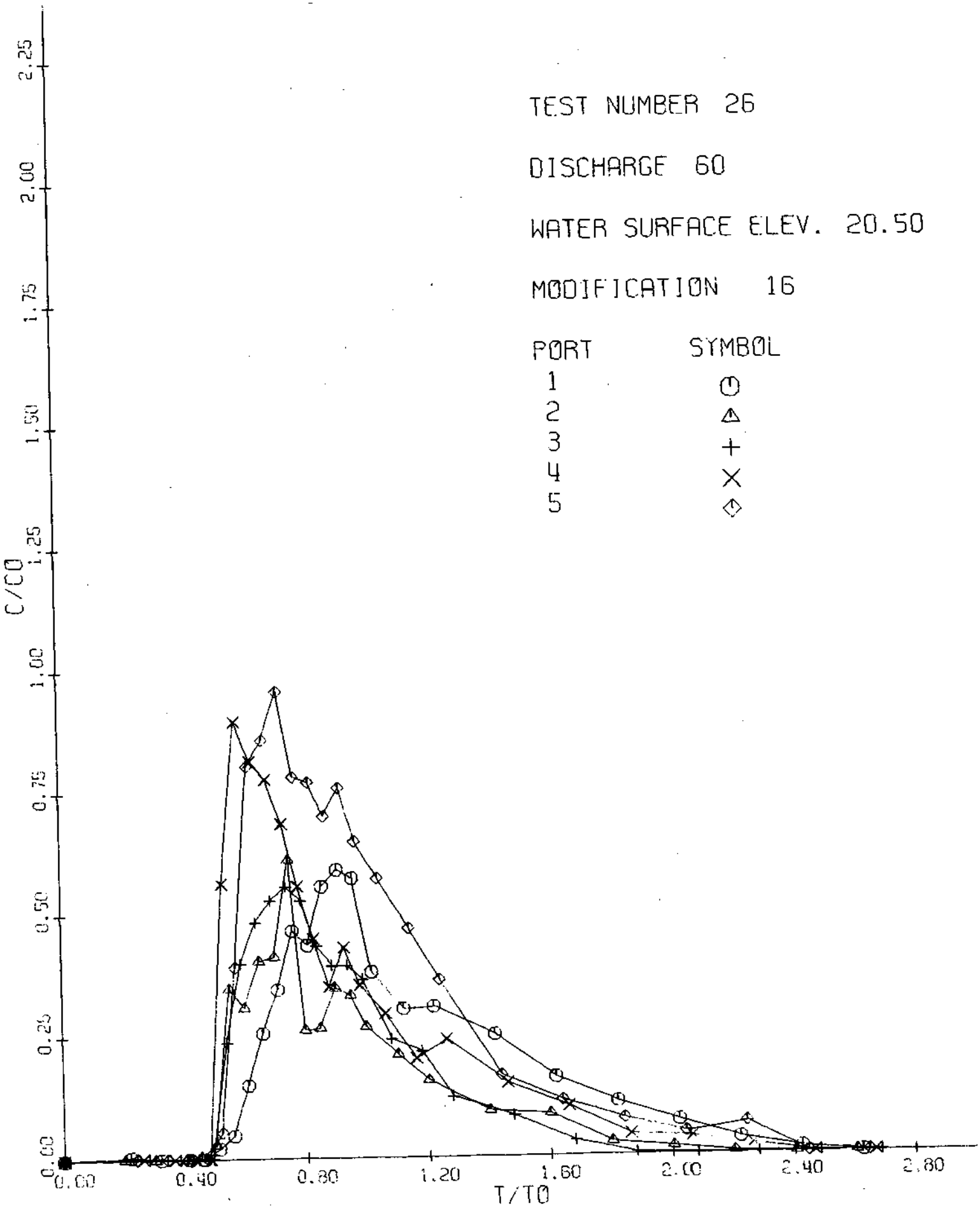

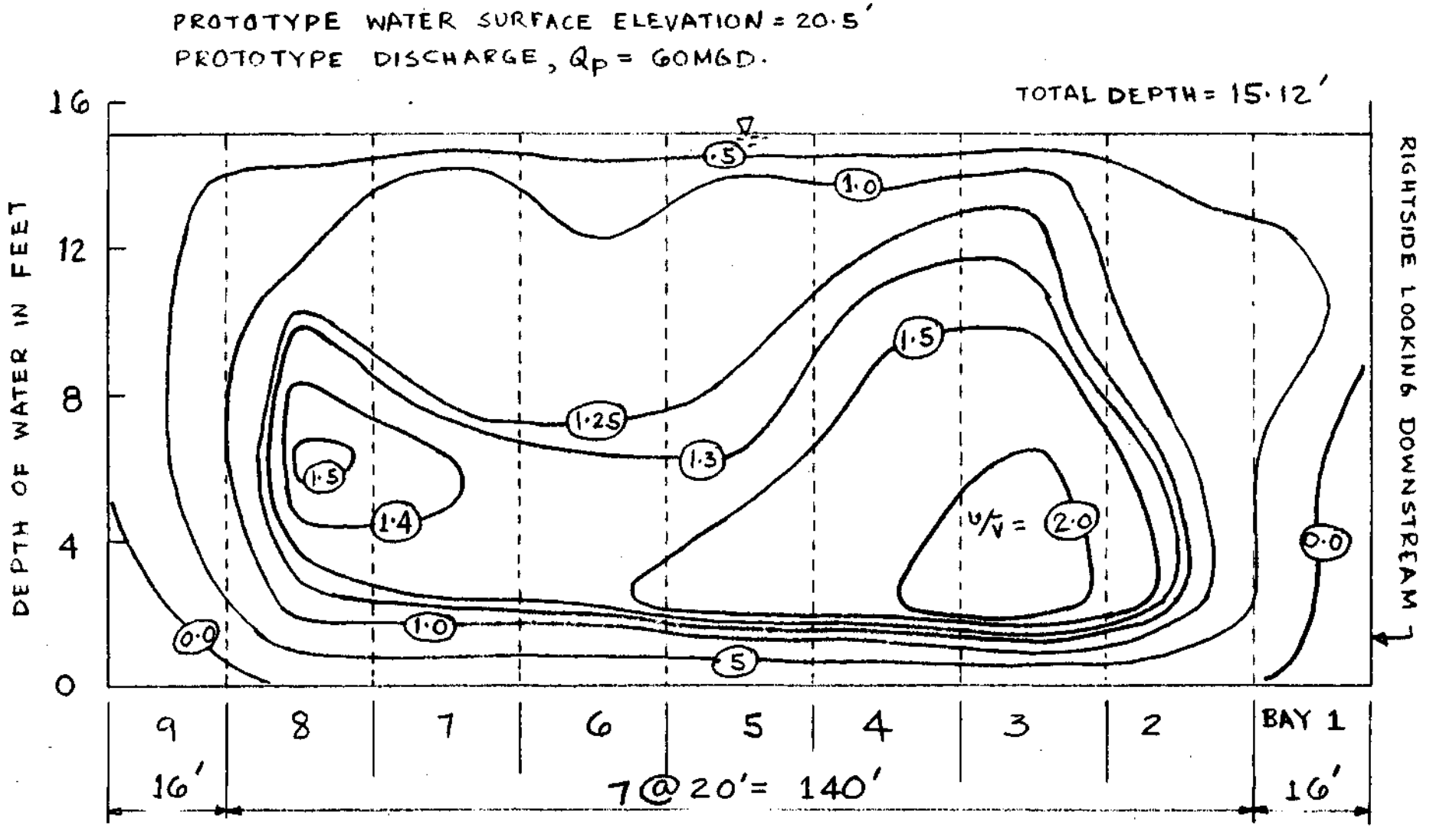


NOTE:- (1) FLOW VELOCITY IS EQUAL TO ZERO AT THE WALLS AND ALSO AT THE WATER SURFACE.

(2) RATIO OF THE POINT VELOCITY TO THE AVERAGE VELOCITY IN THE CROSS-SECTION IS SHOWN AS THE THIRD VARIABLE, $(v/\bar{v})$.

FIGURE 23a. VELOCITY PISTRIBUTION IN THE UPPER SETTLING BASIN AT SECTION 1 FOR MODIFICATION 16.

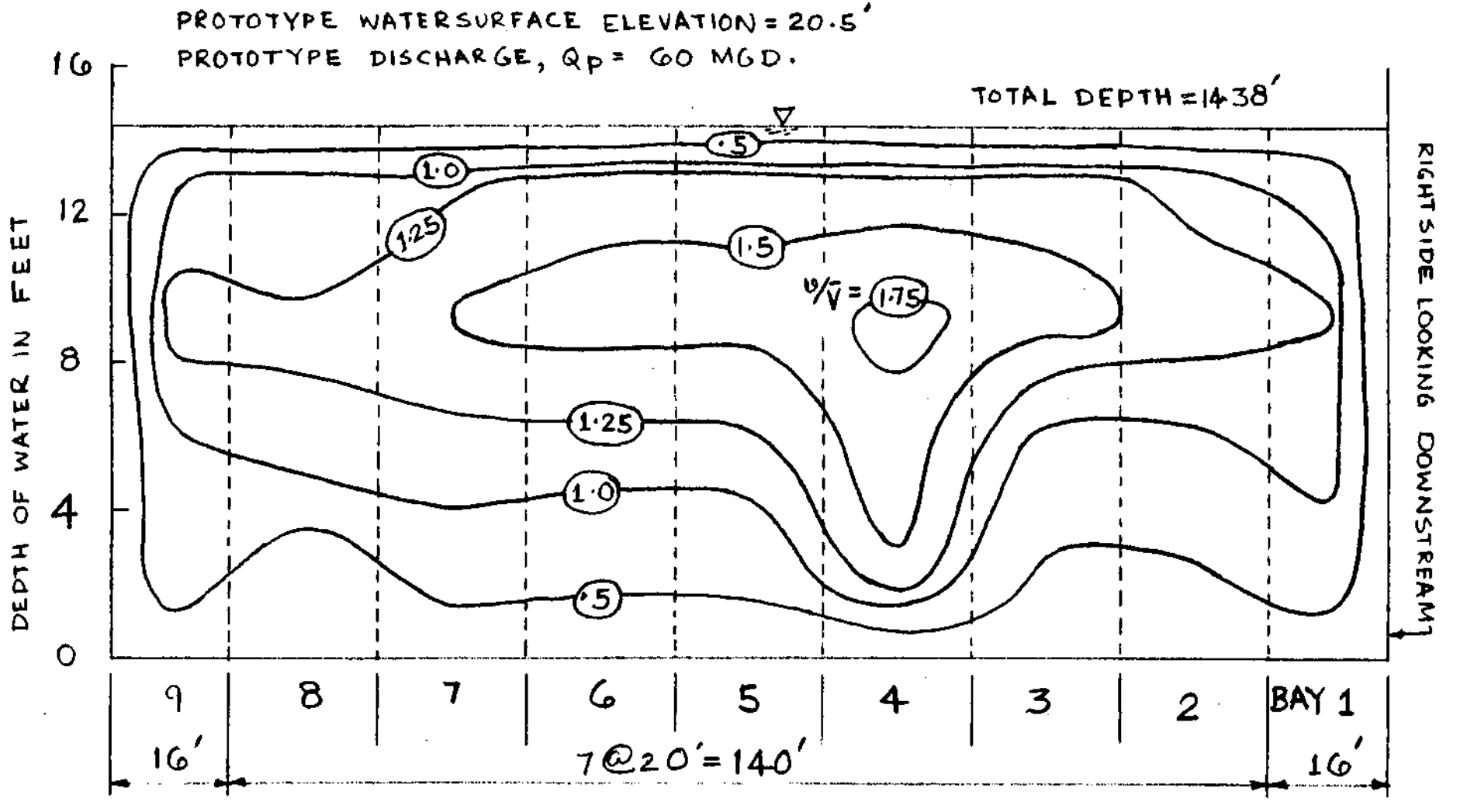


NOTE:- ① FLOW VELOCITY IS EQUAL TO ZERO AT THE WALLS AND ALSO AT THE WATER SURFACE.

② RATIO OF THE POINT VELOCITY TO THE AVERAGE VELOCITY IN THE CROSS-SECTION IS SHOWN AS THE THIRD VARIABLE, $(v/\bar{v})$.

FIGURE 23b. VELOCITY DISTRIBUTION IN THE UPPER SETTLING BASIN AT SECTION 3 FOR MODIFICATION 16.

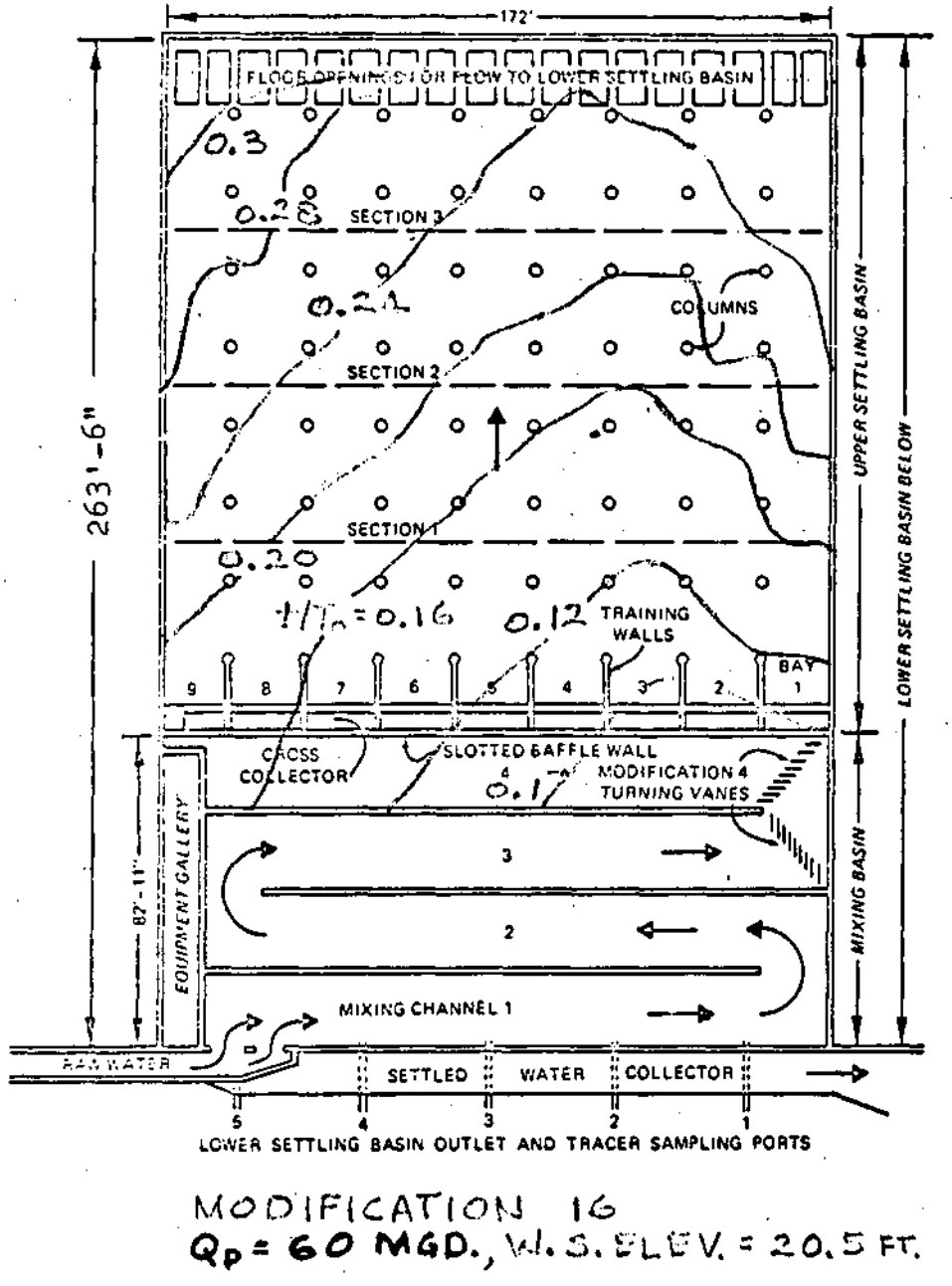


FIGURE 24. DYE FRONT LOCATION IN UPPER SETTLING BASIN AS OBSERVED FROM MOVIES FOR INDICATED RELATIVE TIME $t/T_0$.

Figure 25a. Tracer Results, Modification 18

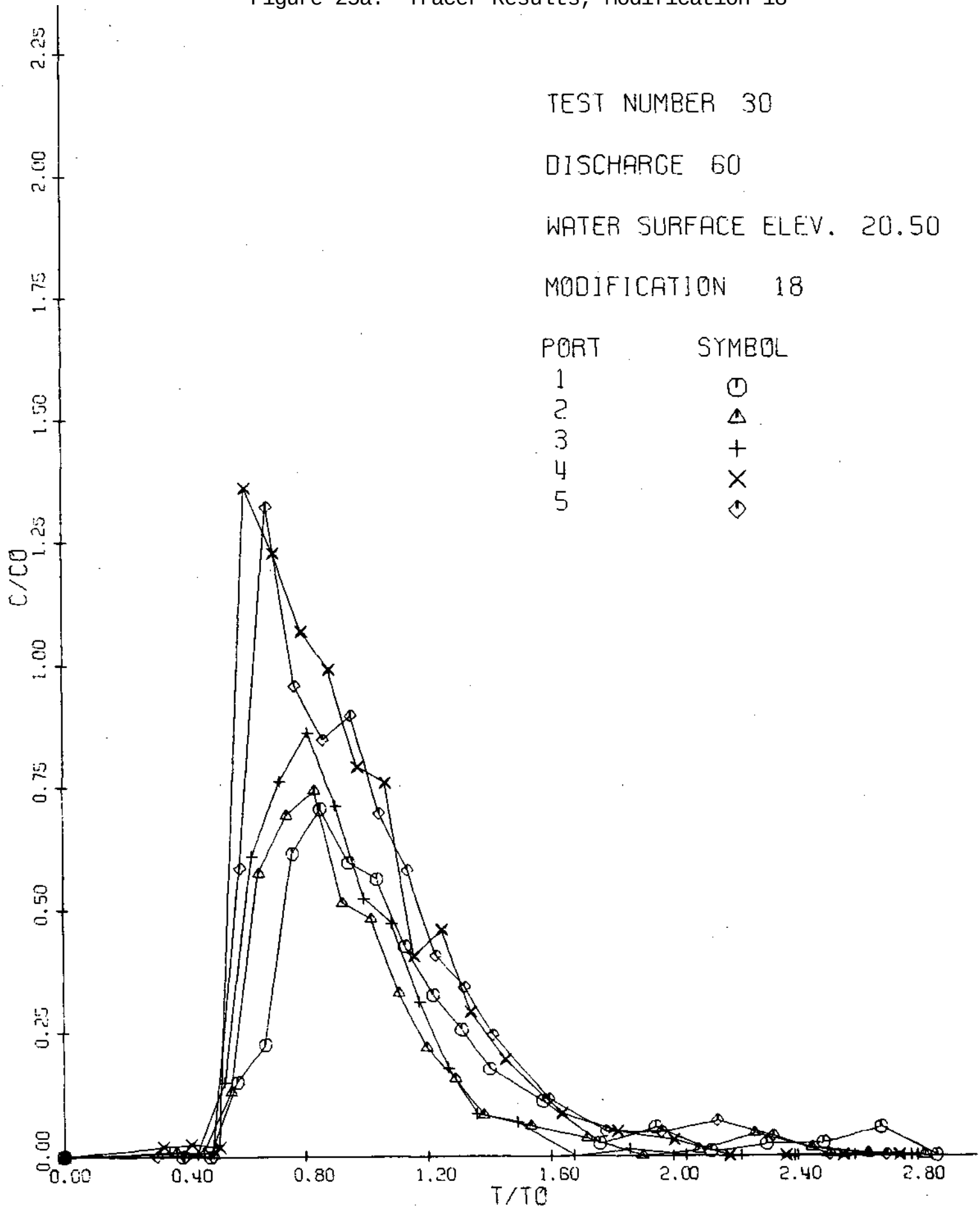

Figure 25b. Tracer Results, Modification 18

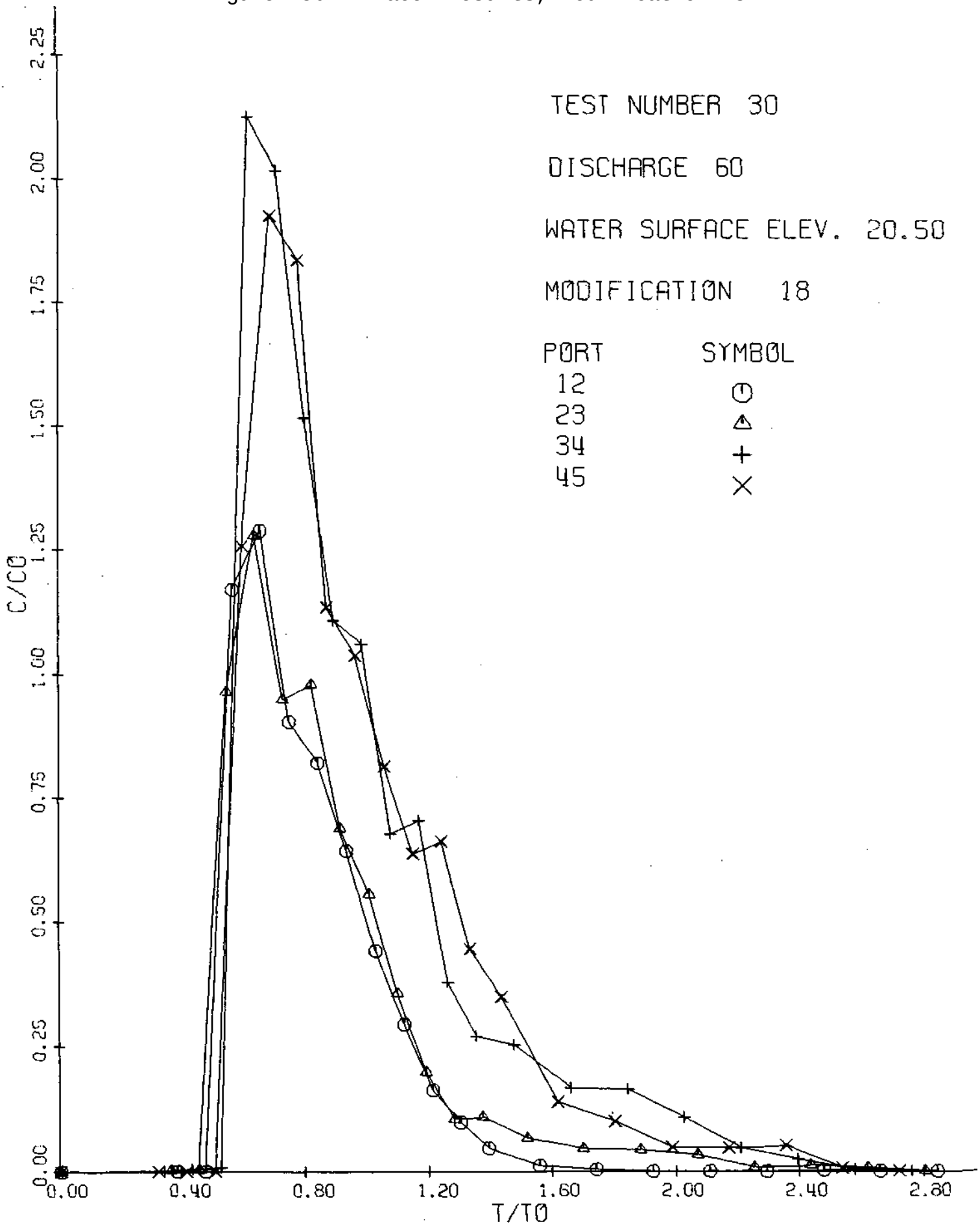

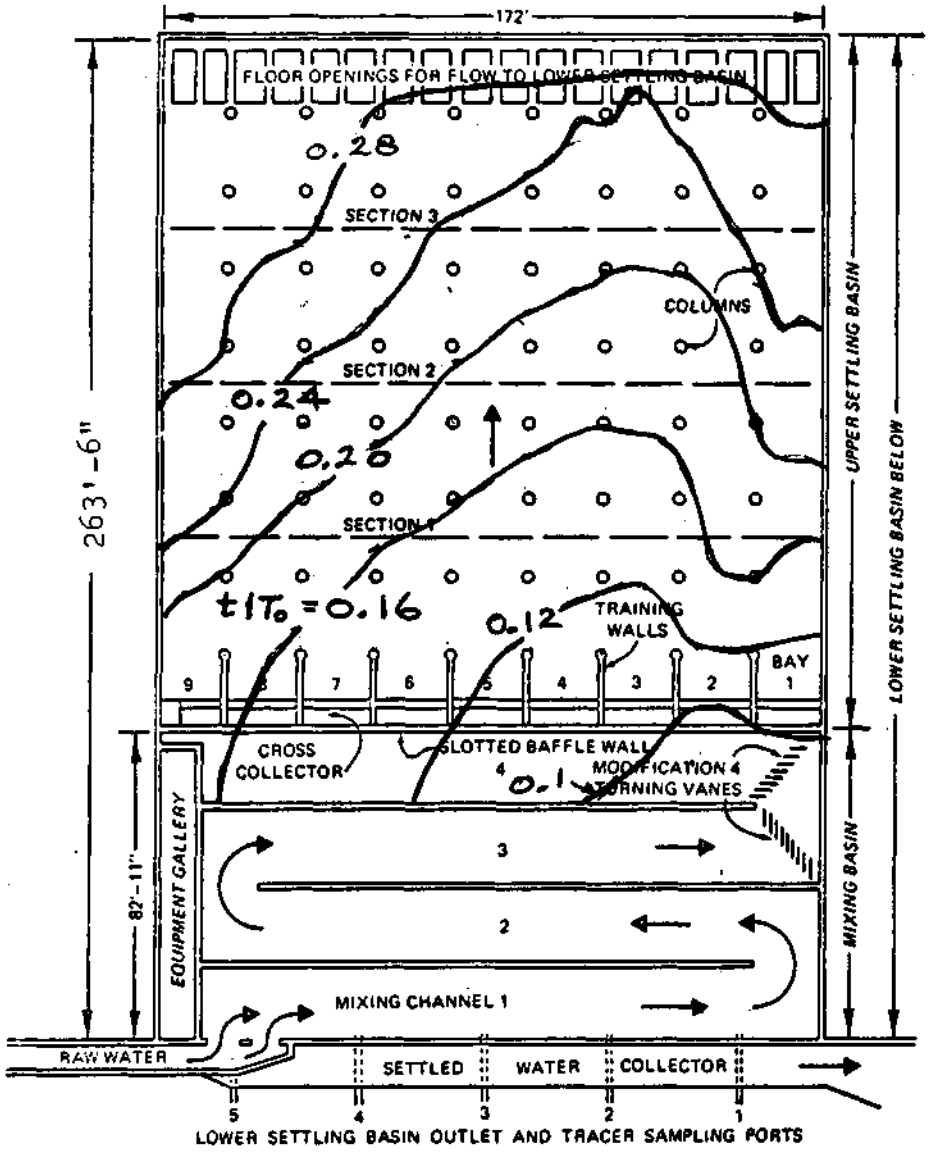


MODIFICATION 18
$Q_p$ = 60 MGD., W.S. ELEV. = 20.5 FT.

FIGURE 26/ DYE FRONT LOCATION IN UPPER SETTLING BASIN AS OBSERVED FROM MOVIES FOR INDICATED RELATIVE TIME t/To.

Figure 27a. Tracer Results, Modification 19

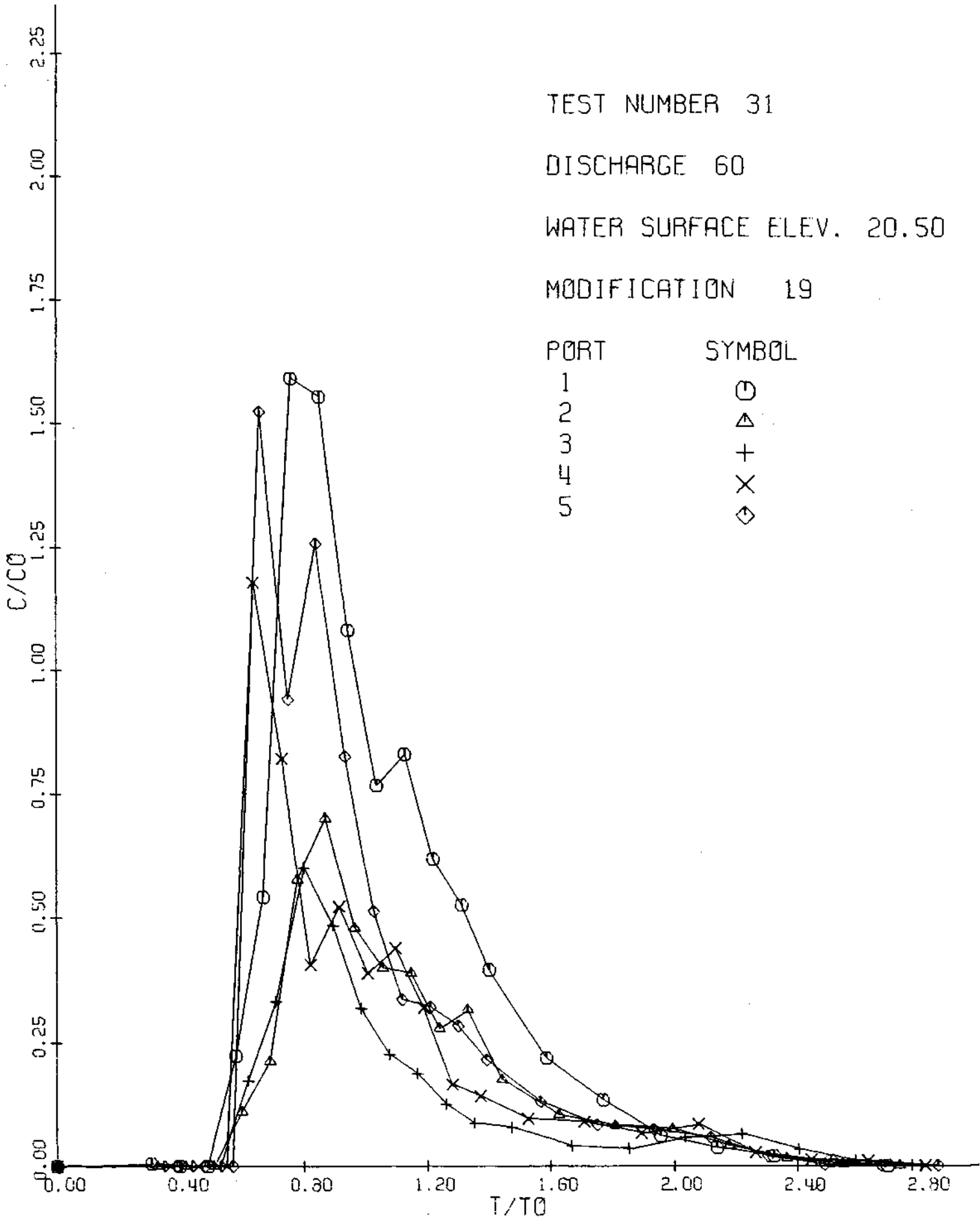

Figure 27b. Tracer Results, Modification 19

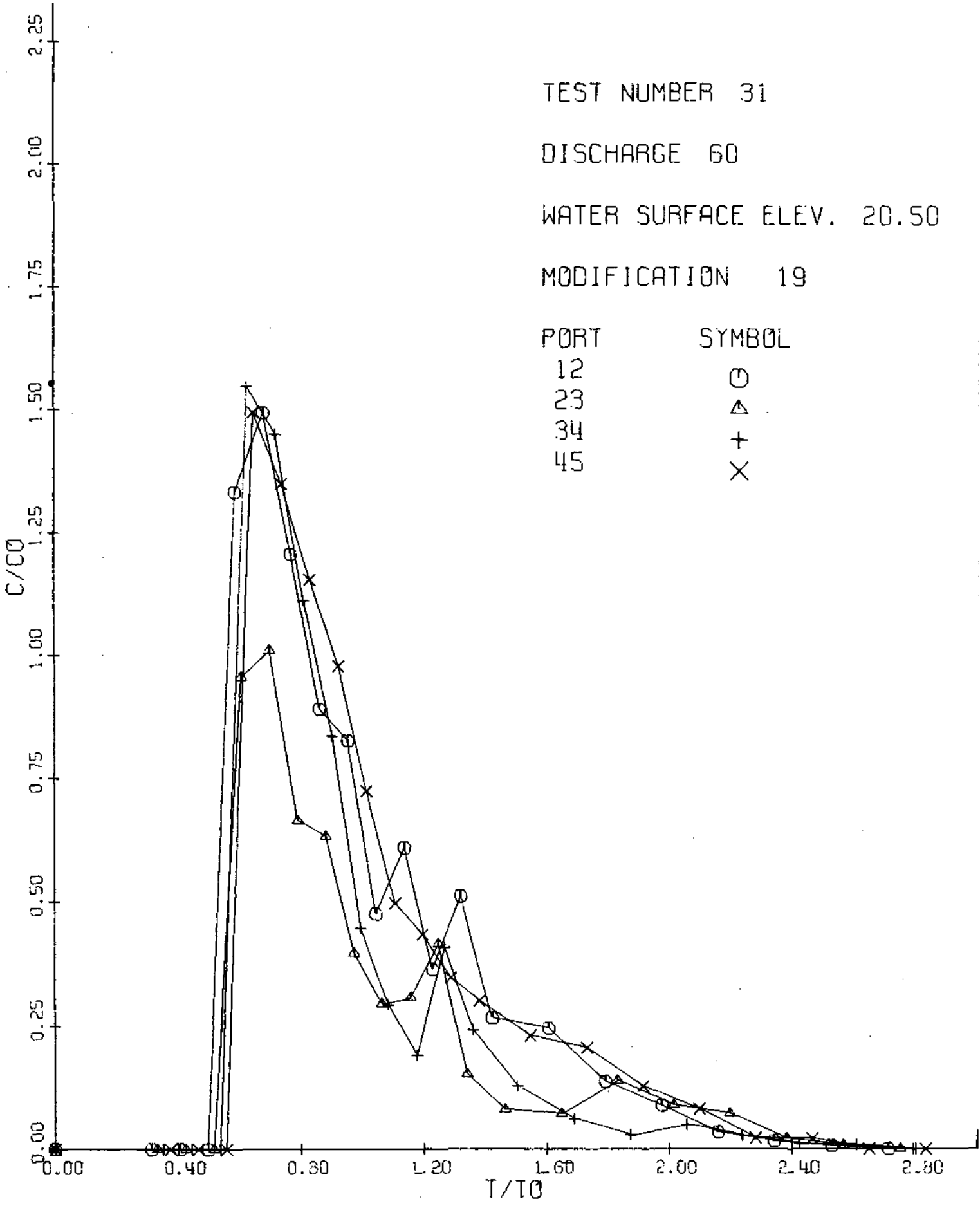

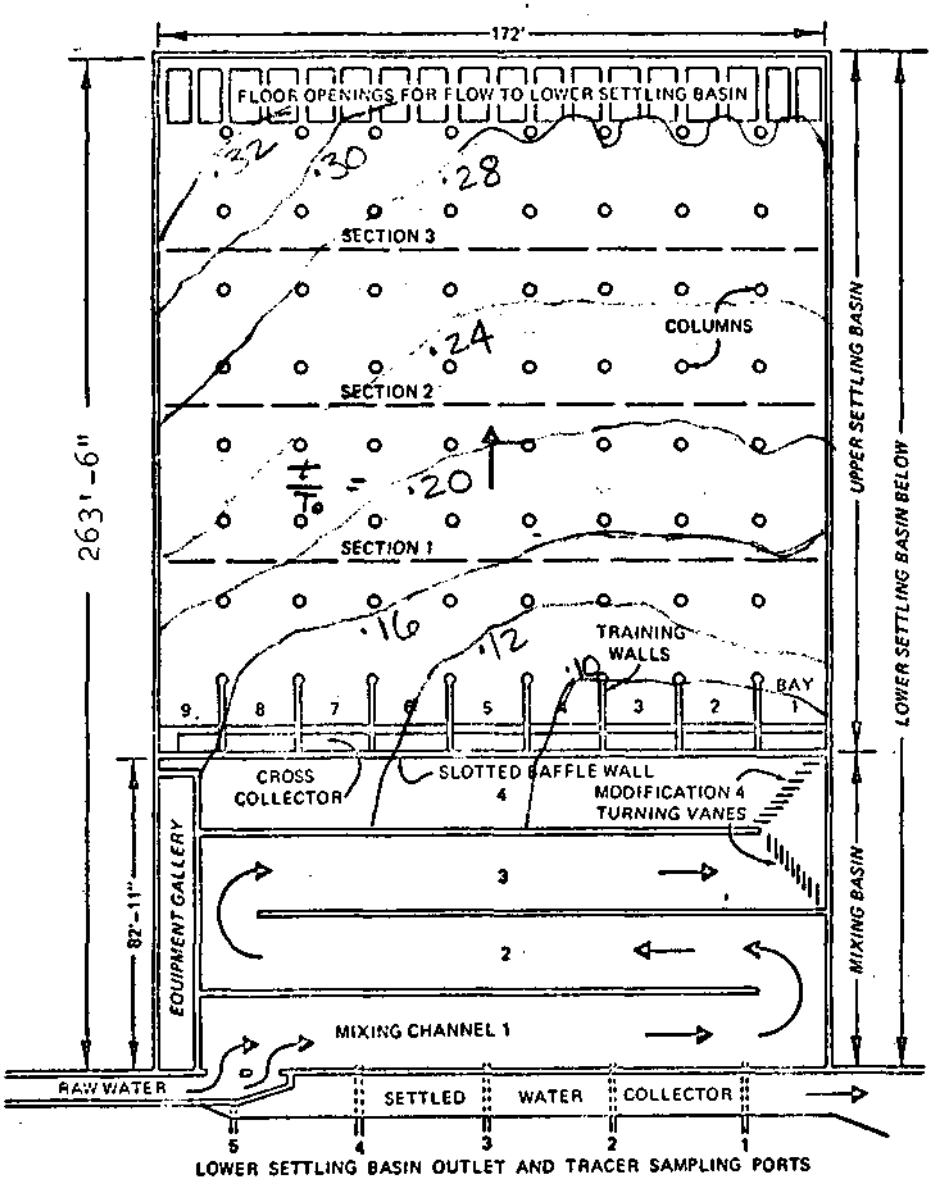


Figure 28. Dye front location in upper settling basin, Modification 19

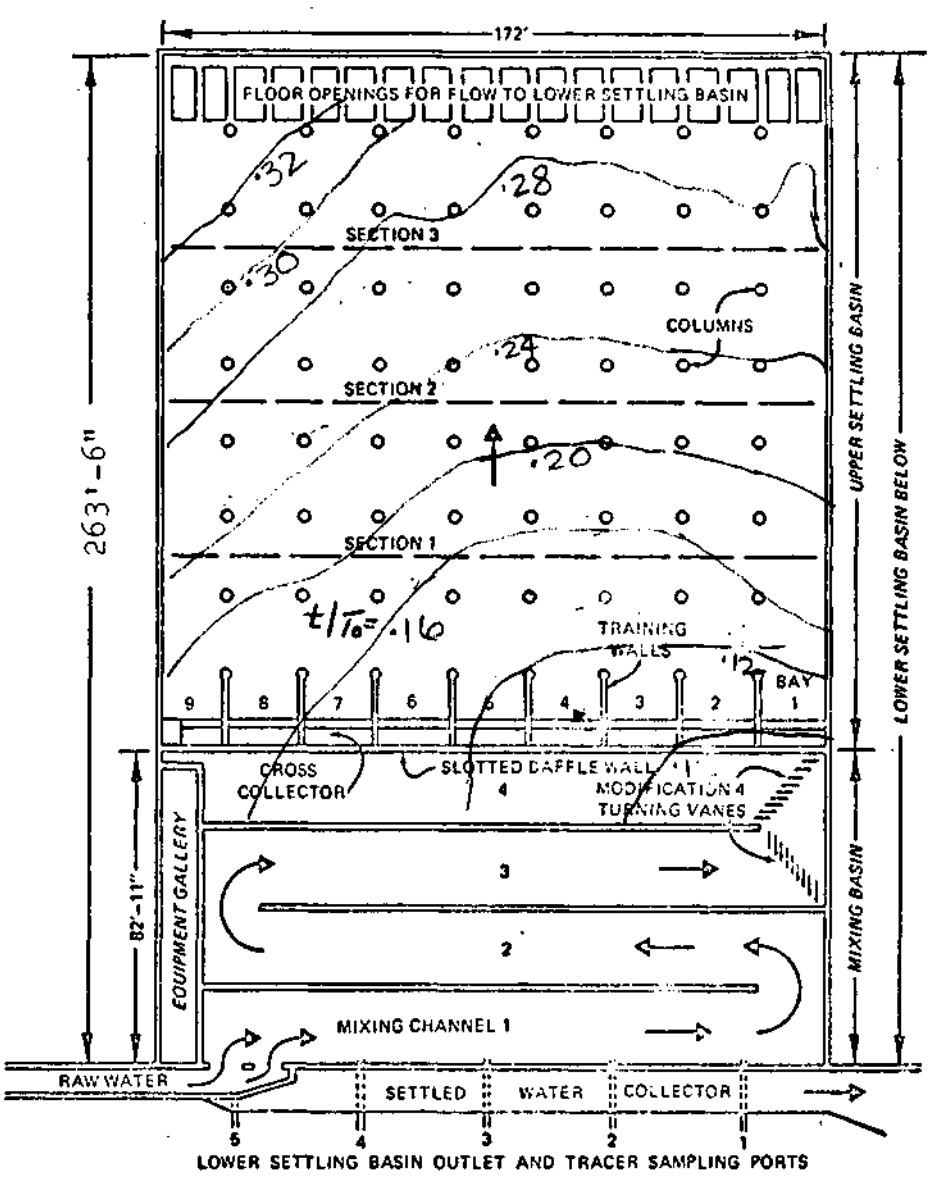


Figure 29. Dye front location in upper settling basin, Modification 20

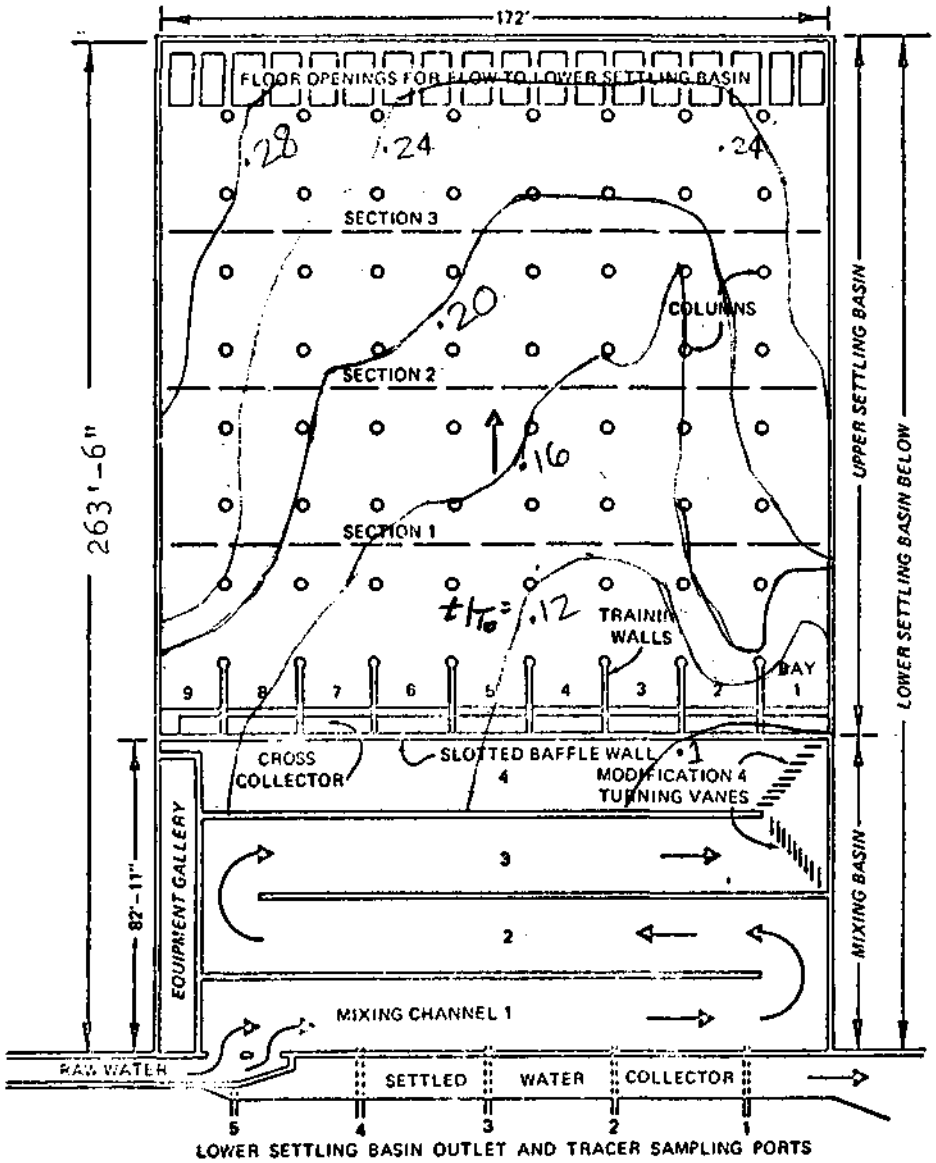


Figure 30. Dye front location in upper settling basin, Modification 21

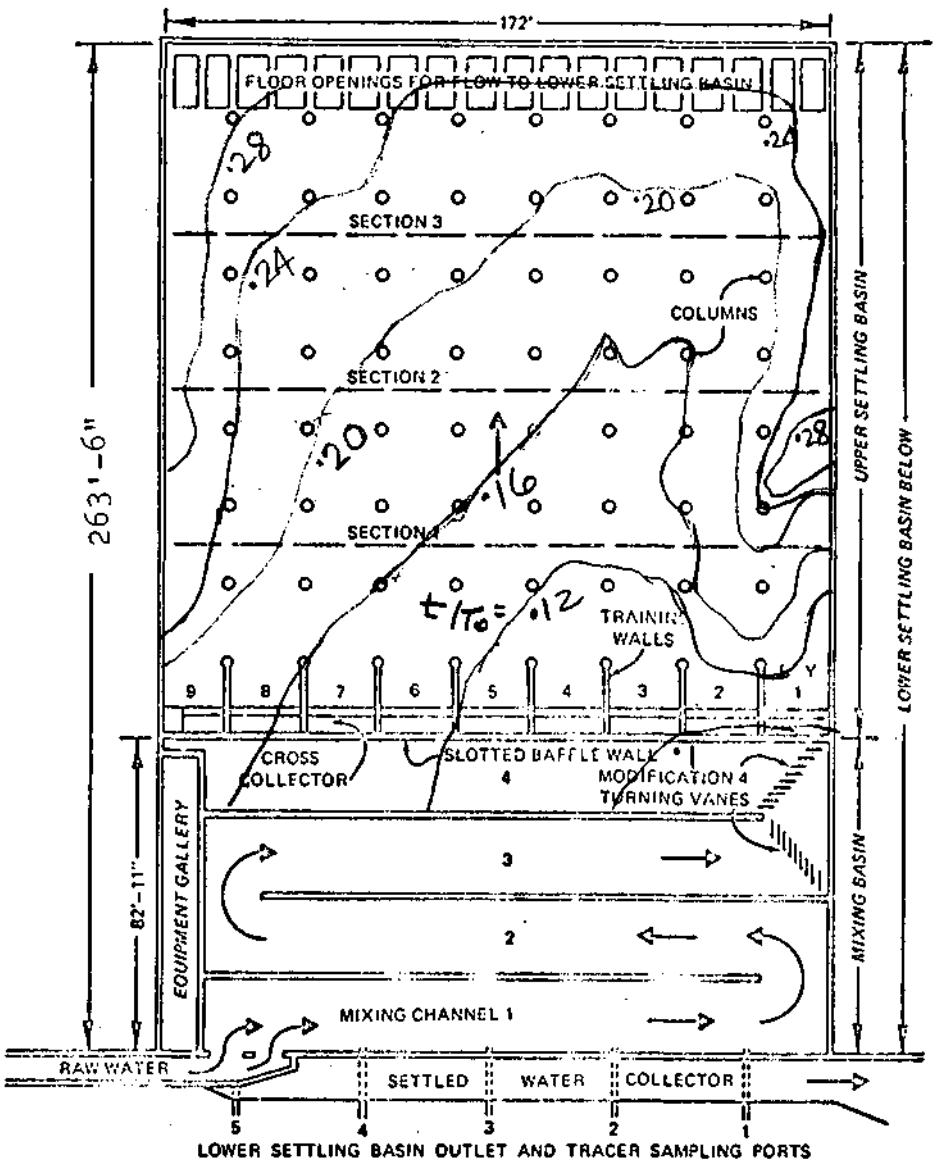


Figure 31. Dye front location in upper settling basin, Modification 22

Figure 32. Tracer Results, Modification 24

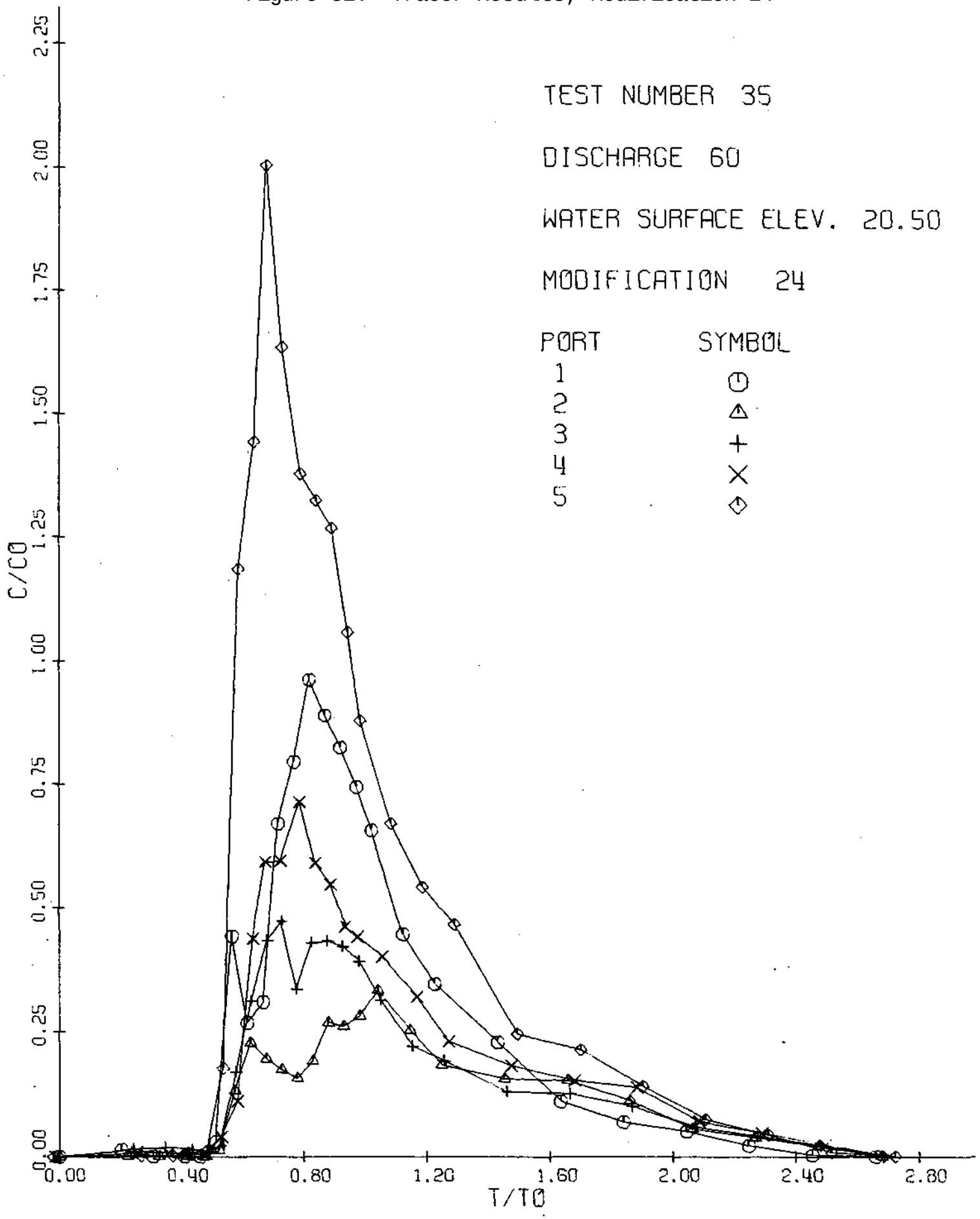

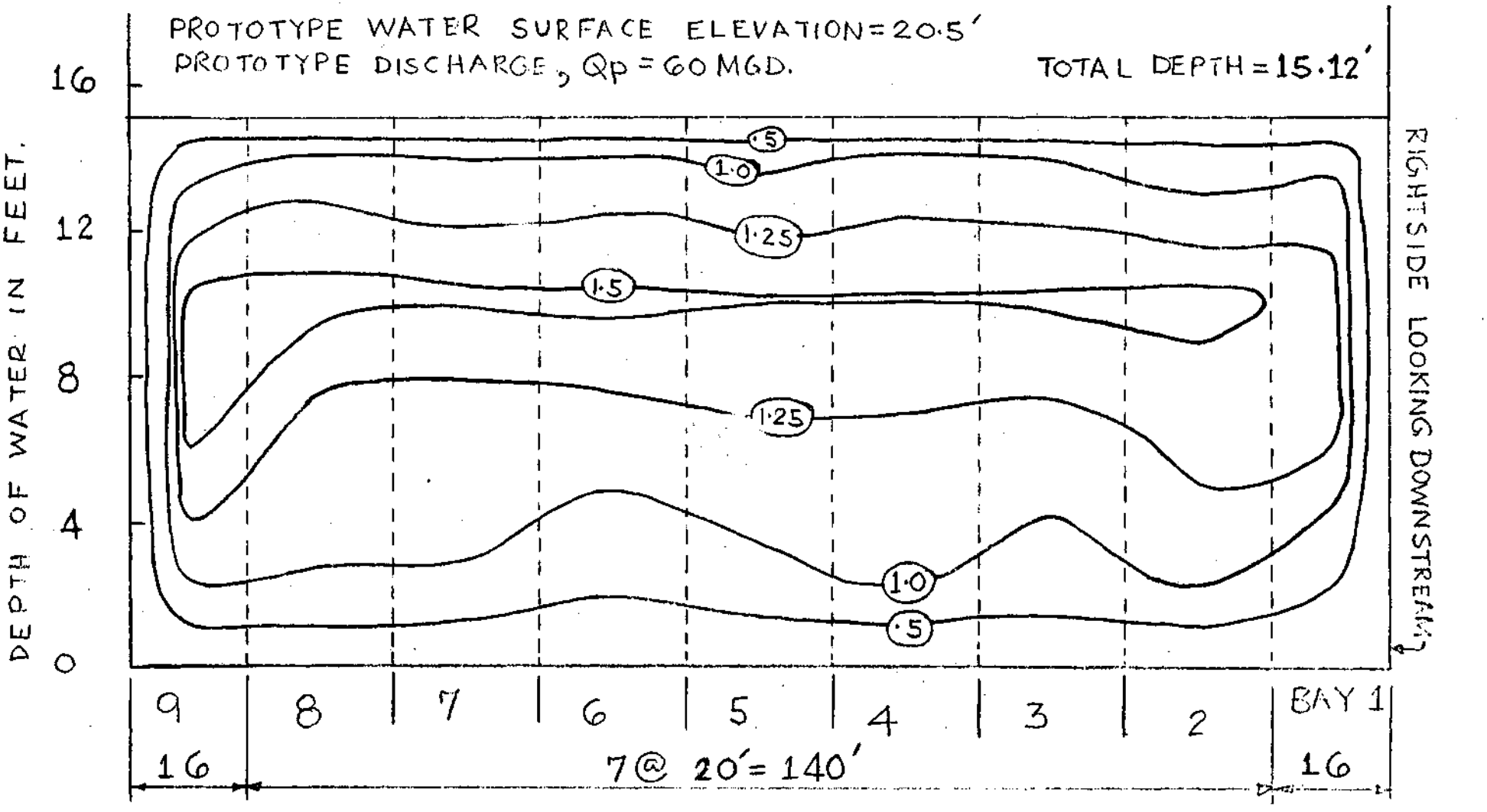


NOTE :- ① FLOW VELOCITY IS EQUAL TO ZERO AT THE WALLS AND ALSO AT THE WATER SURFACE.

② RATIO OF THE POINT VELOCITY TO THE AVERAGE VELOCITY IN THE CROSS-SECTION IS SHOWN AS THE THIRD VARIABLE, $(v/\bar{v})$.

FIGURE 33a. VELOCITY DISTRIBUTION IN THE UPPER SETTLING BKSIN AT SECTION 1 FOR MODIFICATION 24.

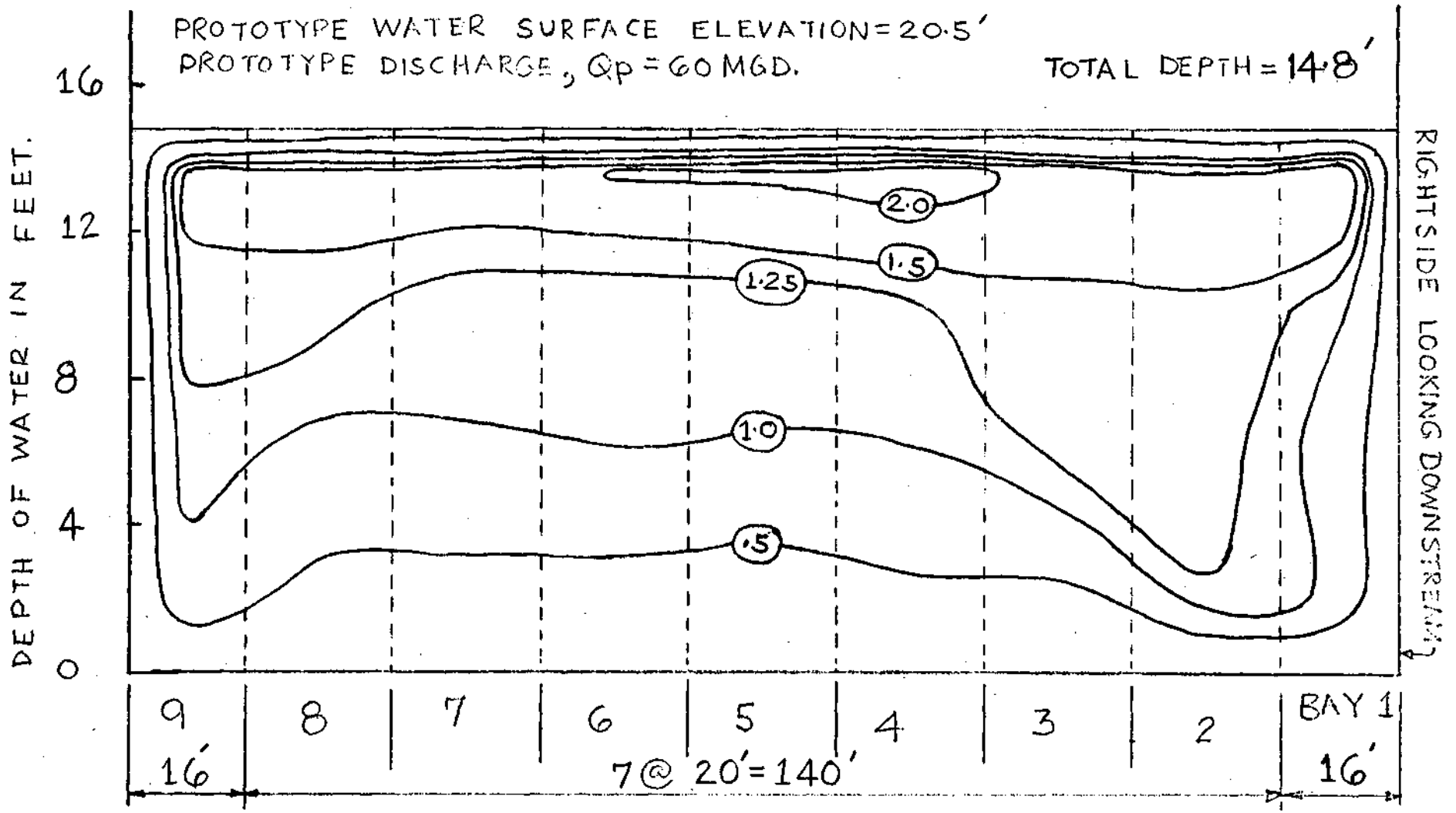


NOTE :- ① FLOW VELOCITY IS EQUAL TO ZERO AT THE WALLS AND ALSO AT THE WATER SURFACE.

② RATIO OF THE POINT VELOCITY TO THE AVERAGE VELOCITY IN THE CROSS-SECTION IS SHOWN AS THE THIRD VARIABLE, $(v/\bar{v})$.

FIGURE. 33b. VELOCITY DISTRIBUTION IN THE UPPER SETTUN6, BKSIN AT SECTION 2 . FOR MODIFICATION 24.

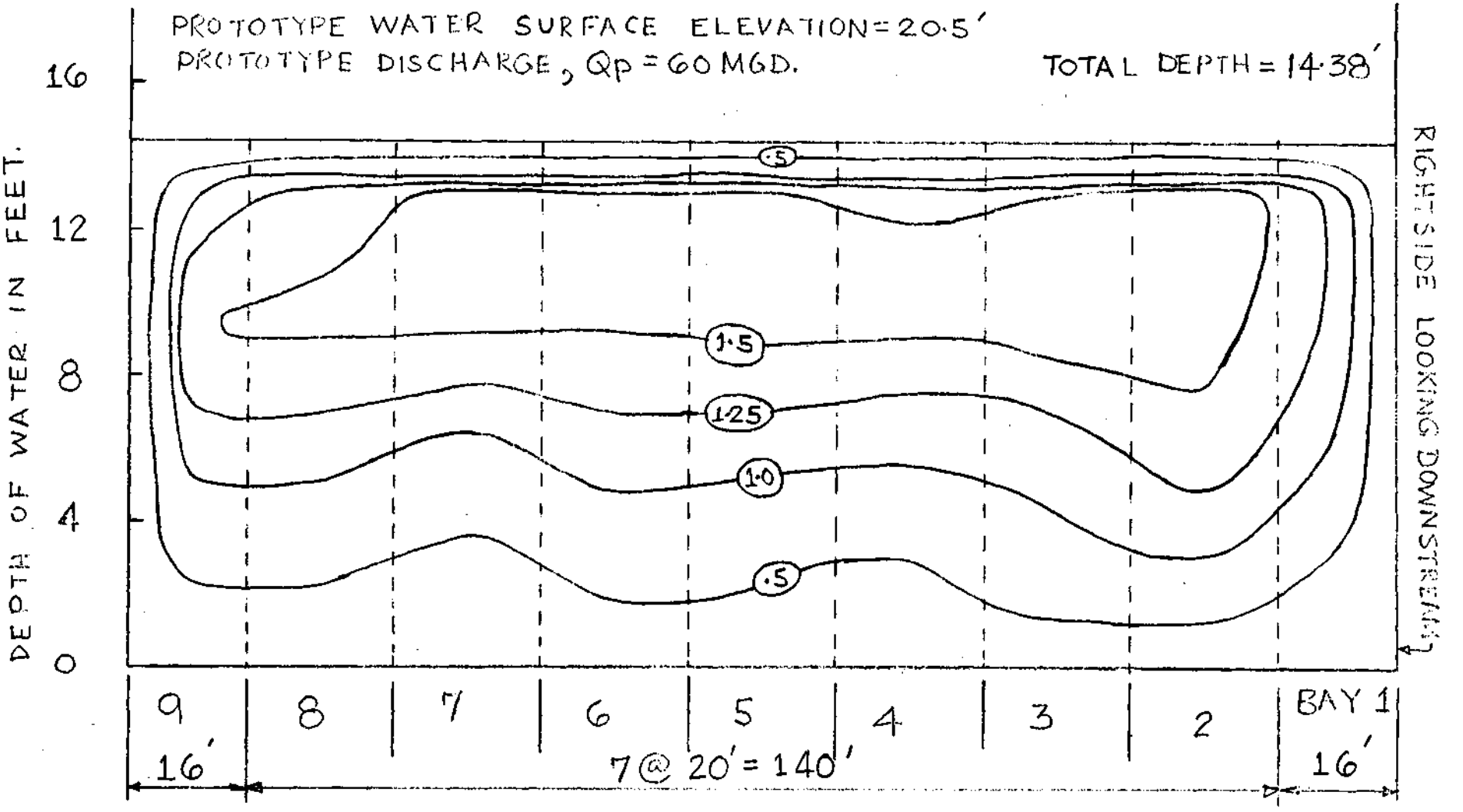


NOTE :- ① FLOW VELOCITY IS EQUAL TO ZERO AT THE WALLS AND ALSO AT THE WATER SURFACE.

② RATIO OF THE POINT VELOCITY TO THE AVERAGE VELOCITY IN THE CROSS-SECTION IS SHOWN AS THE THIRD VARIABLE, $(v/\bar{v})$.

FIGURE .33c. VELOCITY DISTRIBUTION IN UPPER SETTLING BKSIN AT SECTION 3 FOR MODIFICATION^'

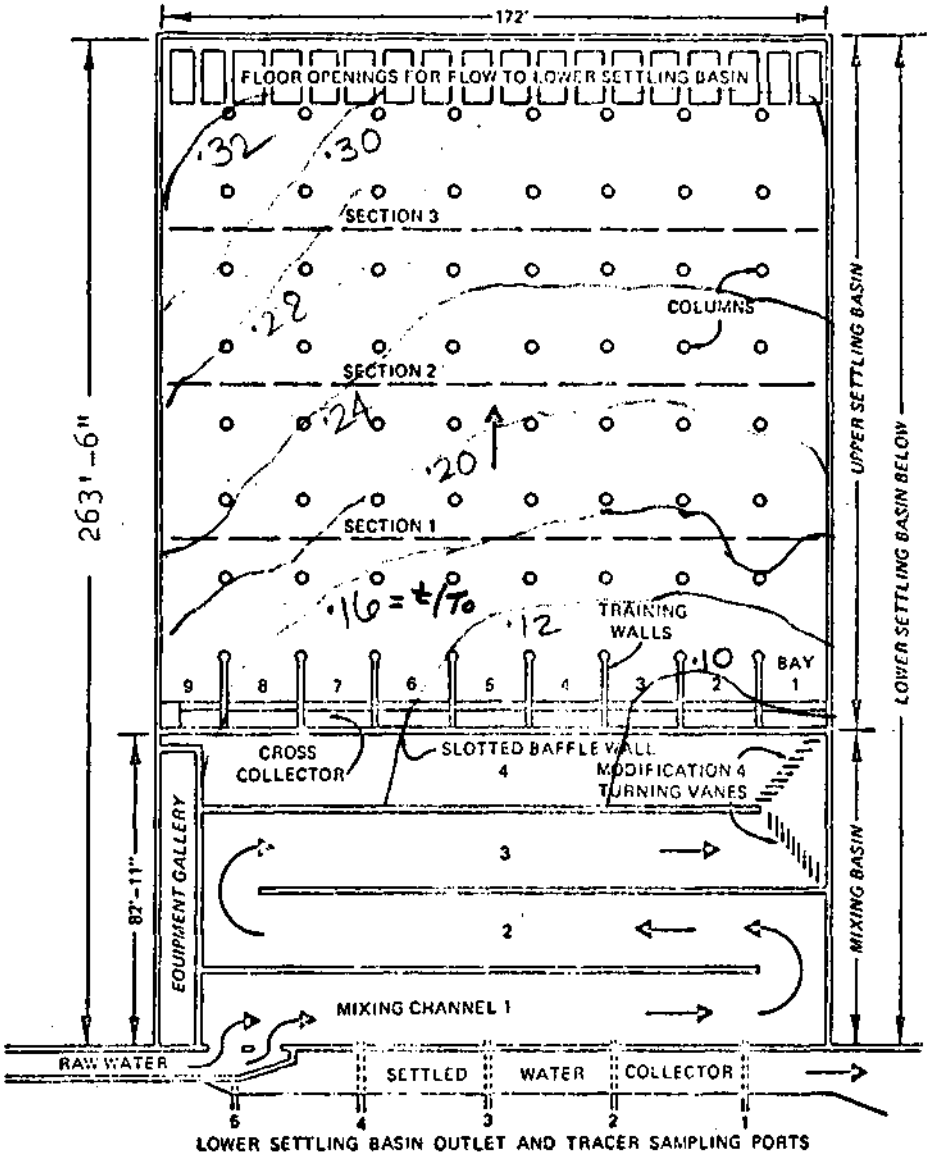


Figure 34. Dye front location in upper-settling basin, Modification 24

Figure 35. Tracer Results, Modification 25

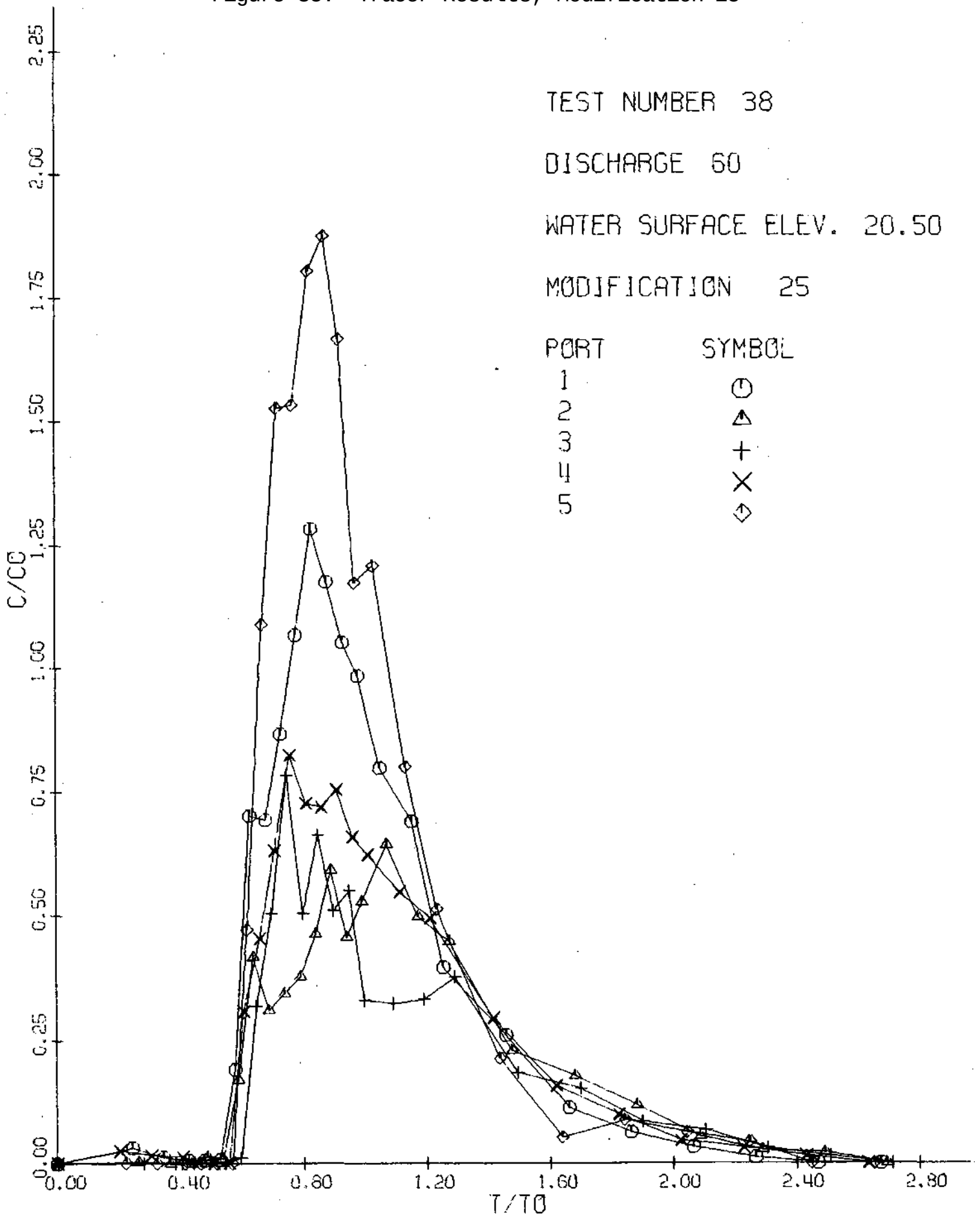

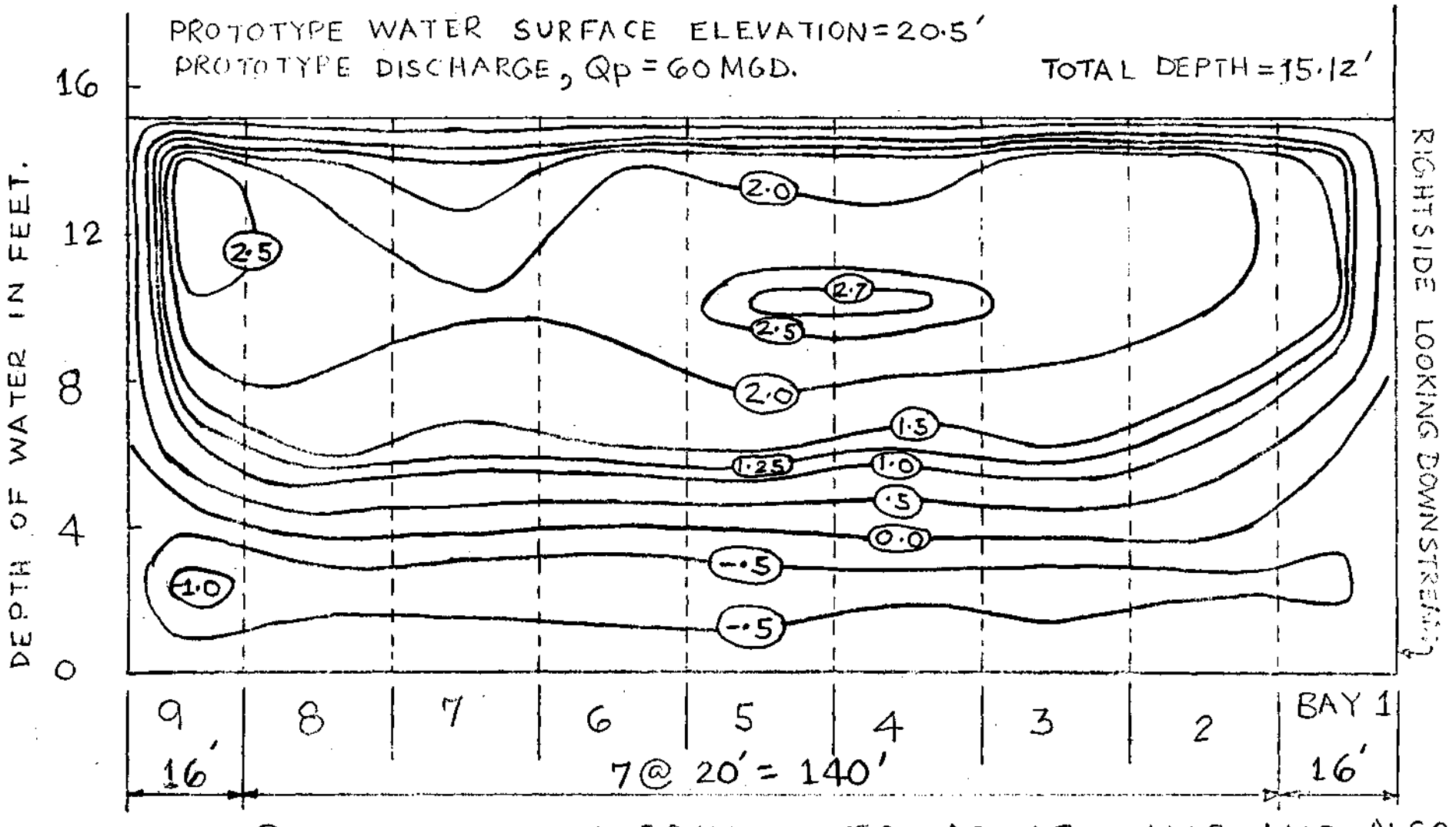


NOTE :- ① FLOW VELOCITY IS EQUAL TO ZERO AT THE WALLS AND ALSO AT THE WATER SURFACE.

② RATIO OF THE POINT VELOCITY TO THE AVERAGE VELOCITY IN THE CROSS-SECTION IS SHOWN AS THE THIRD VARIABLE, $(v/\bar{v})$.

FIGURE .36a. VELOCITY DISTRIBUTION IN THE UPPER SETTLING BASIN AT SECTION 1 FOR MODIFICATION 25.

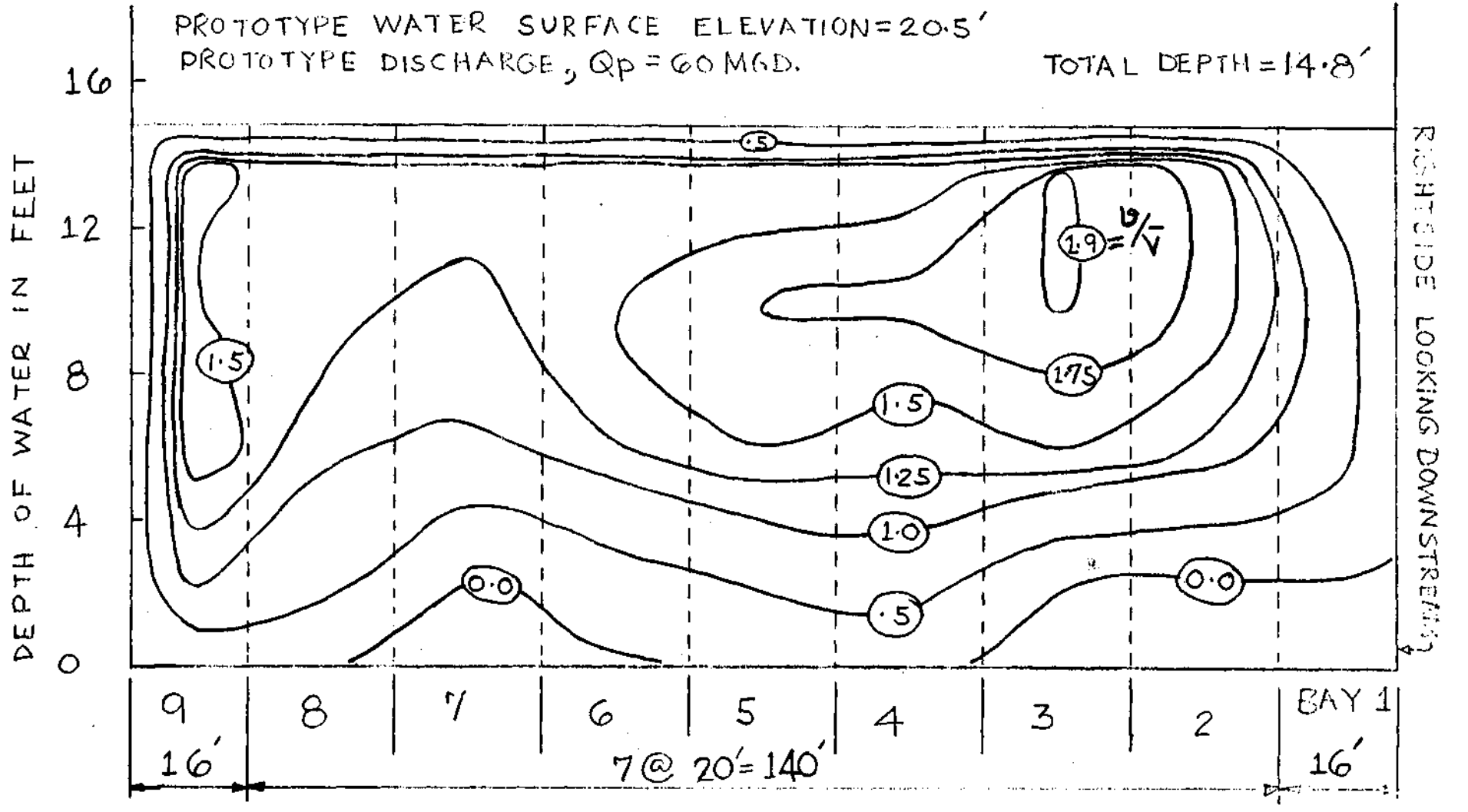


NOTE :- ① FLOW VELOCITY IS EQUAL TO ZERO AT THE WALLS AND ALSO AT THE WATER SURFACE.

② RATIO OF THE POINT VELOCITY TO THE AVERAGE VELOCITY IN THE CROSS-SECTION IS SHOWN AS THE THIRD VARIABLE, $(v/\bar{V})$.

FIGURE, 36b. VELOCITY DISTRIBUTION IN THE UPPER SETTLING BASIN AT SECTION 2 FOR MODIFICATION 25.

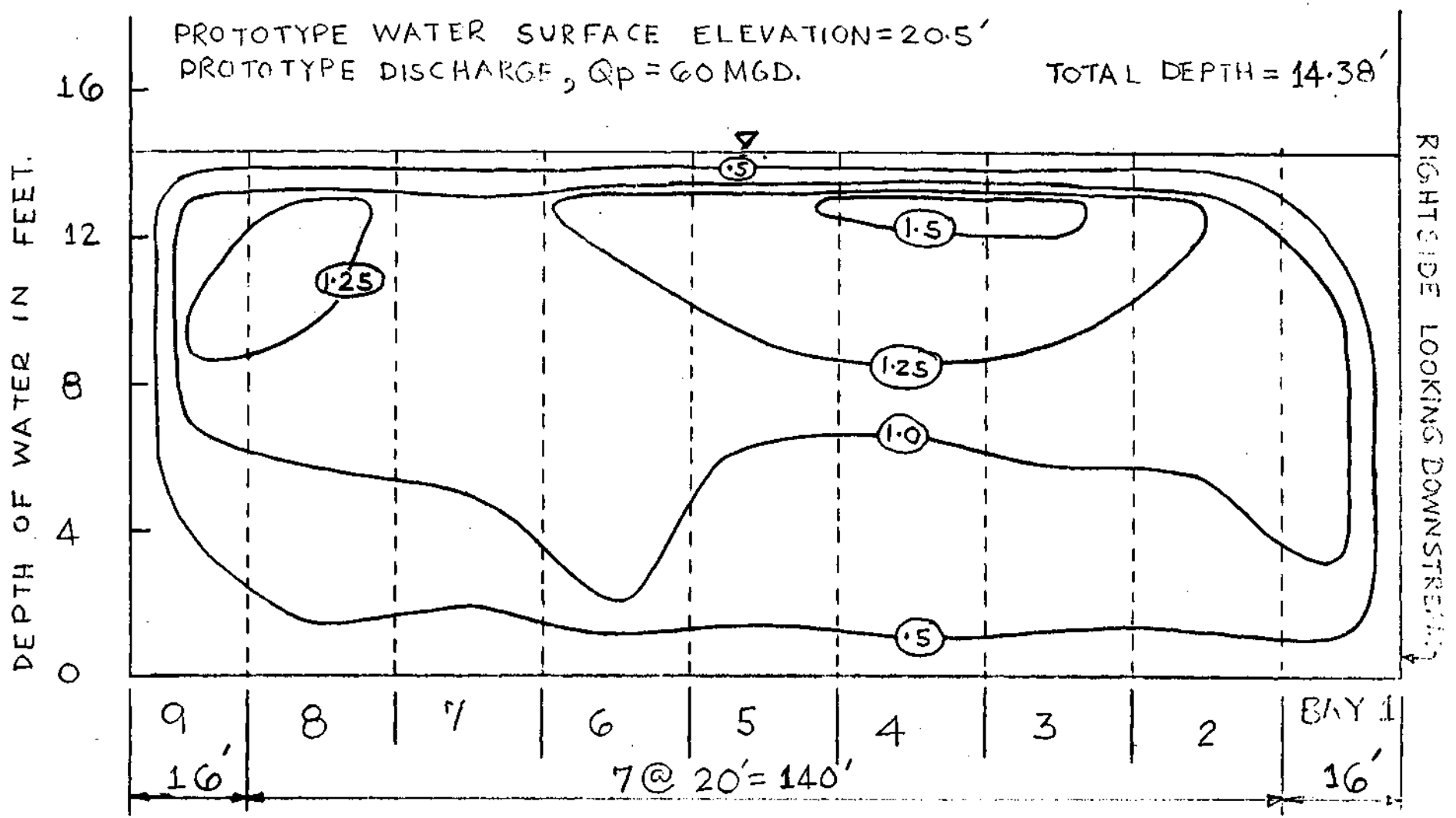


NOTE :- ① FLOW VELOCITY IS EQUAL TO ZERO AT THE WALLS AND ALSO AT THE WATER SURFACE.

② RATIO OF THE POINT VELOCITY TO THE AVERAGE VELOCITY IN THE CROSS-SECTION IS SHOWN AS THE THIRD VARIABLE, $(v/\bar{v})$.

FIGURE.36c. VELOCITY DISTRIBUTION IN THE UPPER SETTLING, BASIN AT SECTION 3 FOR MODIFICATION 25.

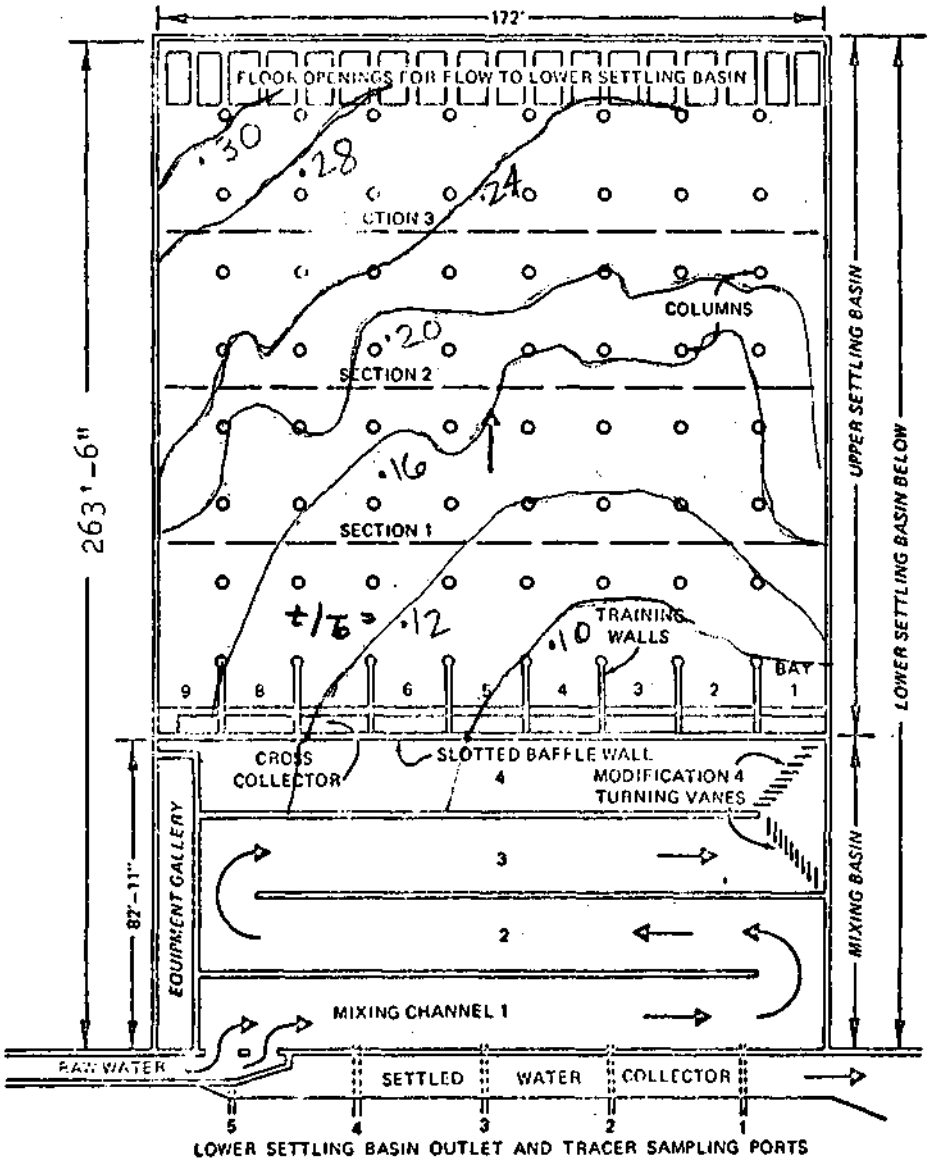


Figure 37. Dye front location in upper settling basin, Modification 25

Figure 38. Tracer Results, Modification 26

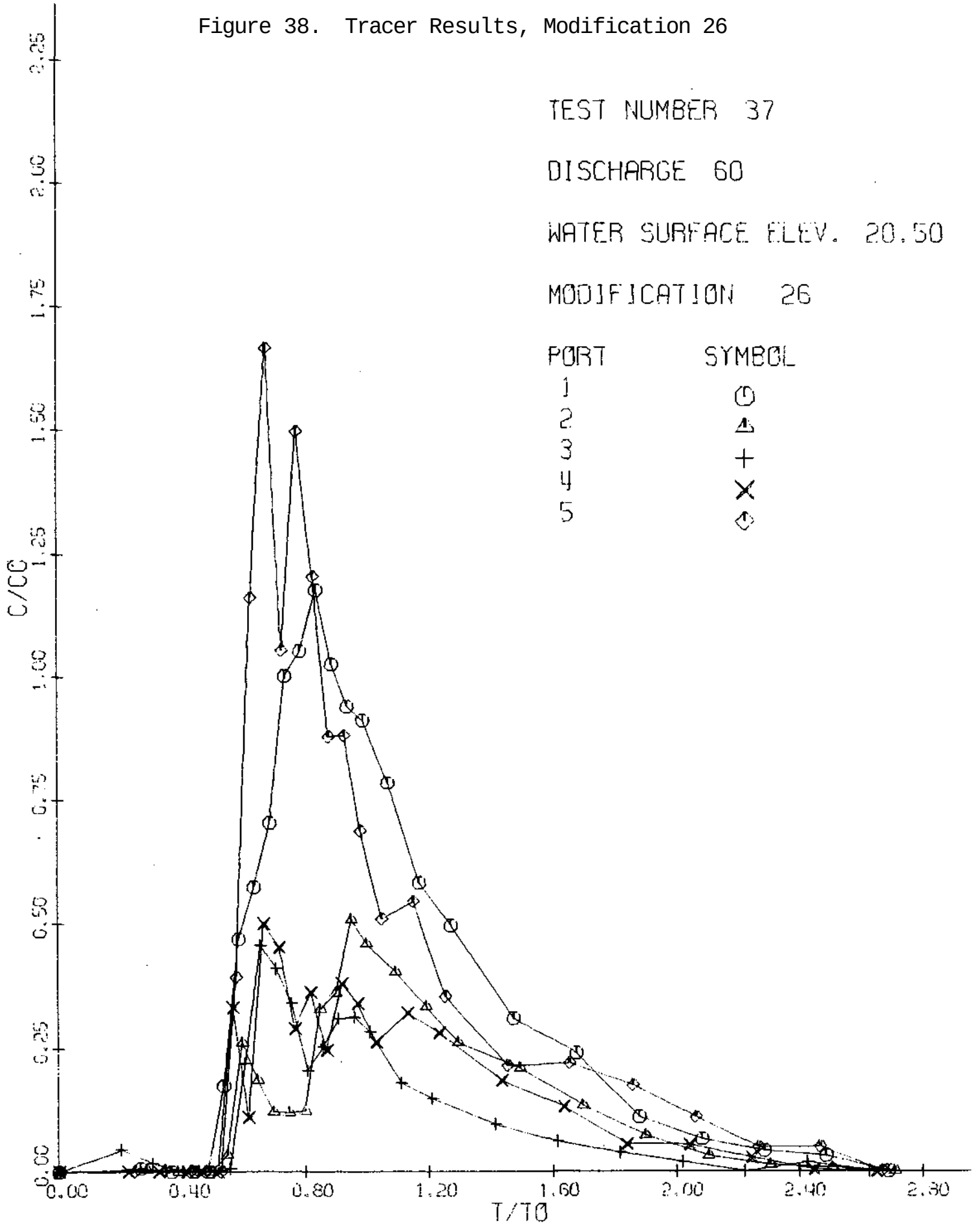

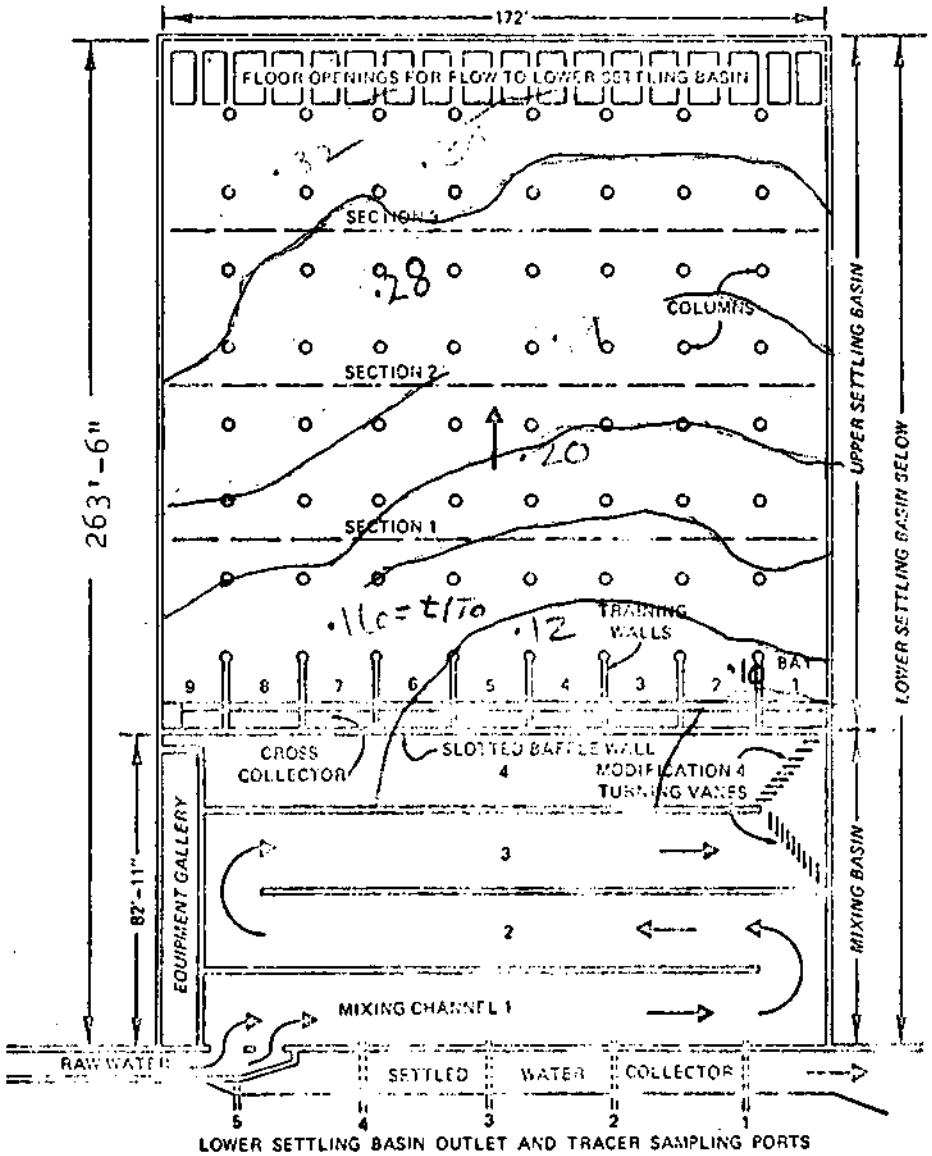


Figure 39. Dye front location in upper settling basin, Modification 26

Figure 40. Tracer Results at Model Outlet

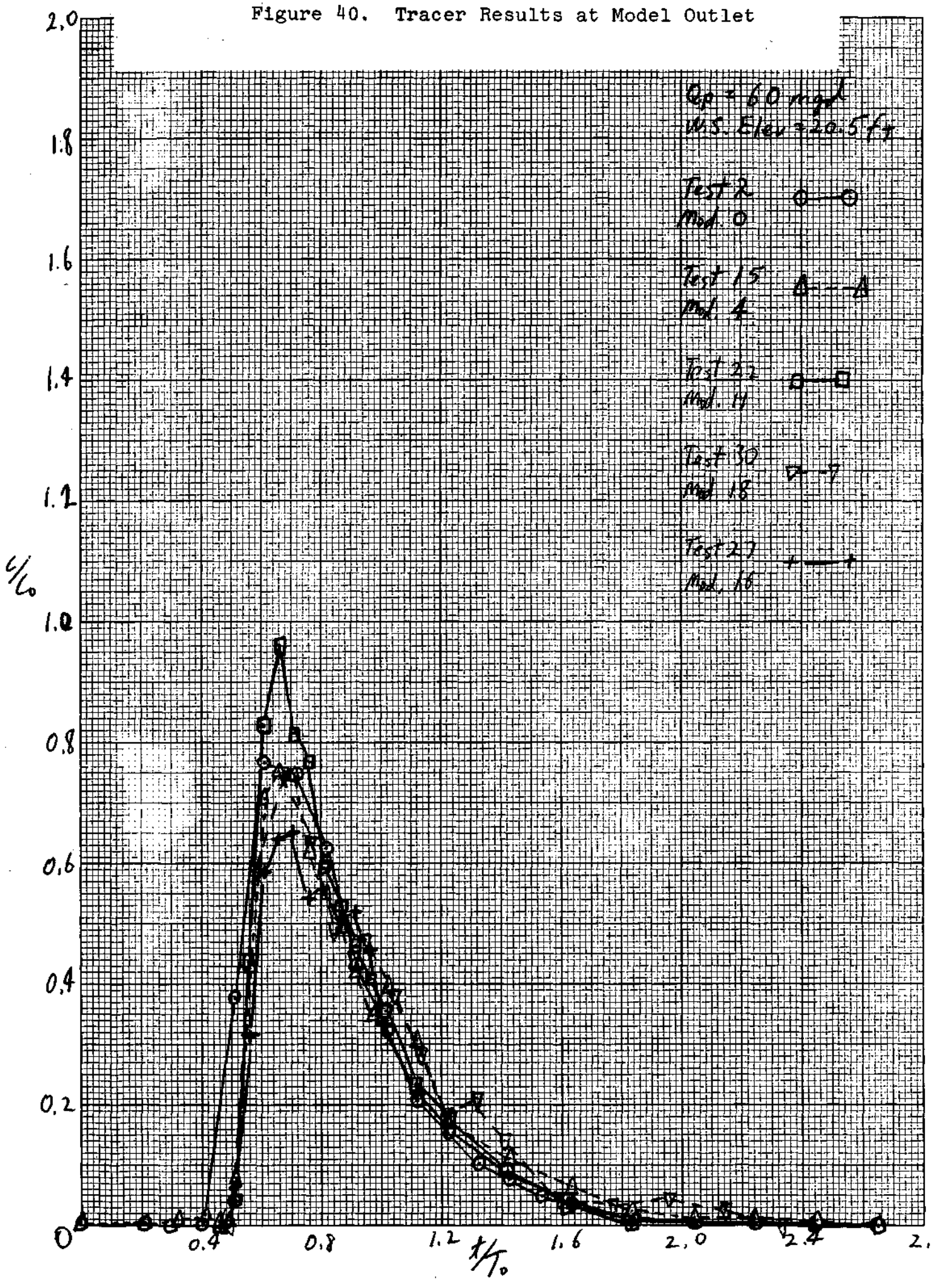

Figure 41, Tracer Distributions for Dispersion Test

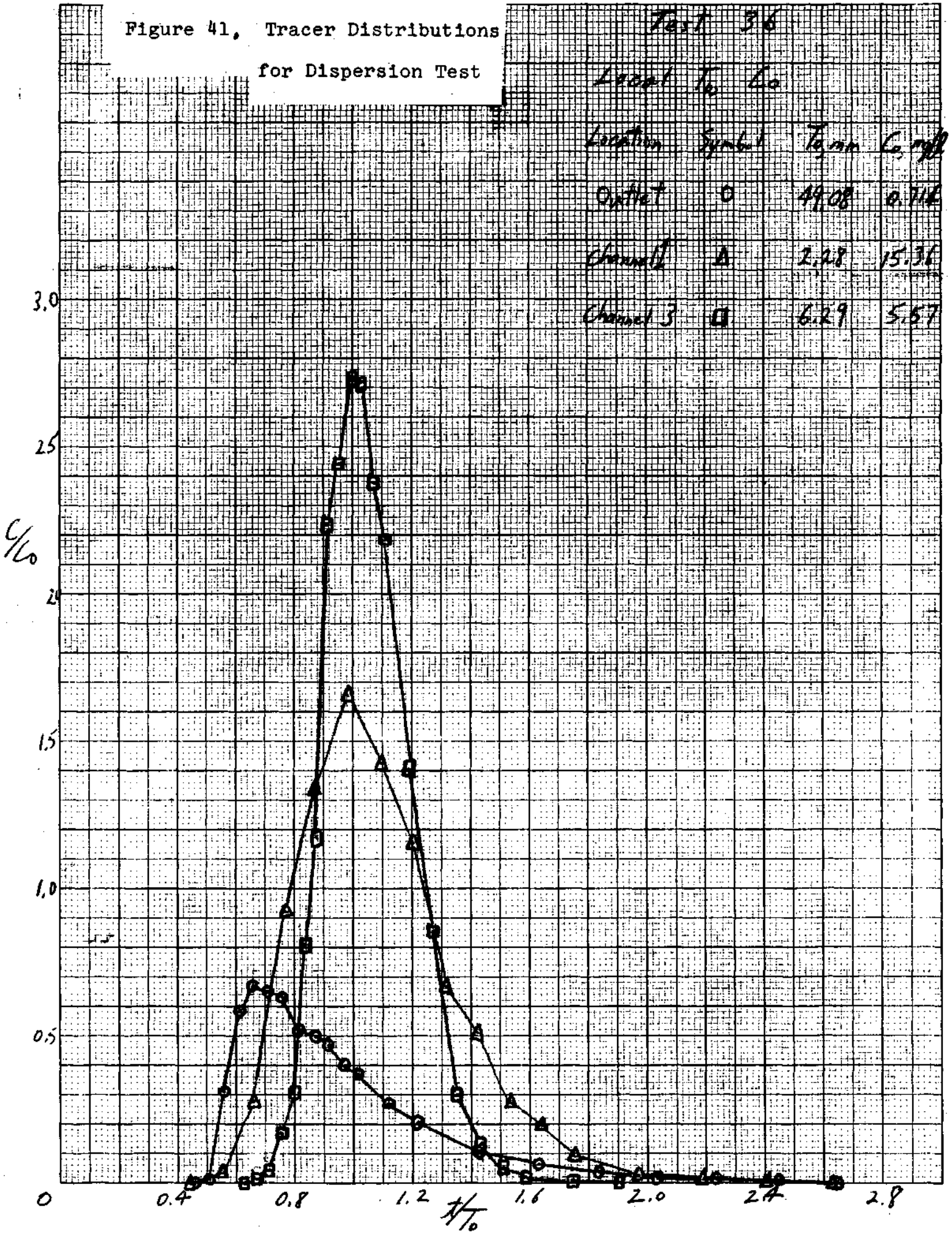

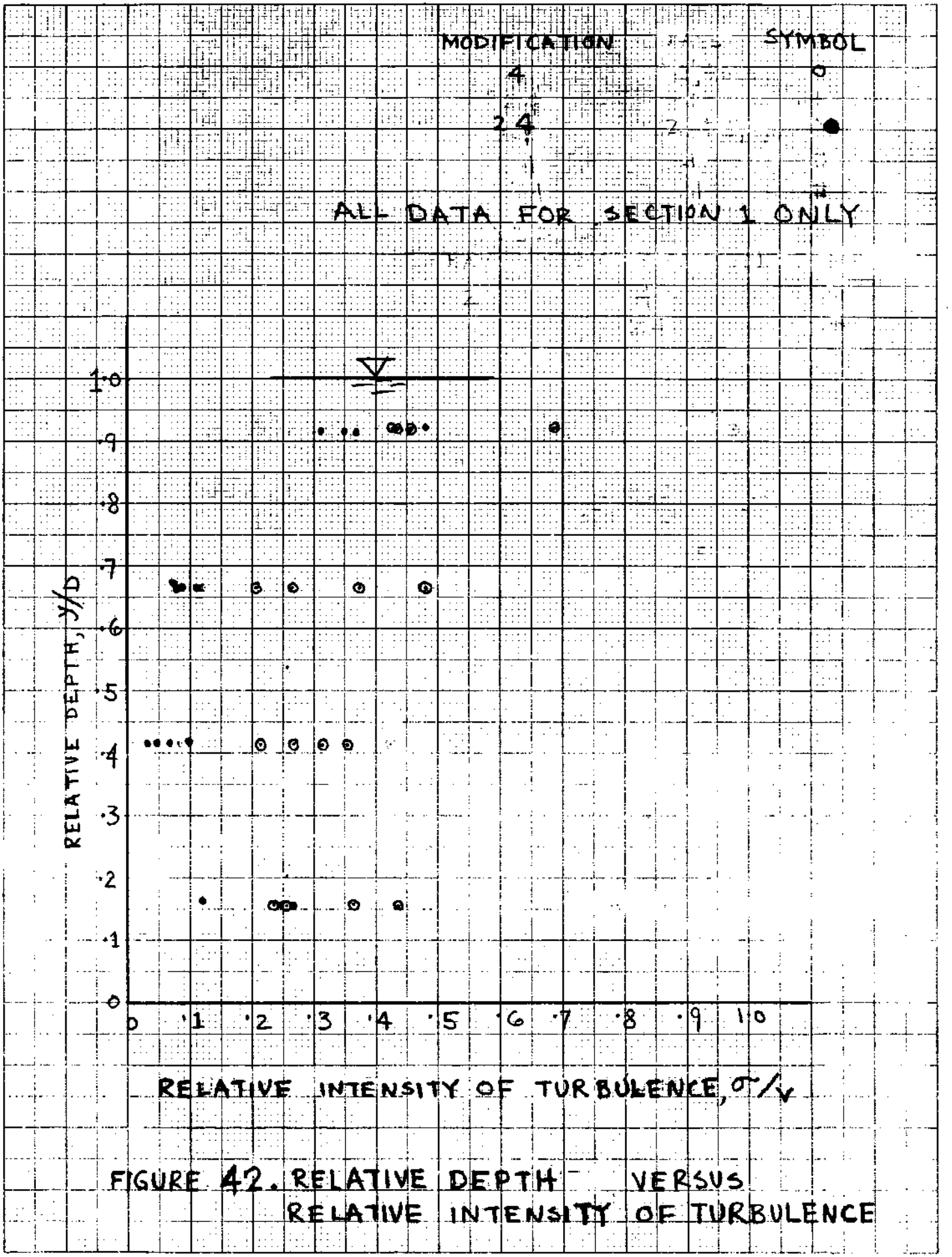


FIGURE 42. RELATIVE DEPTH VERSUS RELATIVE INTENSITY OF TURBULENCE

# APPENDICES

# APPENDIX A

## Water Deaeration

Operation of the velocity meter using thermistors required the partial removal of dissolved gases from the water, since at very small velocities gas bubbles gathered on the thermistors and changed their heat transfer characteristics. This change in heat transfer characteristics was not predictable and resulted in an unstable calibration of the velocity meter. Laboratory water used to supply the model becomes essentially saturated with air as it is recirculated through the laboratory system. The degree of air saturation was assumed to be the same as that for dissolved oxygen since the concentration of dissolved oxygen was readily measured with a dissolved oxygen meter. Therefore, based upon the solubility of oxygen it was estimated that a reduction of dissolved oxygen to about 55-60 percent of saturation would be satisfactory for operation of the velocity meter. Operation of the model required a system capable of continuously deaerating a maximum flow rate of 25 gpm at room temperature.

The deaeration system developed was based upon a method suggested by Maxwell and Holley[A1]. Their method suggested "_____the creation of a region of locally high velocity and low pressure at the entrance to the suction line of a pump. If the pressure is sufficiently low, dissolved gases come out of solution and pass into the pump suction line as small bubbles. The gases do not readily return to solution in a region of high pressure and can be discharged through the pump and allowed to escape to the atmosphere. The pressure may be reduced to the extent that cavitation occurs in the vena contracta just downstream of the suction line entrance. Then, as the flow expands to fill the suction line downstream of the vena contracta, the pressure increase causes the water to return to the liquid state upstream of the suction part of the pump. Thus, only gas bubbles and water pass through the pump. Care must be taken to avoid loss of prime of the pump, preferably by providing positive static suction head."

The system developed includes the two tanks shown in figure 1 and a recirculating deaeration pump with an orifice attached to the inlet of the pump suction pipe.

The smaller tank is a constant-level tank supplied with saturated laboratory water. The purpose of this tank is to supply the required model flow rate to the larger deaeration tank under controlled conditions and to hold to a minimum the quantity of water to be continuously deaerated. The water is deaerated by pumping it from near the bottom of the tank through an orifice attached to the inlet of the pump suction pipe. The

pump discharge of water and air bubbles is returned to the tank. The pump discharge pipe is enlarged with an elbow on the outlet to direct the flow towards the water surface. A wave suppressor is positioned above the discharge from the elbow. The combination of enlarged piping, elbow and wave suppressor minimizes water surface disturbances, speeds the removal of air bubbles and minimizes reaeration.

The dissolved air is removed by creating a low pressure in the vena contracta downstream from the orifice attached to the pump suction pipe. The velocity-pressure relationship at the vena contracta is derived by assuming that the orifice head loss is negligible and writing the Bernoulli equation between the tank water surface and the vena contracta. This equation is

$$V_c^2/2g = -p_g/w + z \qquad (A1)$$

where $V_c$ = mean velocity in the vena contracta, g = acceleration of gravity, $p_g$ = gage pressure in the vena contracta, w = specific weight of water, and z = difference in elevation from the tank water surface to the pipe center line. If cavitation is to occur for the maximum release of dissolved gases $p_g$ must equal $p_v$, the vapor pressure of the water at the operating temperature. At this temperature and a constant tank water level the right side of equation Al is a constant and the value of $V_c$ can be computed. If the pump discharge, Q, is known the area, A, of the vena contracta will be $Q/V_c$. The area, $A_o$, of the orifice equals $A/C_c$. The coefficient of contraction, C , can be assumed to be 0.6l for a sharp edged orifice. Using this value the diameter of the orifice is readily computed.

Initially the required pump capacity and head for continuously deaerating 25 gpm of saturated water to 55-60 percent saturation were unknown. Therefore, an experiment was conducted to determine the required pump capacity relative to the saturated water flow rate. An available pump with a 50 gpm capacity at a head of 30 ft was used. Three orifices were designed using equation Al for flow rates of 12 gpm, 27 gpm and 48 gpm.

The deaerating capability of the pump and orifices were tested in two deaeration tanks. One tank had a diameter of 13.5 inches with a water depth of 22 inches above the orifice and a water volume of 14.5 gallons. The second tank had a diameter of 22.5 inches with a water depth of 22 inches above the orifice and a water volume of 37 gallons. The water depth above the suction pipe for each tank was sufficient to prevent air insufflation from the water surface. In each test the dissolved oxygen measurement was taken near the bottom of the tank where the deaerated water was withdrawn.

For each orifice installed saturated laboratory water was supplied to the deaeration tank and the same amount of deaerated water was withdrawn from near the tank bottom. The withdrawal flow rate was measured with a calibrated flow meter. The flow rate being pumped through the orifice for deaeration was assumed to be the orifice design discharge. The ratio of pumped flow rate to the laboratory inflow rate could be varied from 1.5 to 6 by using the three orifices in combination with various saturated water flow rates.

Dissolved oxygen measurements were made near the deaeration tank bottom until the dissolved oxygen meter indicated the oxygen concentration was essentially in equilibrium. The equilibrium concentration was obtained after 25 minutes of operation.

These tests indicated that to continuously deaerate the water to 55-60 percent saturation the orifice should be cavitating and the deaeration pump flow rate would need to be about five times the flow rate of the water being deaerated. Therefore, to continuously deaerate 25 gpm required a pump capacity of 125 gpm.

The required average velocity in the vena contracta downstream from the orifice was determined from equation Al. The value of z was taken as 1.92 ft and a water temperature of 80°F was selected for determining the vapor pressure. The orifice diameter of 1.331 inches was determined in the manner previously described.

The required pump head is that needed to overcome the head losses as the water is pumped from the deaeration tank through the piping and returned to the tank. The total head loss computed for the piping arrangement was 27.4 ft. Therefore, a standard centrifugal pump with a 125 gpm capacity at a head of 30 ft was used.

The deaeration system assembled had a deaeration tank 32 in. in diameter with a total water depth of 27 in. The water depth above the suction pipe center line was 23 in.

Operation of this system was checked and found to be capable of continuously deaerating 25 gpm of saturated water to 48 percent saturation. Cavitation did occur continuously in the suction pipe supplying the pump. However, a comparison of the computed pump cavitation index with the recommended cavitation limits for single-suction pumps given by DailyA2 indicated the pump operation is in the safe region. Also, there have been no problems in keeping the pump primed.

## REFERENCES


Al Maxwell, W. H. C, and Holley, E. R., 1969. A Method for Deaeratlng Water. Technical Notes, Proceedings ASCE, Journal of the Hydraulics Division v. 96 (HY1): 577-580.

A2 Daily, James W., 1950. Hydraulic Machinery (chapter Xlll). In Engineering Hydraulics, by Hunter Rouse (ed.), John Wiley & Sons, Inc., New York.


## NOTATIONS

A = area of vena contracta in square feet

Ao = area of orifice in square feet

$C_C$ = orifice contraction coefficient, non-dimensional

g = acceleration of gravity in feet per second per second

$p_g$ = gage pressure at orifice vena contracta in pounds per square foot

$p_v$ = gage vapor pressure of water in pounds per square foot

Q = discharge through orifice in cubic feet per second

$V_c$ = average velocity in vena contracta in feet per second

w = unit weight of water in pounds per cubic foot

z = elevation difference between deaeration tank water surface and orifice centerline in feet

# APPENDIX B

## Velocity Meter

Measurement of the spatial velocity distribution in the model settling basin requires an instrument which can measure water velocities less than about 0.08 ft/sec. Several varieties of instruments have successfully been developed to measure low fluid velocities. Unfortunately these instruments were mainly utilized for measuring low air velocities and thus did not encounter the problems associated with the measurement of low velocities in water.

### Thermistor Anemometry

One of the more recent developments in instrumentation for measuring low velocities in water is the application of solid state device known as thermistor. This device transfers heat to the moving fluid in proportion to the local fluid velocity. The power required to maintain or generate this heat can be measured and under proper calibration it will provide an indication of the magnitude of the local fluid velocity.

Wingo[B1] developed a velocity meter using thermistors to measure the velocity distribution of filtered deionized water in a large partially baffled tank. Eagleson and Watering[B2] developed and utilized a thermistor probe to measure orbital velocities in shallow water waves of laboratory scale. The probe developed by Eagleson and Watering could measure the velocity vector in the range of 0.1 to 3.0 feet per second. The determination of the wave energy required only the magnitude of the velocity rather than its direction and therefore the probe developed was directionally insensitive.

### Velocity Meter Developed at State Water Survey

A special velocity measuring meter utilizing thermistors has been developed at State Water Survey for the present. study. A brief description and the related calibration procedures for this meter are presented.

A self-heated thermistor left alone in a flowing fluid can indicate the magnitude of the flow velocity with proper transformation and calibration. But a meter with an open thermistor will not show the direction of the velocity vector. The evaluation of the hydraulic performance of the settling basin requires the knowledge of both the direction and the magnitude of the velocity vector or its components. Therefore, at the beginning of the meter development it was necessary to consider the design of a thermistor housing that

would indicate the direction of the velocity vector. The meter developed for the present study is called Meter D.

Figure Bl shows a sketch of the velocity meter geometry with its housing and the support. Flow direction is from left to right, with flow entering the horizontal tube at the extreme left, traversing the tube and exiting at the extreme right of the tube. The two thermistors inside the 1/4 inch diameter tube are positioned at the center line of the tube. The third thermistor located outside the horizontal tube was found to be unnecessary. All Joints are made water tight. The arrangements and the geometry shown in figure Bl are the end-products of various combinations of positions and geometries of the meter support, nose-extension and tail-extension tried in the laboratory to arrive at an acceptable design geometry of the meter.

Figure B2 shows a photograph of the lower portion of Meter D.

The system consists of two thermistors in a bridge circuit. The active element in this meter is a low resistance heated thermistor, which is maintained at a temperature greater than ambient by a constant increment. As the velocity past the meter increases, the active thermistor is cooled, its resistance increases and more power is required to maintain this temperature, and the bridge voltage provides the output signal.

The other thermistor is of higher resistance, remaining very close to ambient temperature, and serves as a temperature compensator. This temperature compensator thermistor was also used to measure the water temperature. The thermistor was switched to a calibrated temperature measuring circuit and its output signal recorded.

A simplified schematic diagram is shown in figure B3. $T_1$ is the heated thermistor, and $T_2$ is the reference thermistor which senses the ambient temperature. Amplifiers $A_1$, and $A_2$ provide the voltage required to balance the bridge, $A_3$ adjusts the negative voltage to the bridge to minimize the common mode voltage to A,, and the amplifiers F are current amplifiers.

One of the problems encountered in developing this meter is temperature compensation, i.e., obtaining the same output signal for the same velocity regardless of ambient temperature. By appropriate selection of $R_3$ the temperature compensating resistor, the output can be made fairly constant over a span of 8 to 10°C, at one signal level. With one probe it was found that, when compensation was satisfactory at zero velocity, the output varied by about 15 percent over this temperature span at a high signal level, equivalent to a velocity of 0.05 ft/sec. This difficulty was due to a variation in power level with temperature.

For Meter D, the load resistor, $R_1$, for the active thermistor was selected to minimize the power variation over the temperature span used. In this case, when temperature compensation was obtained at zero velocity for a range of temperature of 22°C to 28°C, the output remained constant at a high signal level, for a range of temperature 23.2°C to 27.2°C. This high signal level was equivalent to a velocity of 0.053 ft/sec. These variations are shown in figure B4. Therefore, based on these data, a single calibration curve should be valid for the range of temperature of 23.2°C to 27.2°C for any signal level. Figure B4 can be utilized to extend the calibration curve beyond the constant-calibration curve temperature range of 23.2°C to 27.2°C.

## Calibration of Meter D

Utilization of Meter D for actual measurement of velocity distribution in the settling basin required its calibration in a known, well-established steady velocity field. After few initial trials, the calibration set-up adopted for this purpose is shown skematically in figure B5, and is described here.

The water from the laboratory system is supplied to Tank 1. This head tank is fitted with an overflow pipe which maintains a constant head in the deaeration tank, Tank 2, figure B5•

The dissolved gases in a flowing liquid may collect on the hot surfaces of a hot-wire, hot-film or thermistor and consequently change the heat transfer characteristics of the sensor. Since the bridge-signal is related to the power input required to maintain a constant temperature in the thermistor, the dissolved gases can change the bridge output signal. The deaeration set-up shown on the extreme left in figure B5 consists of a tank, pump, valve and an orifice at the inlet pipe to the pump. The mechanics of deaeration are discussed in detail in Appendix A, Water Deaeration.

The deaerated water from tank number 2 is piped to the small constant head tank which in turn supplies water to the 4 inch diameter stainless steel pipe line. Flow to the head tank is controlled by a valve in the supply line. The water from the head tank is allowed to pass initially through a 3/4 inch diameter pipe, then through a gradual concentric expansion before entering the 4 inch diameter pipe line. At the entrance to the 4 inch pipe line a nest of 1/4 inch tubes 12 inches long is installed to equalize flow.

The pipeline is also positioned on an adverse slope of 0.5 percent toward the outlet to minimize the chance of trapping air pockets along the top of the pipe while filling it. Since the flow velocity in the pipeline must be very small for the range of calibration the precautions and the arrangements

described above were deemed essential. This arrangement of the calibration apparatus resulted in a stable and repeatable flow condition in the pipeline.

The meter was positioned at a distance of about 120 diameters from the pipe inlet and velocity distribution data in a vertical plane were collected.

The downstream section of the pipeline consists of a concentric contraction to the discharge pipe of 5/l6 inch diameter. A control valve was installed on the discharge pipe to control the flow in the main pipeline.

The final piece of apparatus utilized for the calibration consists of a weighing tank with a drain pipe and a weighing scale. The discharge from the outlet pipe was collected in the weighing tank for a known interval of time, the water temperature was measured to determine its unit weight, and from this data the volume of water collected in the tank was computed. Finally the average velocity in the pipeline was computed based on its cross-sectional area and the volume of the water collected for the known interval of time.

## Calibration Curve

Tests were conducted to check the establishment of a fully developed laminar flow in the pipeline. For this condition the maximum velocity is theoretically on the pipe centerline and is equal to twice the average velocity. The velocity distribution is given by the following equation.

$$u/2U = u/U_{max} = [1 - (r/R)^2] \qquad (B1)$$

where u is the point velocity at a distance of r from the pipe centerline, R is the radius of the pipeline, U is the average velocity and $U_{max}$ is the maximum velocity in the pipeline.

Data collected from the calibration set-up indicated that for most cases the maximum velocity in the vertical plane was located within 3/8-inch of the pipe centerline. Therefore, a calibration curve was developed on the assumption that this maximum velocity was equal to twice the average velocity.

Data collected for vertical velocity profiles for different average velocities were converted to point velocities with use of the typical calibration curve. A non-dimensional plot of the experimental velocity data and the theoretical velocity profile for laminar flow, equation Bl, is shown in figure B6. Most of the data are within + 3 percent of the theoretical curve. This indicates that although the maximum velocity may

be located as much as 3/8-inch from the pipe centerline, the shape of the velocity profile remains parabolic when referenced to the maximum velocity. Therefore a calibration curve obtained by measuring the velocity meter output signal for the maximum velocity should be satisfactory.

The actual calibration process consisted of: 1) establishing a stable velocity profile in the pipeline, 2) making sure the ambient water temperature did not vary more than about 0.5°C throughout a full run, 3) collecting the discharge in the weighing tank for a known interval of time and 4) obtaining the output signal on the recorder when the probe was positioned at the centerline or moved in the vertical plane to locate the maximum velocity corresponding to the maximum output signal.

The calibration curve thus obtained for Meter D relating output signal in millivolts to point velocity in feet per second is shown in figure B7. The calibration curve indicates that the meter is very sensitive. This calibration curve was subsequently utilized in the model settling basin.

For correct operation the long nose of the meter, figure Bl, must face in the upstream direction. However, in a settling basin with varying circulation patterns it may not be possible to know before hand the actual flow direction. Consequently a direction detection device was incorporated in the geometric design of the meter. Whenever the flow direction is from the tail-end toward the nose-end of the meter, the output signal drastically reduces in magnitude and the investigator can immediately recognize the reversal of flow. This phenomenon was checked inside the pipeline by rotating the meter 180° and comparing the output signal for the normal and the reversed position of the meter. The location of the thermistors and the length of the tail-end of the meter are instrumental in the reduction of the output signal due to flow reversal.

The calibration curve shown in figure B7 is valid for a range of temperature of 23.2°C to 27.2°C. Figure B4 can be utilized to modify the calibration curve of figure B7 for any other temperature between 20°C to 30°C.

## REFERENCES

Bl Wingo, H. E. , " Thermistors Measure Low Liquid Velocities," Control Engineering 6(10) 131-3, 1959.

B2 Eagleson, P. S. and Van de Watering, W. P. M., "A Thermistor Probe for Measuring Particle Orbital Speed in Water Waves," MIT, Hydrodynamics Laboratory, Report No. 6l, 1963.

## NOTATIONS

R = inside radius of a pipe in feet

r = radial distance from the centerline inside a pipe in feet

U = average flow velocity in a pipeline for laminar flow in feet per second

$U_{max}$ = maximum flow velocity in a pipeline for laminar flow in feet per second

u = velocity at a point inside a pipeline for laminar flow in feet per second

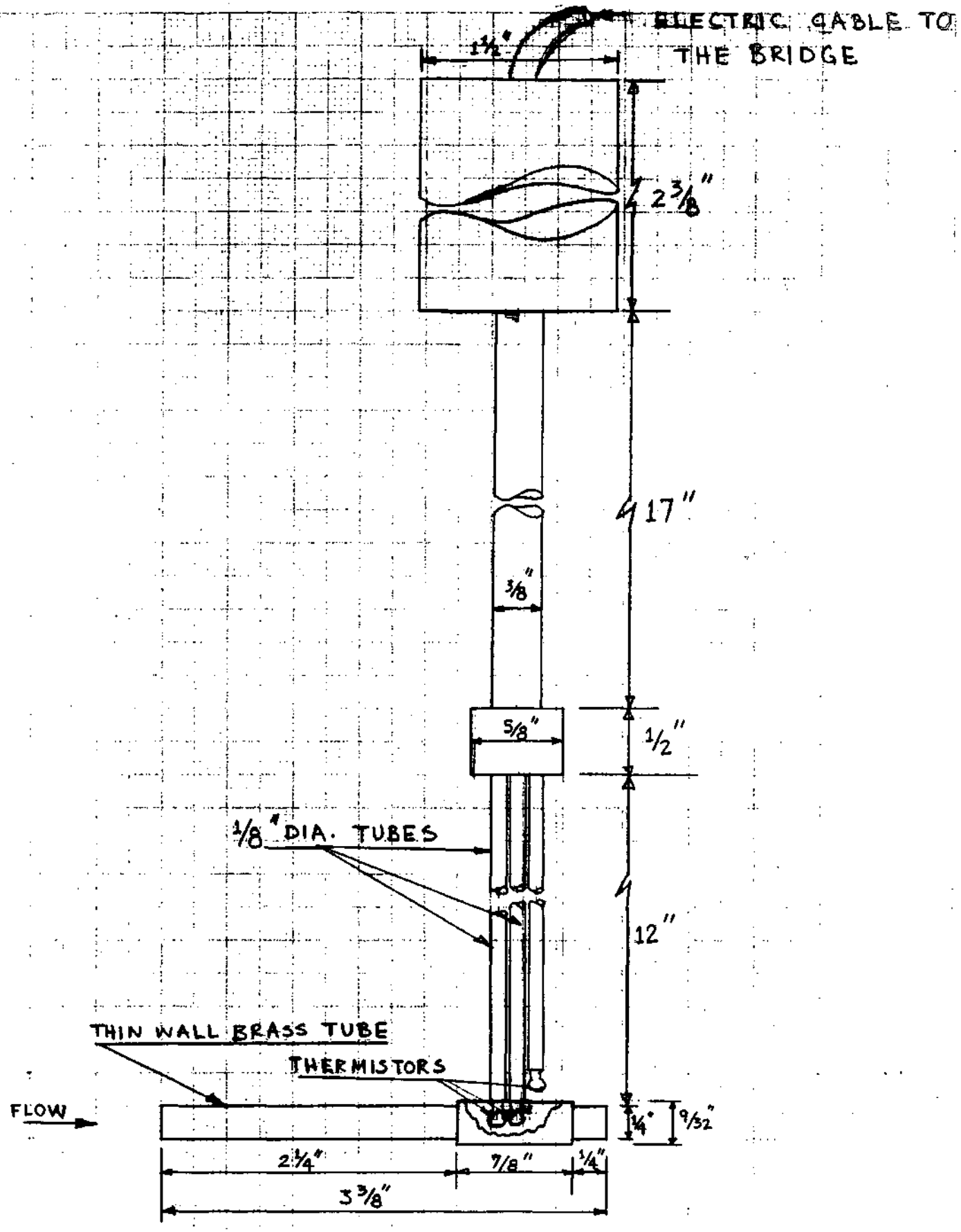


FIGURE B1. VELOCITY METER D

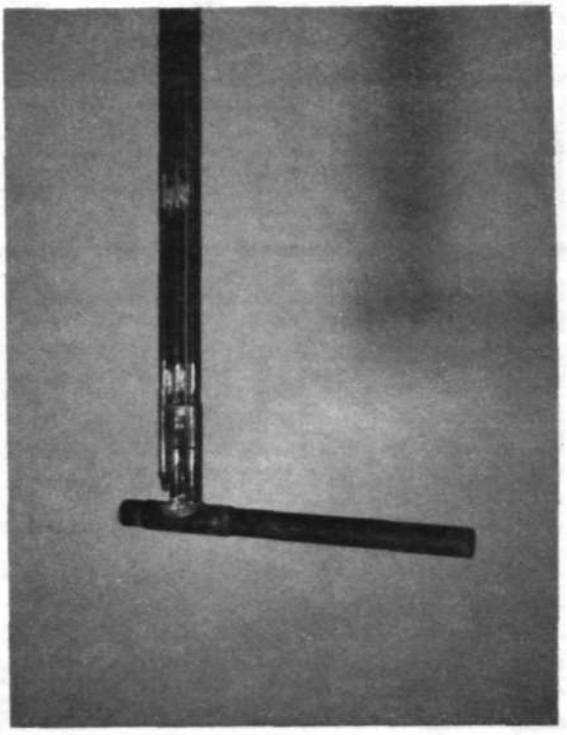

Figure B2. Photograph of the Lower Portion of Velocity Meter D

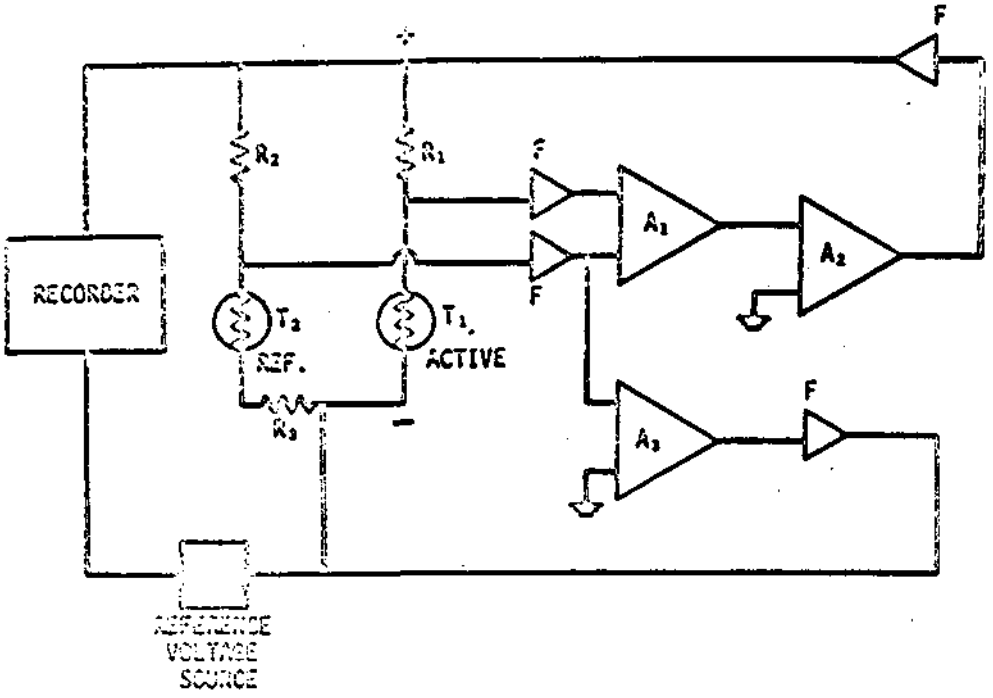


Figure B3. Schematic Circuit for Thermistor Velocity Meter

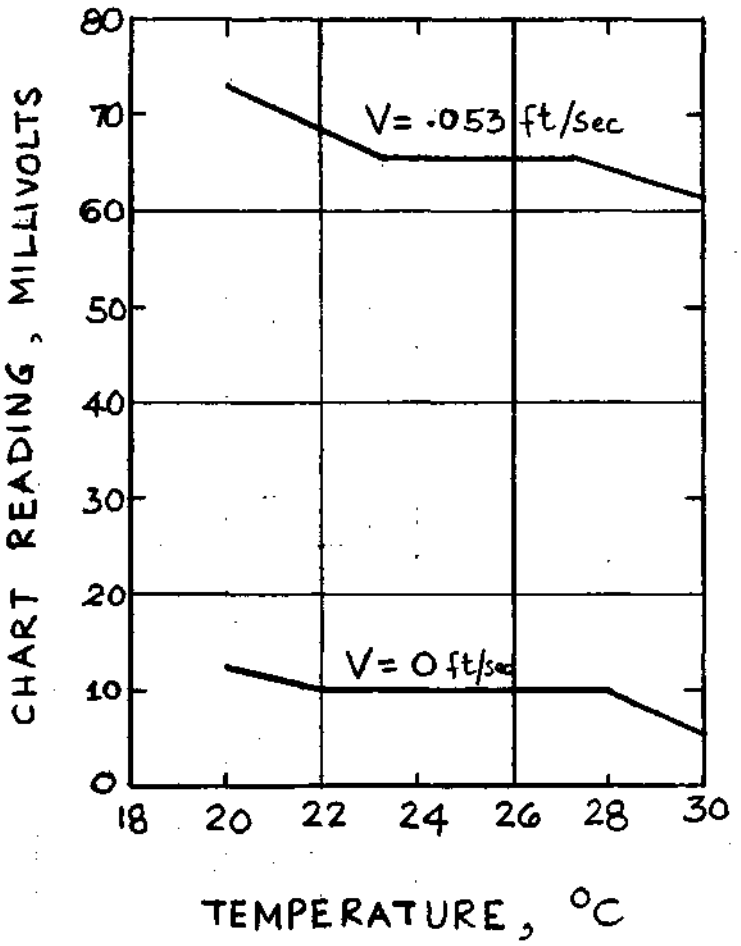


FIGURE B4. METER D, TEMPERATURE EFFECT

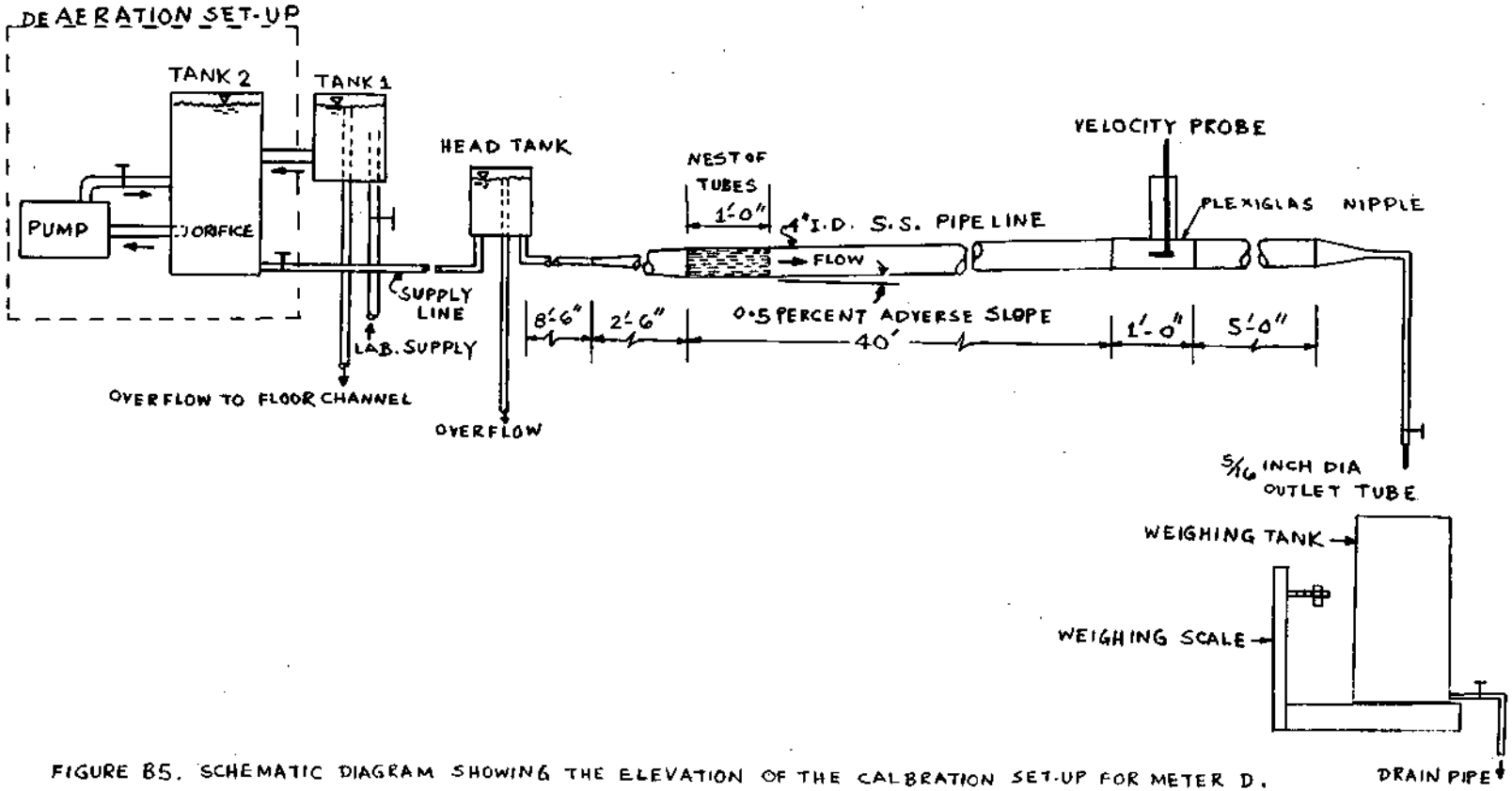


FIGURE B5. SCHEMATIC DIAGRAM SHOWING THE ELEVATION OF THE CALBRATION SET-UP FOR METER D.

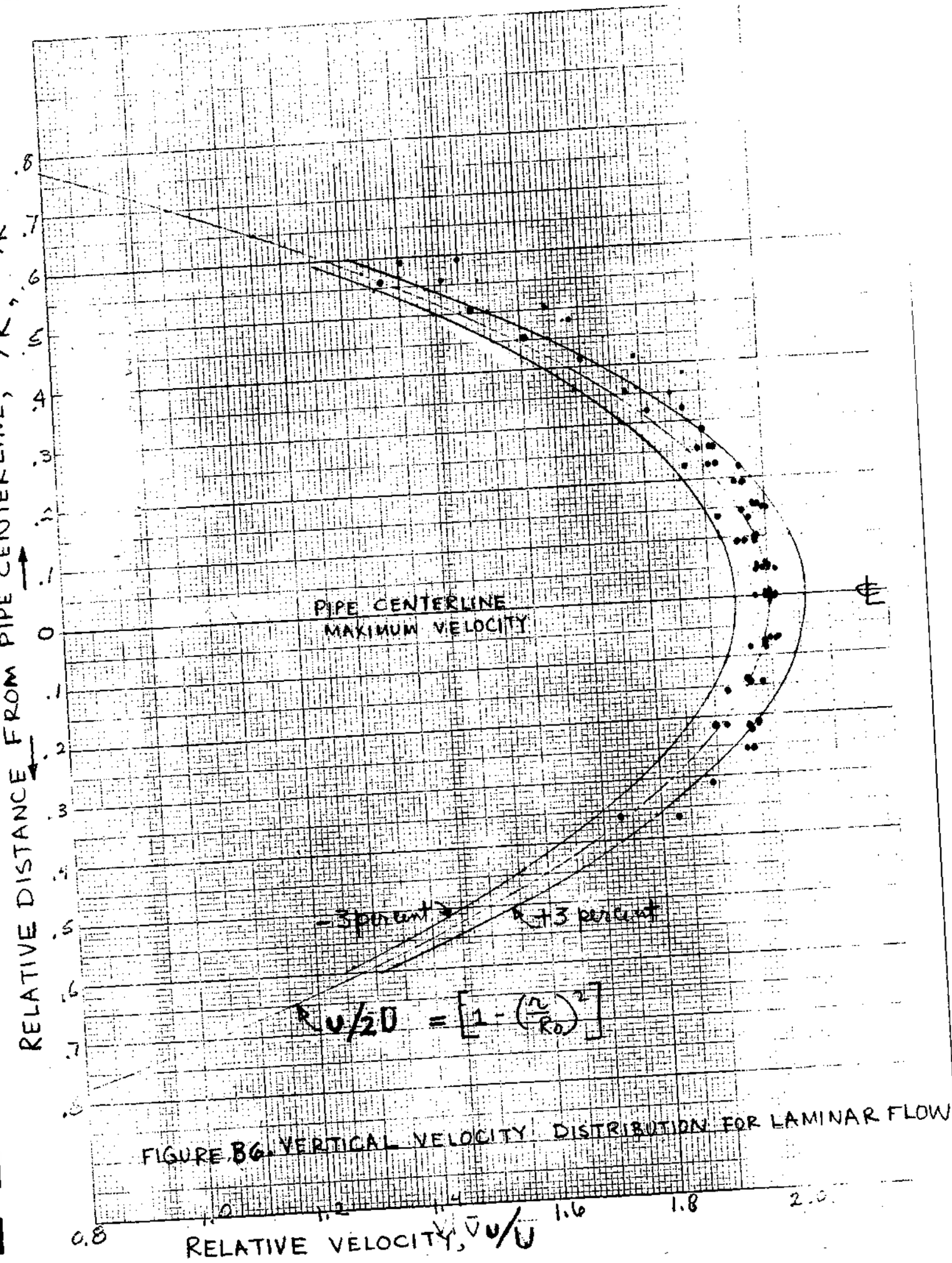


FIGURE B6. VERTICAL VELOCITY DISTRIBUTION FOR LAMINAR FLOW

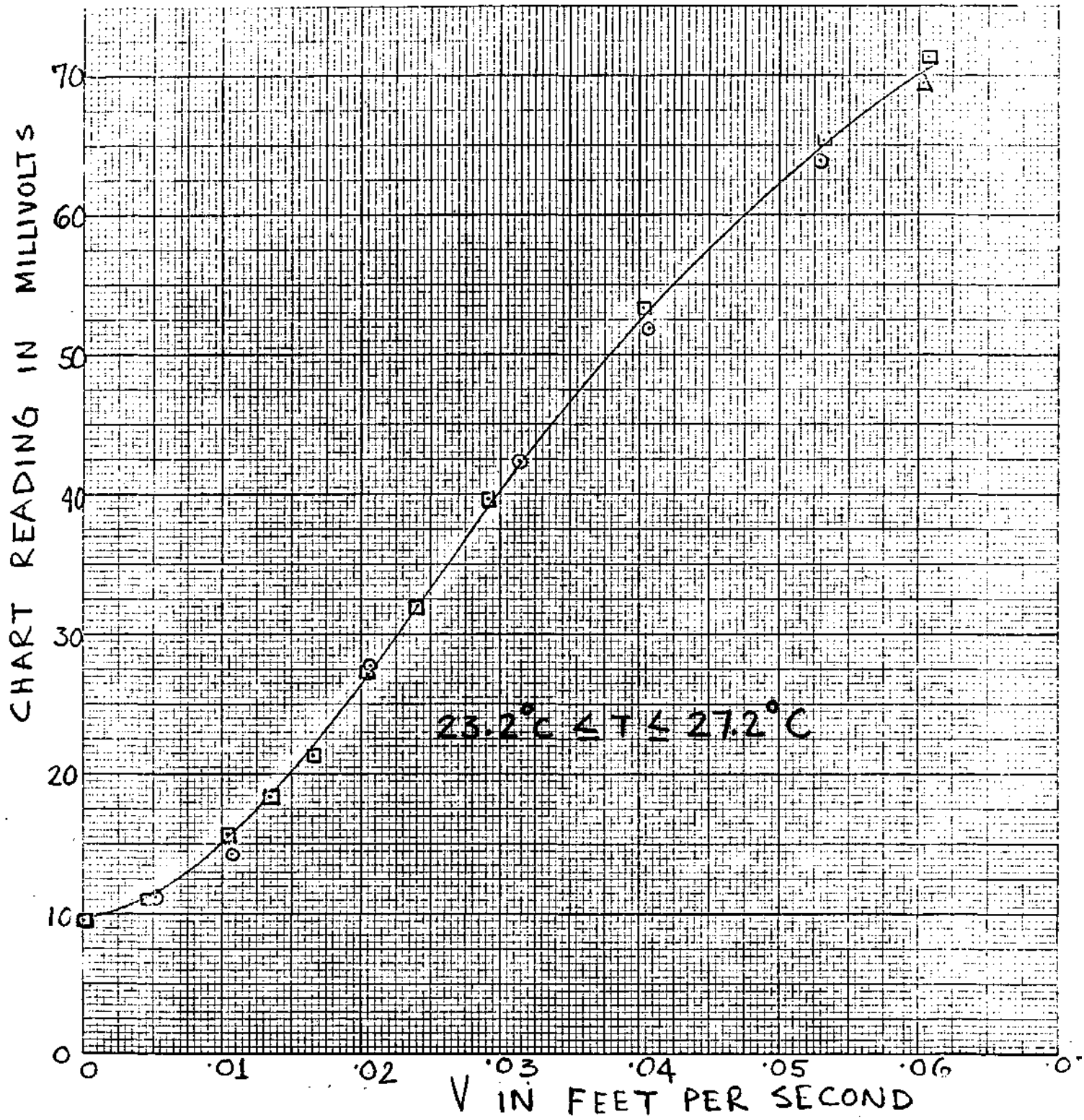


FIGURE B7. CALIBRMIOM CURVE FOR METER D